Topological properties of Rauzy fractals

Anne Siegel

Jörg M. Thuswaldner

IRISA, Campus de Beaulieu, 35042 Rennes Cedex, France
E-mail address: Anne.Siegel@irisa.fr

Chair of mathematics and Statistics, Department of Mathematics and Information Technology, University of Leoben, A-8700 Leoben, Austria
E-mail address: joerg.thuswaldner@unileoben.ac.at

Both authors are supported by the "Amadée" grant FR-13-2008.
The first author is supported by projects ANR-06-JCJC-0073 and BLAN07-1-184548 granted by the French National Research Agency.
The second author is supported by project S9610 granted by the Austrian Science Foundation (FWF). This project is part of the FWF national research network S96 "Analytic combinatorics and probabilistic number theory".
The drawings of the graphs are done with help of the software yFiles.

Abstract. Substitutions are combinatorial objects (one replaces a letter by a word) which produce sequences by iteration. They occur in many mathematical fields, roughly as soon as a repetitive process appears. In the present monograph we deal with topological and geometric properties of substitutions, *i.e.*, we study properties of the *Rauzy fractals* associated to substitutions.

To be more precise, let σ be substitution over the alphabet $\mathcal{A}$. We assume that the linearized matrix of σ is primitive and its dominant eigenvalue is a unit Pisot number (*i.e.*, an algebraic number whose norm is one and all of whose Galois conjugates are of modulus strictly smaller than one). It is well-known that one can attach to σ a set $\mathcal{T}$ which is now called *central tile* or *Rauzy fractal* of σ. Such a central tile is a compact set that is the closure of its interior and decomposes in a natural way in $n = \#\mathcal{A}$ subtiles $\mathcal{T}(1), \ldots, \mathcal{T}(n)$. The central tile as well as its subtiles are graph directed self-affine sets that often have fractal boundary.

Pisot substitutions and central tiles are naturally of high relevance in several branches of mathematics like tiling theory, spectral theory, Diophantine approximation, the construction of discrete planes and quasicrystals as well as in connection with numeration like generalized continued fractions and radix representation. The questions coming up in all these domains can often be reformulated in terms of questions related to the topology and geometry of the underlying central tile.

After a thorough survey of important properties of unit Pisot substitutions and their associated Rauzy fractals the present monograph is devoted to the investigation of a variety of topological properties of $\mathcal{T}$ and its subtiles. Our approach is an algorithmic one. In particular, we dwell upon the question whether $\mathcal{T}$ and its subtiles induce a tiling, calculate the Hausdorff dimension of their boundary, give criteria for their connectivity and homeomorphy to a disk and derive properties of their fundamental group.

The basic tools for our criteria are several classes of graphs built from the description of the tiles $\mathcal{T}(i)$ $(1 \leq i \leq n)$ as graph directed iterated function systems and from the structure of the tilings induced by these tiles. These graphs are of interest in their own right. They can be used to construct the boundaries $\partial\mathcal{T}$ as well as $\partial\mathcal{T}(i)$ $(1 \leq i \leq n)$ and all points where two, three or four different tiles of the mentioned tilings meet.

When working with central tiles in one of the above mentioned contexts it is often useful to know such intersection properties of tiles. In this sense the present monograph also aims at providing tools for "everyday's life" when dealing with topological and geometric properties of substitutions.

Many examples to illustrate our results are given. Moreover, we give perspectives for further directions of research related to the topics discussed in this monograph.

Contents

CHAPTER 1

Introduction

The present monograph deals with topological and geometric properties of substitutions. In this introduction we first emphasize on the great importance of substitutions in many fields of mathematics, theoretical physics and computer science. Already in this first part it becomes evident on several places that geometrical objects like *Rauzy fractals* are intimately related to substitutions and their topological as well as geometric properties deserve to be studied in order to get informations about the underlying substitution. After this general part we give an introductory overview over Rauzy fractals with special emphasis on their topology. We discuss their history and give some details on different ways of their construction. The introduction closes with an outline of the content of the present monograph.

1.1. The role of substitutions in several branches of mathematics

Substitutions are combinatorial objects which produce sequences by iteration. They are given by a replacement rule of the letters of a finite alphabet by nonempty, finite words over the same alphabet. They are also called *iterated morphisms*. Since they simply consist in an iteration process on a finite set, they can be recovered in many fields of mathematics, theoretical physics and computer science to describe repetitive processes or replacement rules.

1.1.1. Combinatorics. In combinatorics of words, since the beginnings of this domain, substitutions have been used in order to exhibit examples of finite words or infinite sequences with very specific or unusual combinatorial properties. The most famous example is the Thue-Morse sequence defined over the two letter alphabet $\{1, 2\}$ as $\sigma(1) = 12$, $\sigma(2) = 21$. This substitution admits two infinite fixed points: the first one begins with all iterations $\sigma^n(1)$ $(n \geq 1)$, the second one begins with the words $\sigma^n(2)$ $(n \geq 1)$. Thue and Morse proved for instance that this infinite sequence is square-free, meaning that is contains no repetition with the shape uu, where u is a finite word (see for instance [**35, 66, 88**] where many other properties of this famous sequence are discussed).

Other well-known infinite sequences that can be defined in terms of substitutions are the so-called *sturmian sequences*. They were introduced in the 1940s as sequences having the smallest complexity among all nonperiodic infinite sequences over a two letter alphabet. In particular, the number of their factors of size n is always equal to $n+1$. A famous characterization relates these sequences with to geometry. Indeed, sturmian sequences are exactly cutting sequences of lines in $\mathbb{R}^2$. In particular, first draw grid lines, which are the horizontal and vertical lines through the lattice $\mathbb{Z}^2$ in the first quadrant of the plane. Then, travelling along the line $y = \alpha x + \beta$ away from the origin, write down a 1 each time a vertical grid line is crossed, and a 2 each time a horizontal grid line is crossed [**66**, Chapter 6]. When the slope α of the line is a quadratic irrational with a Galois conjugate outside of $(0, 1)$, we know that the associated sturmian cutting sequence is the fixed point of a substitution. The most famous case is the fixed point of the Fibonacci substitution $\sigma(1) = 12$, $\sigma(2) = 1$ [**15, 55**]. When the slope α is not a quadratic number, then a recoding process is used to describe the factors of the sequence as produced by the suitable compositions of two "basic" substitutions (see [**66**, Chapter 6]). Their complexity properties are used in a large scale of applicative domains, such as compression to recover repetitions in DNA sequences [**57**] or optimal allocation in networks [**69**].

1.1.2. Number theory. Since the time when they appeared, substitutions have been deeply related to number theory: following Thue, the Thue-Morse sequence classifies integers with respect to parity of the sum of their binary digits. The Baum-Sweet sequence describes whether the binary expansion of an integer n contains at least one odd string of zeros. It is obtained as the projection of a substitution on a 4 letter alphabet [**16**]. A bridge between substitutions and number theory is also given by the Cobham theorem, which states that an infinite sequence is a letter-to-letter projection of the fixed point of a substitution of constant length k if and only if each element u_n of the sequence is produced by feeding a finite automaton with the expansion in base k of n [**51**]. This theorem allows to derive deep transcendence properties: for instance, the real numbers with continued fraction expansions given by the Thue-Morse sequence, the Baum-Sweet sequence or the Rudin-Shapiro sequence are all transcendental, the proof being based on the "substitutive" structure of these sequences [**2**]. Additionally, irrational numbers whose binary expansion is given by the fixed point of a substitution are all transcendental [**1**]. In the field of diophantine approximation, substitutions produce transcendental numbers which are very badly approximable by cubic algebraic integers [**113**]; the description of greedy expansions of reals in noninteger basis [**5, 123**] by the means of substitutions also results in best approximations characterizations (see [**72**] and [**88**, Chapter 10]).

1.1.3. Dynamical systems. Another independent reason of the introduction of substitutions is related to dynamical systems. Indeed, ten years after Thue, Morse rediscovered the Thue-Morse sequence in the field of dynamical systems. Following Poincaré at the beginning of the 20th century, the study of dynamical systems shifted from the research of analytical solutions of differential equations to the study of all possible trajectories and their relations. The research then focused on exhibiting recurrence properties of orbits, that is, properties ensuring that all points will return close to their initial positions. To perform this task in the context of connected surfaces with constant negative curvature, Morse followed an idea proposed by Hadamard: he studied the orbits qualitatively. Here, this means to code a curve by an infinite sequence of 1 and 2's according to which boundary of the surface it meets. With this approach and by using the Thue-Morse substitution fixed point, Morse succeeded in proving that there indeed exists uniformly non-closed recurrent geodesics [**100**]. This result initiated the field of *symbolic dynamics*, that is, studying dynamical systems by coding their orbits as infinite sequences; therefore, a complex dynamics over a quite simple space is replaced by a simple dynamics (the shift map) over an intricate but combinatorial space made of infinite sequences.

For dynamical systems for which past and future are disjoint, the symbolic dynamical systems are particularly simple and well understood: they are described by a finite number of forbidden words, and they are called *shifts of finite type* [**85**]. A partition that induces a coding from a dynamical system onto such a shift of finite type is called a *Markov partition* [**3**]: such a partition gives rise to a semiconjugacy from a bi-infinite shift to the dynamical system which is one-to-one almost everywhere. A first example has been implicitly given in the invariant Cantor sets of the diffeomorphisms of the sphere studied by Smale [**121**]. After that the existence of Markov partitions has been established for several classes of dynamical systems, including hyperbolic automorphisms of n-dimensional tori and pseudo-Anosov diffeomorphisms of surfaces [**45**]. The existence of Markov partitions and their associated semiconjugacies is extremely useful in studying many dynamical properties (especially statistical ones); as an example, they are used to prove that hyperbolic automorphisms of the two-dimensional torus are measure-theoretically isomorphic if and only if they have the same entropy [**4**].

Explicit Markov partitions, however, are generally known only for hyperbolic automorphisms of the two-dimensional torus [**3**], and they have rectangular shapes. In higher dimensions, a sightly different behavior appears since several results attest that the contracting boundary of a member of a Markov partition cannot be smooth [**46, 50**]. Markov partitions have then been proposed by arithmetical means for irreducible hyperbolic toral automorphisms: using homoclinic points of the dynamics [**62, 81**] allows to build constant-to-one factor maps

for the dynamical system; however, switching to semiconjugacy maps is performed only in examples, and the topological properties of the pieces of the partition are not explicit. Another approach was proposed, based on the representation of integers in non-integer basis [**105**] or referring to two-dimensional iteration processes [**24, 75**]. These constructions are explicit and geometrical, based on substitutions. The same problem as before occurs when switching from a factor map to a semi-conjugacy, but this question is tackled in some cases by using symbolic dynamics and the combinatorics of substitutions as we shall detail soon.

At the opposite to Markov shifts we mention highly ordered self-similar systems with zero entropy, which can be loosely defined as systems where the large-scale recurrence structure is similar to the small-scale recurrence structure, or more precisely as systems which are topologically conjugate to their first return map on a particular subset. Naturally, their symbolic dynamical systems are generated by substitutions [**66, 108**]. The codings of recurrent geodesics studied by Morse in [**100**] belongs to this class, as well as the return map of the expanding flow onto the contracting manifold for hyperbolic toral automorphisms with a unique expanding direction [**31**]. For these systems, the natural question is to determine their ergodic properties, among which we mention mixing properties or pure discrete spectrum. A very large literature is dedicated to this task (see [**66**, Chapters 5 and 7]). It was shown that symbolic dynamical systems generated by substitutions have a variety of interesting properties. A specific case is of great interest: when the incidence matrix of the substitution has a unique expanding direction (its dominant eigenvalue is a Pisot number). In this case explicit combinatorial conditions characterize systems with pure discrete spectrum [**31, 78**]. We will come back to this property in Chapter 3. These conditions are used to prove that the factor map induced by the Markov partitions proposed in [**24, 75, 105**] are indeed semiconjugacies.

1.1.4. Applications to tiling theory, theoretical physics and discrete geometry. Substitutions also appeared in physics in connection with quasicrystals. In 1984, aluminium-manganese crystals with icosahedral symmetry where synthesized. However, crystals were proved to have rotational symmetries confined to orders 2, 3, 4 and 6. The term *quasicrystal* was invented to describe new classes of crystals with forbidden symmetry. The definition of quasicrystals and crystals in general has then evolved and it is not entirely fixed nowadays [**44, 89, 117**]. Nevertheless, a solid is usually considered as a quasicrystal when is has an essentially discrete diffraction diagram. The mathematical question here was to identify atomic structures (or point sets) with a discrete diffraction diagram.

In this context, substitutions are ubiquitous. Indeed, starting from a substitution, one can build a tiling space by considering tilings of the real line by intervals with specific length. The order of intervals in the tilings that are considered in the space is governed by the factors of a periodic point of the initial substitution. Such tiling spaces support a natural topology and a minimal and uniquely ergodic $\mathbb{R}$-translation flow.

However, a natural relation exists between tilings and models atoms in crystals: a one-dimensional tiling can be mapped to a one-dimensional discrete set of points by placing an atom at the end of each tile. The question whether such a material is a quasi-crystal has been studied in the 1990s: Lee, Moody and Solomyak proved that if the substitution is Pisot (its abelianized matrix has a unique expanding direction), then its diffraction spectrum is purely discrete if and only if the dynamical spectrum of the translation flow on the substitution tiling space is purely discrete from a topological point of view [**84**]. Recalling that the translation flow on a tiling space is related (even if not exactly equal) to the spectrum of substitutive dynamical systems as mentionned in the previous subsection [**31**], we realize that a strong bridge exists between theoretical physics and spectral theory of substitutive systems. Criterions for pure discrete spectrum provided in [**31, 78**] and already used for Markov partitions can be directly applied in the context of quasicrystals.

One-dimensional tiling flows also appeared in classification of dynamical systems since every orientable hyperbolic one-dimensional attractor is proved to be either a one-dimensional

substitution tiling space or a classical solenoid [**17, 31, 127**]. The consequences of this result will be discussed in Chapter 7.

From a more combinatorial point of view, a quasicrystal is given by an aperiodic but repetitive structure that plays the role of the lattice in the theory of crystalline structures. Mathematically, we then speak of *Meyer sets* and such Meyer sets are obtained by exhibiting the *cut-and-project scheme* [**99**]. In the one-dimensional case, a well-studied family of Meyer sets is given by integers in non-integral basis, in relation with sturmian sequences [**70**]. In higher-dimensional cases, however, all these questions are quite open. The well-known Penrose tiling is a quasicrystal since it has essentially discrete diffraction diagram, but defining a wide class of examples of quasicrystals is an open question [**17, 80, 81, 112**]. By analogy with the one-dimensional case, good candidates for cut-and-project schemes (hence quasicrystals) are given by discrete approximations of planes that are orthogonal to Pisot directions [**20, 32**]. Still by analogy with sturmian sequences, such approximations of planes can be generated from one-dimensional substitutions by applying suitable continued fractions algorithms [**20, 76**]. However, the large literature dedicated to ergodic properties of multi-dimensional substitutive tiling flows [**122**] applies with difficulty since the definition of substitutive planar tilings is not stable yet [**106**] and much work remains to be done in this direction.

As a final direction, let us mention that the use of substitutions to describe discrete planes in $\mathbb{R}^3$ have recently proved to be very useful in discrete geometry to algorithmically decide whether a discrete patch is the part of a discrete plane [**21, 37, 65**]. We will discuss this question in Chapter 7.

1.2. The geometry of substitutions: Rauzy fractals

In the world of substitutions, geometrical objects appeared in 1980 in the work of Rauzy [**110**]. The motivation of Rauzy was to build a domain exchange in $\mathbb{R}^2$ that generalized the theory on interval exchange transformations [**79, 126**]. Thurston introduced this object in the context of numeration systems in non-integer basis in [**123**]. As we shall see, this object was finally used in many other context.

1.2.1. The Rauzy fractal for the Tribonacci substitution. To build a Rauzy fractal (also called *central tile*) we restrict to the case of a *unit Pisot substitution*, *i.e.*, a substitution such that its abelianization matrix is primitive and its dominant eigenvalue is a Pisot unit (its Galois conjugates all have a modulus strictly less than 1). There are mainly two methods of construction for Rauzy fractals. The first approach is based on formal power series and projections of broken lines to hyperplanes and is inspired by the seminal paper [**110**]. The principle is to consider a periodic point for the substitution, then to represent this sequence as a stair in $\mathbb{R}^n$, where n denotes the size of the alphabet on which the substitution applies. The next step is to project the vertices of the stair onto a contracting subspace of the abelianization matrix, spanned by the eigenvectors corresponding to Galois conjugates of the dominant eigenvalue of the matrix. Since the projection is performed on a contracting stable space of the matrix, and the object that was projected is a periodic point for the substitution (hence somewhat "contracted" by the abelianization matrix) the closure of the projection is a compact set. A final step consists in drawing several colors with respect to the direction used in the stair to arrive on each vertex before the projection, and we get the Rauzy fractal.

The standard example is given by the so-called *Tribonacci substitution* defined as $\sigma(1) = 12$, $\sigma(2) = 13$, $\sigma(3) = 1$ which was first studied by Rauzy [**110**]. The abelianization matrix counts the number of occurrences of letters in the images of the letters of the substitution; here it is $\begin{bmatrix} 1 & 1 & 1 \\ 1 & 0 & 0 \\ 0 & 1 & 0 \end{bmatrix}$. The dominant eigenvalue satisfies the relation $X^3 - X^2 - X - 1 = 0$, justifying the name *Tribonacci* for the substitution. The contracting space is two-dimensional. Projecting the "broken line" related to the unique fixed point of the Tribonacci substitution to the contracting

plane yields a nice fractal picture, the so-called *Rauzy fractal* $\mathcal{T}$ which is depicted here with its basic subtiles $\mathcal{T}(1)$ (larger subtile), $\mathcal{T}(2)$ (middle size subtile), $\mathcal{T}(3)$ (smallest subtile).

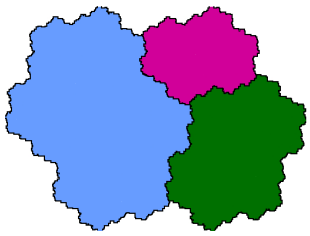

Since this compact set is obtained from the fixed point of the substitution, the self-induced properties of the fixed point have geometrical consequences: we represent the contracting space as the complex plane $\mathbb{C}$. We denote by α one of the two complex conjugate roots of the polynomial; one has $|\alpha| < 1$. With help of α, the Rauzy fractal can be written as graph directed iterated function system in the flavor of [**95**] as

$$\mathcal{T}(1) = \alpha(\mathcal{T}(1) \cup \mathcal{T}(2) \cup \mathcal{T}(3)), \qquad \mathcal{T}(2) = \alpha(\mathcal{T}(1)) + 1 \qquad \mathcal{T}(3) = \alpha(\mathcal{T}(2)) + 1.$$

Hence, each basic tile can be mapped onto a finite union of translates of basic tiles, when multiplied by the parameter α^{-1}. The maps in the GIFS are contractive, thus the nonempty compact sets $\mathcal{T}(1)$, $\mathcal{T}(2)$ and $\mathcal{T}(3)$ satisfying this equation are uniquely determined [**95**]; they have nonzero measure and are the closure of their interior [**120**]. Let us note that the subdivision matrix in the graph directed iterated function system is closely connected to the substitution σ, since it is the transpose of the abelianization matrix.

The unicity of the solution of such a graph directed iterated function system equation allows to build the Rauzy fractal in a second way, actually used by Rauzy during its attempts to perform the construction of the fractal (but not published in this way). The principle is to start from a decomposition of an hexagon splitted into three rhombi. There are actually two ways for cutting an hexagon into three rhombi: this defines a *domain exchange* dynamical system on the hexagon. Then, we add pieces to the hexagon and define a new domain exchange so that the first return map from the new shape to the hexagon is described by the substitution; then the process is iterated infinitely often. This idea is formalized by homology-like objects in [**25, 114**], and produces Rauzy fractals.

From Rauzy's seminal paper [**110**], generalizations of the construction have been proposed in different contexts: starting from the investigation of irreducible Pisot units [**25, 49, 96, 97**], reducible Pisot units and beta-numeration [**5, 7, 123**], the case of non-unit Pisot numbers [**39, 118**] and the hyperbolic case with two expanding directions [**24**] have been explored so far.

1.2.2. Using a Rauzy fractal and its topological properties. The large literature dedicated to the Rauzy fractal and its extensions is motivated by the fact that it is useful in many of the domains mentioned in the first section. The main reason for this intensive use is that in each case, the iterative procedure to generate infinite words with the help of a substitution is geometrically shifted into self-similarity properties that can be studied. Then, the main questions to be investigated in each domain can be interpreted as a question related to the topology of the central tile and its tiling properties.

- In number theory, diophantine properties are induced by properties of a distance function to a specific broken line [**72**] related to the Rauzy fractal and the size of the largest ball contained in it. Properties of digits in numeration systems with non-integer basis are related to the fact that $\mathbf{0}$ is an inner point of the Rauzy fractal or not [**14**]. Rauzy fractals also characterize purely periodic orbits in non-integer basis, as a generalization of Galois theorem [**77**].

- The Rauzy fractal allows to explicitly build the largest spectral factor induced by a substitutive dynamical system. Explicit Markov partitions for hyperbolic automorphisms of tori are constructed for instance in [**75, 105**], actually using this piece. Connectivity properties of Rauzy fractals are linked to the generator properties of the Markov partition [**3**].
- In tiling theory, the Rauzy fractal is used to represent the tiling flow; then substitutive systems are proved to be expanding foliations of the space tiling [**26**].
- In theoretical physics, the Rauzy fractal appears as an explicit model set [**38**].
- In discrete geometry, there are numerous relations between generalized Rauzy fractals and discrete planes as studied for instance in [**23**]. The shape of pieces generating a discrete plane is widely related to the shape of the Rauzy fractal.

For all these reasons, a thorough study of the topological properties of Rauzy fractals is of great importance. There are several results scattered in literature. For instance, it is known that the Tribonacci Rauzy fractal has a nice topological behavior ($\mathbf{0}$ is an inner point of $\mathcal{T}$ and $\mathcal{T}$ is homeomorphic to a closed disk [**97**]) but totally different things can appear for other Rauzy fractals: they might be not connected or not simply connected, and $\mathbf{0}$ is not always an inner point of the central tile; see for instance the examples given in [**7**]. Some Rauzy fractals seem not to be homeomorphic to a disk. We will review the different contributions to the topological properties of Rauzy fractal that appear in the literature in the next section and in Chapter 4. However, we have to notice that they are incomplete and often based on examples. Therefore, the main aim of the present paper is to investigate a variety topological properties of Rauzy fractals associated to unit Pisot substitutions in a thorough and systematic way.

1.3. Topological properties of central tiles

We intend to give a thorough systematic study of the topology of central tiles associated to unit Pisot substitutions. In particular, we emphasize on algorithmic criteria for various topological properties.

The monograph starts with two chapters containing a detailed explanation of substitutions, central tiles and the tilings induced by these tiles. These sections are also intended as a survey of basic results related to the geometry of unit Pisot substitutions.

After that, in Chapter 4 we give the statements of the main theorems of the present paper. Among other things we deal with the following properties:

- We give a criterion that decides whether a given tile induces a tiling. A criterion already exists in terms of *super-coincidences* [**26, 61, 78**]. Our criterion has two advantages compared to the previously known ones: firstly, it can be applied to lattice tilings in the reducible case, which was not the case for the other criterions. Secondly, our criterion is an algorithmic necessary and sufficient condition, while the procedure for checking super-coincidences does not terminate when the condition is not satisfied.
- We calculate the box counting dimension of the fractal boundary of the central tile and its subtiles. (Examples of such calculations appeared in [**64, 74, 97, 124**].) In some cases we are even able to give a formula for the Hausdorff dimension.
- We show that the fact that the origin is an inner point of the central tile is equivalent to a finiteness property of the underlying numeration system (Dumont-Thomas numeration [**58**]). This was already known in the beta-numeration context [**7**]. We give a general geometrical proof for this result.
- We give a simple criterion to decide whether the central tile and its subtiles are connected, pursuing the work initiated in [**48, 110**].
- We give criteria for the central tile and its subtiles to be homeomorphic to a closed disk. (Examples for disklikeness previously appeared in [**90, 97, 98**]; in our general approach we use different methods to derive our results.) To this matter we establish a general criterion for a solution of a graph directed iterated function system to be a simple closed curve. This can be applied to the boundary of the subtiles of a central

tile. A similar approach as the one we are going to employ has been used in order to prove the homeomorphy to a disk of a class of solutions of iterated function systems associated to number systems in the ring of Gaussian integers (see [**94**]). However, in our situation there is no possibility to conclude from the connectivity of the interior of a tile to its homeomorphy to a disk like it can be done in the case of iterated function systems (see [**92**]). We have to use several theorems from plane topology to gain our results.

- We give algorithms that can be used to show that the fundamental group of the subtiles of the central tile has certain properties. By doing so, we exhibit examples of fundamental groups that are not free and non-numerable, as the Sierpiński gasket can be.

The underlying idea in all criterions is to match the structure of the graph directed iterated function system that defines the central tile with its tiling properties. All criterions make use and are expressed in terms of graphs.

These graphs are introduced in Chapter 5. Some of them contain the structure of intersections of two or more tiles in the tilings induced by the central tile and its subtiles. Among other informations, they give a description of $\partial\mathcal{T}$ and $\partial\mathcal{T}(i)$ $(1 \leq i \leq n)$ and even permit to draw these boundaries in an easy way. Other graphs defined in this chapter encode the connectivity of the central tile, its subtiles as well as of certain pieces of their boundary. Summing up, apart from checking the topological properties listed above these graphs are very useful in order to study several properties of $\mathcal{T}$, its subtiles and of the tilings induced by them. This is illustrated by many examples scattered throughout this chapter. In particular, the last section contains a detailed example for the use of the criterion for the homeomorphy of $\mathcal{T}(i)$ to a closed disk.

Chapter 6 contains the proofs of our results. Especially Section 6.5 of this chapter deserves special attention. It contains the proof of the criteria for checking whether $\mathcal{T}$ as well as $\mathcal{T}(i)$ is homeomorphic to a closed disk. In proving these criteria we set up a general theory that admits to decide the disklikeness question for arbitrary graph directed self-affine sets. The proofs contained in this chapter make use of general properties of substitutions and central tiles which are reviewed in Chapters 2 and 3, of the graphs defined in Chapter 5 as well as of several results from plane topology. The last section contains the exact statement of our results on the fundamental group of $\mathcal{T}$ and $\mathcal{T}(i)$ as well as detailed examples illustrating their application to concrete substitutions.

Chapter 7 contains perspectives for further research. We are confident that the methods contained in this monograph have high potential to be of use in several branches of mathematics. In this chapter we discuss this in more detail and mention the influence of our results to the topology of fractal sets, to number theory (generalized radix representations and continued fractions), as well as to dynamical systems induced by substitutions.

The Appendix contains all the technical proofs we require and gives the details on those graphs which recognize the points in the tilings in which four different tiles meet.

Acknowledgements: The authors wish to thank P. Arnoux, V. Berthé, A. Hilion, B. Loridant and M. Lustig, for many fruitful discussions, especially to exhibit the applications provided in Chapter 7 which contains further perspectives of research on the topic of the present monograph.

CHAPTER 2

Substitutions, central tiles and beta-numeration

In the present chapter we want to recall the definition and basic properties of the main objects of our study. In the first section we will dwell upon *substitutions*. Then we will survey basic facts of the *tiles* associated to substitutions. Moreover, we shall discuss how these tiles can be represented by a so-called *graph directed iterated function system*. The chapter closes with a description of the relations between substitutions and *beta-numeration*.

2.1. Substitutions

2.1.1. General setting. Let $\mathcal{A} := \{1, \dots, n\}$ be a finite set called *alphabet* whose elements are called *letters*. The *free monoid* $\mathcal{A}^*$ on the alphabet $\mathcal{A}$ with empty word ε is defined as the set of finite words on the alphabet $\mathcal{A}$, that is, $\mathcal{A}^* := \{\varepsilon\} \cup \bigcup_{k\in\mathbb{N}} \mathcal{A}^k$, endowed with the concatenation map. We denote by $\mathcal{A}^{\mathbb{N}}$ and $\mathcal{A}^{\mathbb{Z}}$ the set of one- and two-sided sequences on $\mathcal{A}$, respectively. The topology of $\mathcal{A}^{\mathbb{N}}$ and $\mathcal{A}^{\mathbb{Z}}$ is the product topology of the discrete topology on each copy of $\mathcal{A}$. Both of these spaces are metrizable.

The *length* $|w|$ of a word $w \in \mathcal{A}^*$ is defined as the number of letters it contains. For any letter $a \in \mathcal{A}$, we denote by $|w|_a$ the number of occurrences of a in w. Let $\mathbf{l} : w \in \mathcal{A}^* \mapsto (|w|_a)_{a\in\mathcal{A}} \in \mathbb{N}^n$ be the natural homomorphism obtained by abelianization of the free monoid, called the *abelianization map*.

A *substitution over the alphabet* $\mathcal{A}$ is an endomorphism of the free monoid $\mathcal{A}^*$ such that the image of each letter of $\mathcal{A}$ is nonempty; to avoid trivial cases (projection or permutations of letters), we will always suppose that for at least one letter, say a, the length of the successive iterations $\sigma^k(a)$ tends to infinity. A substitution naturally extends to the set of two-sided sequences $\mathcal{A}^{\mathbb{Z}}$. We associate to every substitution σ its *incidence matrix* $\mathbf{M}$ which is the $n \times n$ matrix obtained by abelianization, that is, $\mathbf{l}(\sigma(w)) = \mathbf{M}\mathbf{l}(w)$ for all $w \in \mathcal{A}^*$.

A two-sided *periodic point* of the substitution σ is an infinite word $u = (u_k)_{k\in\mathbb{Z}} \in \mathcal{A}^{\mathbb{Z}}$ that satisfies $\sigma^\nu(u) = u$ for some $\nu > 0$, and furthermore its central pair of letters $u_{-1}u_0$ belongs to the image of some letter by σ^ℓ for some $\ell \in \mathbb{N}$. All substitutions admit periodic points (see [**108**, Proposition V.1]).

2.1.2. Pisot substitutions. An important property of a substitution is that of *primitivity*: a substitution σ is *primitive* if there exists an integer k (independent of the letters) such that, for each pair $(a, b) \in \mathcal{A}^2$, the word $\sigma^k(a)$ contains at least one occurrence of the letter b.

By the definition of primitivity, the incidence matrix of a primitive substitution is a primitive matrix, so that it has a simple real positive dominant eigenvalue β (Perron-Frobenius Theorem).

- A substitution σ is said to be *Pisot* if the dominant eigenvalue is a *Pisot number*[2.1].
- A substitution σ is said to be *unit* if its dominant eigenvalue is a unit.
- A substitution σ is said to be *irreducible* if the algebraic degree of the dominant eigenvalue is equal to the size of the alphabet.

Note that there exist substitutions whose largest eigenvalue is Pisot but whose incidence matrix has eigenvalues that are not conjugate to the dominant eigenvalue. Examples are $1 \to 12$,

[2.1] Recall that a Pisot number is an algebraic integer $\beta > 1$ such that each Galois conjugate $\beta^{(i)}$ of β satisfies $|\beta^{(i)}| < 1$.

$2 \to 3$, $3 \to 4$, $4 \to 5$, $5 \to 1$ and the Morse substitution $1 \to 12$, $2 \to 21$ (the characteristic polynomial is not irreducible). Such substitutions are not irreducible and they are called *reducible*.

2.2. The central tile associated to a unit Pisot substitution

We now want to give a geometric interpretation of a periodic point u of a unit Pisot substitution. We first need to introduce some algebraic formalism in order to embed u in a hyperplane spanned by the algebraic conjugates of the dominant eigenvalue of the incidence matrix; the closure of the "projections" of the prefixes of u will comprise the so-called *central tile* or *Rauzy fractal*.

In all that follows, we suppose that σ is a primitive unit Pisot substitution.

2.2.1. A broken line associated to a Pisot substitution. Let u be a two-sided periodic point of σ. The bi-infinite word u is embedded as a discrete line in $\mathbb{R}^n$ by replacing each letter of u by the corresponding vector in the canonical basis $(\mathbf{e}_1, \dots, \mathbf{e}_n)$ in $\mathbb{R}^n$. More precisely, the *discrete line* has vertices $\{\mathbf{l}(u_0 \dots u_{N-1});\ N \in \mathbb{N}\}$.

2.2.2. A suitable decomposition of the space. We now need to introduce a suitable decomposition of $\mathbb{R}^n$ with respect to eigenspaces of the incidence matrix $\mathbf{M}$ associated to the dominant eigenvalue β. We denote by d the algebraic degree of β; one has $d \leq n$, since the characteristic polynomial of $\mathbf{M}$ may be reducible.

Let $r-1$ denote the number of real conjugates of β; they are denoted by $\beta^{(2)}$, $\dots$, $\beta^{(r)}$. Each corresponding eigenspace has dimension one according to the assumption of primitivity. Let $2s$ denote the number of complex conjugates of β. They are denoted by $\beta^{(r+1)}$, $\overline{\beta^{(r+1)}}$, $\dots$, $\beta^{(r+s)}$, $\overline{\beta^{(r+s)}}$. Each pair of an eigenvector together with its complex conjugate generates a 2-dimensional plane.

Let $\mathbf{v}_\beta$ be the dominant eigenvector of ${}^t\mathbf{M}$ such that $\langle \mathbf{v}_\beta, \mathbf{e}_1 \rangle = 1$ and $\mathbf{u}_\beta$ be the unique dominant eigenvector of $\mathbf{M}$ such that $\langle \mathbf{v}_\beta, \mathbf{u}_\beta \rangle = 1$ (this normalization is needed to recover beta-numeration in specific examples; see Section 2.5). Both vectors have coordinates in $\mathbb{Q}[\beta]$. Moreover, since $\mathbf{u}_\beta$ is the dominant eigenvector of a primitive matrix, each of the entries of $\mathbf{u}_\beta$ has the same sign. The same is true for $\mathbf{v}_\beta$. We obtain eigenvectors $\mathbf{u}_{\beta^{(i)}}$ and $\mathbf{v}_{\beta^{(i)}}$ for the algebraic conjugates $\beta^{(i)}$ of β by replacing β by $\beta^{(i)}$ in the coordinates of the vectors. By construction, these vectors satisfy $\langle \mathbf{v}_{\beta^{(i)}}, \mathbf{u}_{\beta^{(k)}} \rangle = 0$ if $i \neq k$ and $\langle \mathbf{v}_{\beta^{(i)}}, \mathbf{u}_{\beta^{(k)}} \rangle = 1$ if $i = k$ (*cf.* [**49**, Section 2] for details and note that we identify $\mathbb{R}^2$ with $\mathbb{C}$).

From these vectors we introduce a decomposition of $\mathbb{R}^n$ as follows.

- The *beta-contracting space* of the matrix $\mathbf{M}$ is the subspace $\mathbb{H}_c$ generated by the eigenspaces associated to the beta-conjugates, that is $\mathbf{u}_{\beta^{(2)}}$, $\dots$, $\mathbf{u}_{\beta^{(r)}}$, $\Re(\mathbf{u}_{\beta^{(r+1)}})$, $\Im(\mathbf{u}_{\beta^{(r+1)}})$, $\dots$, $\Re(\mathbf{u}_{\beta^{(r+s)}})$, $\Im(\mathbf{u}_{\beta^{(r+s)}})$. It has dimension $r + 2s - 1 = d - 1$.
  We denote by $\mathbf{h} :\ \mathbb{H}_c \to \mathbb{H}_c$ the restriction of $\mathbf{M}$ to $\mathbb{H}_c$; it is a contraction whose eigenvalues are the conjugates of β. We define a suitable norm on $\mathbb{H}_c$ by

$$\forall \mathbf{x} \in \mathbb{H}_c, \quad ||\mathbf{x}|| = \max\{|\langle \mathbf{x}, \mathbf{v}_{\beta^{(i)}} \rangle|;\ i = 2, \dots, r+s\}. \tag{2.1}$$

  This implies that

$$\forall \mathbf{x} \in \mathbb{H}_c, \quad ||\mathbf{M}\mathbf{x}|| = ||\mathbf{h}\mathbf{x}|| \leq \max\{|\beta^{(i)}|;\ i = 2, \dots, r+s\}||\mathbf{x}||. \tag{2.2}$$

- We denote by $\mathbb{H}_e$ the *beta-expanding line* of $\mathbf{M}$, *i.e.*, the real line generated by the beta-eigenvector $\mathbf{u}_\beta$.
- Let Min_β be the minimal polynomial of β. The *beta-supplementary space* is defined to be $\mathbb{H}_s = \mathrm{Min}_\beta(\mathbf{M}(\mathbb{R}^n))$. One checks that it is an invariant space of $\mathbf{M}$ that satisfies $\mathbb{R}^n = \mathbb{H}_c \oplus \mathbb{H}_e \oplus \mathbb{H}_s$. The space $\mathbb{H}_s$ is generated by the eigenspaces corresponding to the eigenvalues of $\mathbf{M}$ that are not conjugate to β. It is trivial if and only if the substitution is irreducible.

From the definition of $\mathbb{H}_s$ and the fact that $\mathbf{v}_\beta$ belongs to the kernel of $\mathrm{Min}_\beta({}^t\mathbf{M})$, we deduce that the space $\mathbb{H}_s$ is orthogonal to $\mathbf{v}_\beta$ (see [**61**, Lemma 2.5] and [**26**]), indeed

$$\langle \mathbf{v}_\beta, \mathbb{H}_s\rangle = \langle \mathbf{v}_\beta, \mathrm{Min}_\beta(\mathbf{M}(\mathbb{R}^n))\rangle = \langle \mathrm{Min}_\beta({}^t\mathbf{M})\mathbf{v}_\beta, \mathbb{R}^n\rangle = 0.$$

Let $\pi : \mathbb{R}^n \to \mathbb{H}_c$ be the projection onto $\mathbb{H}_c$ along $\mathbb{H}_e \oplus \mathbb{H}_s$, according to the natural decomposition $\mathbb{R}^n = \mathbb{H}_c \oplus \mathbb{H}_e \oplus \mathbb{H}_s$. Then, the relation $\mathbf{l}(\sigma(w)) = \mathbf{M}\mathbf{l}(w)$, for all $w \in \mathcal{A}^*$ implies the commutation relation

$$\forall w \in \mathcal{A}^*,\ \pi(\mathbf{l}(\sigma(w))) = \mathbf{h}\pi(\mathbf{l}(w)). \tag{2.3}$$

By considering the orthogonality between the vectors $\mathbf{v}_{\beta^{(i)}}$ and the vectors $\mathbf{u}_{\beta^{(j)}}$, we obtain the following representation of π in the eigenvectors basis

$$\forall \mathbf{x} \in \mathbb{R}^n, \qquad \pi(\mathbf{x}) = \sum_{2\le i\le r+2s} \langle \mathbf{x}, \mathbf{v}_{\beta^{(i)}}\rangle \mathbf{u}_{\beta^{(i)}}. \tag{2.4}$$

(Again we identified $\mathbb{R}^2$ with $\mathbb{C}$.)

For vectors with rational coordinates, the following relation follows by considering Galois conjugates of (2.4).

$$\forall \mathbf{x}, \mathbf{y} \in \mathbb{Q}^n, \qquad \pi(\mathbf{x}) = \pi(\mathbf{y}) \iff \langle \mathbf{x}, \mathbf{v}_\beta\rangle = \langle \mathbf{y}, \mathbf{v}_\beta\rangle. \tag{2.5}$$

Concretely, this equation means that as soon as two points with rational coordinates coincide in the beta-contracting space, they also coincide along the beta-expanding line. We will often use this property in the following.

2.2.3. Definition of the central tile. In the irreducible case it is well known that the Pisot assumption implies that the discrete line of σ remains at a bounded distance of the expanding direction of the incidence matrix (see [**25**]). In the reducible case, the discrete line may have other expanding directions, but (2.4) implies that the projection of the discrete line by π still provides a bounded set in $\mathbb{H}_c \simeq \mathbb{R}^{d-1}$ (see details in [**61**, Section 3.2]).

Definition 2.1 (Central tile / Rauzy fractal). Let σ be a primitive unit Pisot substitution with dominant eigenvalue β. The *central tile* (or *Rauzy fractal*) of σ is the projection on the beta-contracting plane of the discrete line associated to any periodic point $u = (u_k)_{k\in\mathbb{Z}}$ of σ, *i.e.*,

$$\mathcal{T} := \overline{\{\pi(\mathbf{l}(u_0 \dots u_{k-1}));\ k \in \mathbb{N}\}}.$$

Subtiles of the central tile $\mathcal{T}$ are naturally defined, depending on the letter associated to the vertex of the discrete line that is projected. One thus sets for $i \in \mathcal{A}$

$$\mathcal{T}(i) := \overline{\{\pi\left(\mathbf{l}(u_0 \dots u_{k-1})\right);\ k \in \mathbb{N},\ u_k = i\}}.$$

Remark 2.2. It follows from the primitivity of the substitution σ that the definition of $\mathcal{T}$ and $\mathcal{T}(i)$ ($i \in \mathcal{A}$) does not depend on the choice of the periodic point u (see *e.g.* [**25, 49, 108**]).

By definition, the central tile $\mathcal{T}$ consists of the finite union of its subtiles, *i.e.*,

$$\mathcal{T} = \bigcup_{i\in\mathcal{A}} \mathcal{T}(i).$$

Examples of central tiles and their subtiles are discussed in Section 2.4.

2.3. Central tiles viewed as graph directed iterated function systems

The tiles $\mathcal{T}(i)$ ($i \in \mathcal{A}$) can be written as a so-called *graph directed iterated function system*, GIFS for short. For the convenience of the reader we recall the definition of GIFS (*cf.* [**95**] for a variant of our definition).

Definition 2.3 (GIFS). Let G be a finite directed graph with set of vertices $\{1, \dots, q\}$ and set of edges E. Denote the set of edges leading from i to j by E_{ij}. To each $e \in E$ associate a contractive mapping $\tau_e : \mathbb{R}^n \to \mathbb{R}^n$. If for each i there is some outgoing edge we call $(G, \{\tau_e\}_{e\in E})$ a GIFS.

DEFINITION 2.4 (Open set condition). If there exist nonempty open sets $J_1, \ldots, J_q$ such that $\{\tau_e(J_j)\ ;\ e \in E_{ij}\}$ is a disjoint family for each fixed i and

$$J_i \supseteq \bigcup_{e\in E_{ij}} \tau_e(J_j) \qquad (i \in \{1, \ldots, q\})$$

we say that the GIFS satisfies the *generalized open set condition*.

It can be shown by a fixed point argument that to a GIFS $(G, \{\tau_e\}_{e\in E})$ there corresponds a unique collection of nonempty compact sets $K_1, \ldots, K_q \subset \mathbb{R}^n$ having the property that

$$K_i = \bigcup_{e\in E_{ij}} \tau_e(K_j).$$

The sets K_i are called *GIFS attractors* or *solutions of the GIFS*.

The graph we are going to define now will permit us to view the subtiles $\mathcal{T}(i)$ $(i \in \mathcal{A})$ as solution of a GIFS. The corresponding result is stated immediately after the definition.

DEFINITION 2.5 (Prefix-suffix graph). Let σ be a substitution over the alphabet $\mathcal{A}$ and let $\mathcal{P}$ be the finite set

$$\mathcal{P} := \{(p, a, s) \in \mathcal{A}^* \times \mathcal{A} \times \mathcal{A}^*;\ \exists\, b \in \mathcal{A},\, \sigma(b) = pas\}.$$

We call *prefix-suffix graph of* σ the graph Γ_σ with nodes in $\mathcal{A}$ and such that there is an edge labelled by $(p, a, s) \in \mathcal{P}$ from a towards b if $pas = \sigma(b)$.

THEOREM 2.6. *Let σ be a primitive unit Pisot substitution over the alphabet $\mathcal{A}$. Let d be the degree of its dominant eigenvalue. The central tile $\mathcal{T}$ is a compact subset of $\mathbb{R}^{d-1}$ with nonempty interior. Each subtile is the closure of its interior. The subtiles of $\mathcal{T}$ are solutions of the GIFS*

$$\forall i \in \mathcal{A},\ \mathcal{T}(i) = \bigcup_{\substack{j\in\mathcal{A},\\ i\xrightarrow{(p,i,s)}j}} \mathbf{h}\mathcal{T}(j) + \pi\mathbf{l}(p). \tag{2.6}$$

Here the union is extended over all edges in the prefix-suffix graph of σ leading away from the vertex i.

PROOF. In the irreducible case, the fact that $\mathcal{T}$ is compact with nonempty interior is proved in [**120**] and the GIFS equation is contained in [**38**, Theorem 2]. The generalization to the reducible case is given in [**26, 61**]. Let S be the shift operator on $\mathcal{A}^{\mathbb{Z}}$ and let u be a periodic point of the substitution σ. Denote by $\overline{\mathcal{O}}$ the closure of the orbit of u under S. The GIFS structure (2.6) comes from the decomposition of every two-sided sequence $w \in \overline{\mathcal{O}}$. In particular, $w = S^\nu(\sigma(v))$, with $v \in \overline{\mathcal{O}}$ and $0 \le \nu < |\sigma(v_0)|$, where v_0 is the 0^{th} coordinate of v. For more details see the survey [**38**]. □

We use the GIFS equation to expand every point of the central tile.

COROLLARY 2.7. *Let σ be a primitive unit Pisot substitution over the alphabet $\mathcal{A}$. A point $\gamma \in \mathbb{H}_c$ belongs to the subtile $\mathcal{T}(i)$ $(i \in \mathcal{A})$ if and only if there exists a walk $(p_k, i_k, s_k)_{k\ge0}$ starting at $i = i_0$ in the prefix-suffix graph such that*

$$\gamma = \sum_{k\ge0} \mathbf{h}^k \pi\mathbf{l}(p_k). \tag{2.7}$$

The sequence $(p_k, i_k, s_k)_{k\ge0}$ is called a **h**-ary representation *of γ.*

In what follows the letter γ will always be used to refer to points on the contractive space $\mathbb{H}_c$.

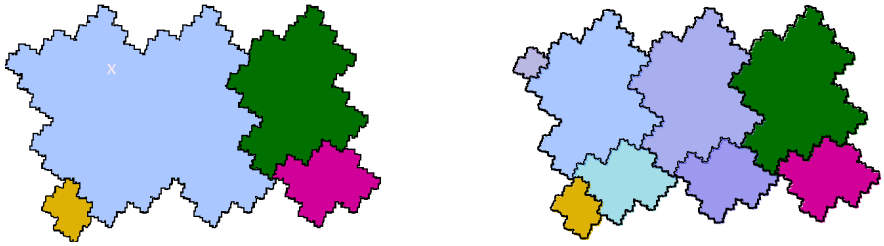

FIGURE 2.1. The central tile $\mathcal{T}$ of σ_0. On the left hand side the decomposition $\mathcal{T} = \mathcal{T}(1) \cup \mathcal{T}(2) \cup \mathcal{T}(3) \cup \mathcal{T}(4)$ is shown. On the right hand side the GIFS decomposition of each subtile is illustrated. The white cross "X" indicates the position of the origin $\mathbf{0}$.

PROOF. Suppose that $\gamma \in \mathcal{T}(i)$. Then the GIFS equation allows to express γ as $\gamma = \mathbf{h}\gamma_1 + \pi\mathbf{l}(p_0)$ where $\gamma_1 \in \mathcal{T}(i_1)$ and $\sigma(i_1) = p_0 i s_0$. By iterating this we get $\gamma = \pi\mathbf{l}(p_0) + \cdots + \mathbf{h}^k\pi\mathbf{l}(p_k) + \mathbf{h}^k\gamma_k$. Since γ_k is bounded and $\mathbf{h}$ is contracting, the power series is convergent and $\gamma = \sum_{k\geq 0} \mathbf{h}^k\pi\mathbf{l}(p_k)$. □

2.3.1. Disjointness of the subtiles of the central tile. To ensure that the subtiles are disjoint, we introduce the following combinatorial condition on substitutions.

DEFINITION 2.8 (Strong coincidence condition). A substitution σ over the alphabet $\mathcal{A}$ satisfies the *strong coincidence condition* if for every pair $(b_1, b_2) \in \mathcal{A}^2$, there exists $k \in \mathbb{N}$ and $a \in \mathcal{A}$ such that $\sigma^k(b_1) = p_1 a s_1$ and $\sigma^k(b_2) = p_2 a s_2$ with $\mathbf{l}(p_1) = \mathbf{l}(p_2)$ or $\mathbf{l}(s_1) = \mathbf{l}(s_2)$, where $\mathbf{l}$ denotes the abelianization map.

The strong coincidence condition is satisfied by every unit Pisot substitution over a two-letter alphabet [**29**]. It is conjectured that every substitution of Pisot type satisfies the strong coincidence condition.

THEOREM 2.9. *Let σ be a primitive unit Pisot substitution. If σ satisfies the strong coincidence condition, then the subtiles of the central tile have disjoint interiors and the GIFS* (2.6) *satisfies the generalized open set condition.*

PROOF. The proof for the disjointness is given in [**25**] for the irreducible case and generalized to the reducible case in [**38, 61**]. The generalized open set condition is easily seen to be satisfied by the interiors of the sets $\mathcal{T}(i)$ $(i \in \mathcal{A})$. □

2.4. Examples of central tiles and their subtiles

We now want to give some examples of unit Pisot substitutions and their associated central tiles. Moreover, we will state the topological properties of their central tiles here. All these properties will be proved in the present monograph. Indeed, the examples given here will be used frequently throughout the monograph in order to illustrate our results.

σ_0: This substitution is our *main example*. It is defined by

$$\sigma_0(1) = 112, \quad \sigma_0(2) = 113, \quad \sigma_0(3) = 4, \quad \sigma_0(4) = 1.$$

σ_0 is a reducible primitive unit Pisot substitution whose dominant eigenvalue β has degree 3 and satisfies $\beta^3 - 3\beta^2 + \beta - 1 = 0$. Its subtiles $\mathcal{T}(1), \mathcal{T}(2), \mathcal{T}(3), \mathcal{T}(4)$ are shown on the left hand side of Figure 2.1. The GIFS decomposition of these subtiles is given on the right hand side of Figure 2.1. According to (2.6) the largest subtile $\mathcal{T}(1)$ can be decomposed into five pieces, namely two copies $\mathbf{h}\mathcal{T}(1)$ of the largest tile, two copies $\mathbf{h}\mathcal{T}(2)$ of the second largest tile, and a copy $\mathbf{h}\mathcal{T}(4)$ of the smallest tile. This corresponds to the equation $\mathcal{T}(1) = \mathbf{h}\mathcal{T}(1) \cup (\mathbf{h}\mathcal{T}(1) + \pi(e_1)) \cup \mathbf{h}\mathcal{T}(2) \cup (\mathbf{h}\mathcal{T}(2) + \pi(e_1)) \cup \mathbf{h}\mathcal{T}(4)$. Similar decompositions are obtained for the other subtiles: the second largest

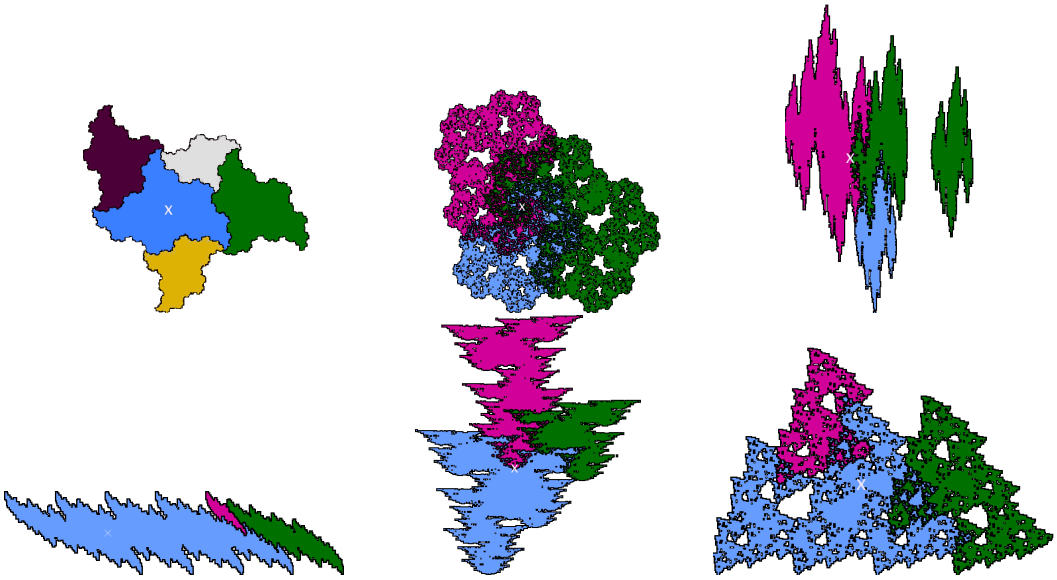

FIGURE 2.2. In the first line (from left to right) the central tiles of the substitutions σ_1, σ_2 and σ_3 can be seen. The second line (also from left to right) contains the central tiles of σ_4, σ_5 and σ_6. In all these central tiles the decomposition in subtiles is indicated by different colors. The white cross "X" indicates the position of the origin $\mathbf{0}$.

tile $\mathcal{T}(2)$ actually is a copy of the largest tile: $\mathcal{T}(2) = \mathbf{h}(\mathcal{T}(1) + 2\pi(e_1))$. The third largest tile $\mathcal{T}(3)$ can be seen as a copy of the second one: $\mathcal{T}(3) = \mathbf{h}(\mathcal{T}(2) + 2\pi(e_1))$. Finally, the smallest tile $\mathcal{T}(4)$ is a copy of the third subtile with the same ratio: $\mathcal{T}(4) = \mathbf{h}(\mathcal{T}(3))$.

Notice that $\mathbf{h}$ includes a rotation of about (but not exactly) $\frac{\pi}{2}$, hence, each subtile $\mathbf{h}\mathcal{T}(i)$ appears with a rotation in the decomposition of $\mathcal{T}(i)$. We will prove that this central tile as well as each of its subtiles is homeomorphic to a closed disk. Moreover, $\mathbf{0}$ is an inner point of $\mathcal{T}(1)$.

σ_1: This substitution is defined by $\sigma_1(1) = 12$, $\sigma_1(2) = 3$, $\sigma_1(3) = 4$, $\sigma_1(4) = 5$, $\sigma_1(5) = 1$. It is reducible and its dominant eigenvalue β satisfies $\beta^3 = \beta - 1$. The central tile as well as each of its subtiles $\mathcal{T}(1), \ldots, \mathcal{T}(5)$ is homeomorphic to a closed disk which has also been proved in Luo [**90**] (see Figure 2.2 for a picture of $\mathcal{T}$ and its subtiles). Moreover, $\mathbf{0}$ is an inner point of $\mathcal{T}$.

σ_2: This substitution is defined by $\sigma_2(1) = 2$, $\sigma_2(2) = 3$, $\sigma_2(3) = 12$. It is irreducible and its dominant eigenvalue satisfies the same equation as the one for σ_1. $\mathcal{T}$ as well as $\mathcal{T}(i)$ $(i = 1, 2, 3)$ are connected and have uncountable fundamental group. $\mathbf{0}$ lies on the boundary of $\mathcal{T}$ (see Figure 2.2).

σ_3: This substitution is defined by $\sigma_3(1) = 3$, $\sigma_3(2) = 23$, $\sigma_3(3) = 31223$. It is disconnected and $\mathbf{0}$ does not lie in the interior of $\mathcal{T}$ (see Figure 2.2).

σ_4: This substitution is defined by $\sigma_4(1) = 11112$, $\sigma_4(2) = 11113$, $\sigma_4(3) = 1$. It is irreducible and its central tile $\mathcal{T}$ has uncountable fundamental group. $\mathbf{0}$ is contained in its interior (see Figure 2.2).

σ_5: This substitution is defined by $\sigma_5(1) = 123$, $\sigma_5(2) = 1$, $\sigma_5(3) = 31$. It is irreducible and its central tile has uncountable fundamental group (see Figure 2.2). Moreover, $\mathbf{0}$ is not an inner point of the central tile.

σ_6: This substitution is defined by $\sigma_6(1) = 12$, $\sigma_6(2) = 31$, $\sigma_6(3) = 1$. It is irreducible and its central tile has uncountable fundamental group (see Figure 2.2).

2.5. Recovering beta-numeration from unit Pisot substitutions

Let $\beta > 1$ be a real number. The (Renyi) *beta-expansion* of a real number $x \in [0,1]$ is defined as the sequence $(a_i)_{i\geq 1}$ over the alphabet $\mathcal{A}_\beta := \{0,1,\dots,\lceil\beta\rceil - 1\}$ produced by the beta-transformation $T_\beta : \ x \mapsto \beta x \pmod 1$ with a greedy procedure, *i.e.*, such that $\forall i \geq 1,\ a_i = \lfloor \beta T_\beta^{i-1}(x)\rfloor$, and $x = \sum_{i\geq 1} a_i \beta^{-i}$ (see [**104**]).

We denote the beta-expansion of 1 by $d_\beta(1) = (t_i)_{i\geq 1}$. When $d_\beta(1)$ is finite with length m, an infinite expansion of 1 is given by $d^*_\beta(1) = (t_1 \dots t_{m-1}(t_m - 1))^\infty$; let us stress the fact that this infinite expansion cannot be obtained by a greedy algorithm. If $d_\beta(1)$ is infinite we define $d^*_\beta(1) = d_\beta(1)$. In the Pisot case, $d^*_\beta(1)$ is ultimately periodic and every element in $\mathbb{Q}(\beta)\cap[0,1]$ has eventually periodic beta-expansion according to [**40, 116**]. Then, beta-expansions of real numbers in $[0,1)$ are completely characterized by $d^*_\beta(1)$: a sequence $w_1 \dots w_k \dots \in \mathcal{A}_\beta^{\mathbb{N}}$ is the beta-expansion of a real number if and only if all truncations $w_{k_0} \dots w_k \dots$ are strictly smaller than $d^*_\beta(1)$ in the lexicographical order [**43, 104**].

We define the set of integers in base β as the set of positive real numbers with no fractional part in their beta-expansion:

$$\mathrm{Int}(\beta) = \left\{ z = \sum_{0\leq i\leq K} a_i\beta^i \in \mathbb{Z}[\beta];\ a_K \dots a_0 \begin{array}{l}\text{are produced by the}\\ \text{beta-transformation applied on } \beta^{-K-1}z\end{array} \right\}.$$

The set $\mathrm{Int}(\beta)$ is a discrete subset of $\mathbb{R}_+$. It has some regularity: two consecutive points in $\mathrm{Int}(\beta)$ can differ only by a finite number of values, namely, the positive numbers $T_\beta^{a-1}(1)$, $a \in \{1,\dots,n\}$ (see [**8, 123**]).

To understand the structure of $\mathrm{Int}(\beta)$, Thurston [**123**] defined a compact representation φ of $\mathrm{Int}(\beta)$ by

$$\begin{array}{rccl} \varphi: & \mathrm{Int} & \to & \mathbb{R}^{r-1}\times\mathbb{C}^s \\ & x & \mapsto & (x^{(2)},\dots,x^{(r+s)}). \end{array}$$

Here $x^{(i)}$ $(i = 2,\dots,r+s)$ are the Galois conjugates of x.

The closure of $\mathrm{Im}\,\varphi$ is denoted by $\widetilde{\mathcal{T}} := \overline{\varphi(\mathrm{Int}(\beta))}$. In this paragraph, this tile will be called the *beta-numeration tile*.

A natural partition of $\mathrm{Int}(\beta)$ is given by the distance between a point and its successor in $\mathrm{Int}(\beta)$. Concretely, this can be done as follows:

- for $i \in \{2,\dots,n\}$, we define $\widetilde{\mathcal{T}^{(i)}}$ as the closure of the representation of points $z = \sum_{0\leq k\leq K} w_k\beta^k \in \mathrm{Int}(\beta)$ such that $w_K \dots w_0$ ends with $t_1 \dots t_{i-1}$, that is: $w_{i-2}\dots w_0 = t_1 \dots t_{n-1}$.
- For $i = 1$, the set $\widetilde{\mathcal{T}^{(1)}}$ is defined as the closure of the representation of points $z = \sum_{0\leq k\leq K} w_k\beta^k \in \mathrm{Int}(\beta)$ such that $w_K \dots w_0$ does not end with any $t_1 \dots t_{j-1}$ for $1 \leq j \leq n$.

We thus obtain a decomposition of the beta-numeration tile $\widetilde{\mathcal{T}}$ into subtiles $\widetilde{\mathcal{T}^{(i)}}$. A precise study of the language generated by the beta-transformation shows that the numeration subtiles satisfy a GIFS equation deduced from the expansion of 1. Indeed, if $d^*_\beta(1) = t_1 \dots t_m(t_{m+1}\dots t_n)^\infty$ (*cf.* [**88, 123**])

$$\left\{ \begin{array}{rcl} \widetilde{\mathcal{T}^{(1)}} & = & \bigcup_{a\in\{1,\dots,n\}} \bigcup_{p<t_a} \left(\varphi(\beta)\widetilde{\mathcal{T}^{(a)}} + \varphi(p)\right) \\ \widetilde{\mathcal{T}^{(m+1)}} & = & \left(\varphi(\beta)\widetilde{\mathcal{T}^{(m)}} + \varphi(t_m)\right) \cup \left(\varphi(\beta)\widetilde{\mathcal{T}^{(n)}} + \varphi(t_n)\right) \\ \widetilde{\mathcal{T}^{(k+1)}} & = & \varphi(\beta)\widetilde{\mathcal{T}^{(k)}} + \varphi(t_k),\ k \in \{1,\dots,n-1\}\setminus\{m\} \end{array} \right. \tag{2.8}$$

(if $m = 0$, *i.e.*, if there is no pre-period then the first part of the union in the second line has to be omitted). In this equation, the notation $\varphi(\beta)\widetilde{\mathcal{T}^{(a)}}$ stands for the multiplication by each conjugate of β on each coordinate, that is defined by $\varphi(\beta)(x_2, \ldots, x_{r+s}) = (\beta^{(2)}x_2, \ldots, \beta^{(r+s)}x_{r+s}) \in \mathbb{R}^{r-1} \times \mathbb{C}^s$.

Now, let us introduce the so called *beta-substitution* over the n-letter alphabet $\mathcal{A} = \mathcal{A}_\beta$, defined as $\sigma(k) = 1^{t_k}(k+1)$ for each $k < n$ and $\sigma(n) = 1^{t_n}(m+1)$ where m stands for the length of the pre-period in $d^*_\beta(1)$ (as mentioned above, m can possibly be equal to 0). One can check easily that β is the largest eigenvalue of this substitution. Its beta-contracting space $\mathbb{H}_c$ is isomorphic to $\mathbb{R}^{r-1} \times \mathbb{C}^s$ (each element of $\mathbb{R}^{r-1} \times \mathbb{C}^s$ corresponds to a coordinate along an eigendirection). Moreover, this isomorphism is a conjugacy between the multiplication by $\varphi(\beta)$ and the contracting map $\mathbf{h}$ on $\mathbb{H}_c$. As a specific example, the isomorphism maps $\varphi(p)$ to $\pi\mathbf{l}(1^p)$ for every $p \in \mathbb{N}$. With this correspondence at hand, one checks that the GIFS in (2.8) is exactly the same as the one in (2.6) satisfied by the central tile of the substitution. By unicity of the solution to an GIFS, we can conclude that beta-numeration tiles as introduced in [**123**] form a special class of central tiles of substitutions (for more details see [**38**]).

CHAPTER 3

Tilings induced by the central tile and its subtiles

One interesting feature of the central tile $\mathcal{T}$ and its subtiles $\mathcal{T}(i)$ ($i \in \mathcal{A}$) is that they can tile the plane in two different ways. Exploiting properties of these tilings will allow us to study the boundary as well as topological properties of $\mathcal{T}$ and $\mathcal{T}(i)$. In the following definition we will make precise what we want to understand by a tiling.

DEFINITION 3.1 ([**81, 83, 109**]). A *multiple tiling* of $\mathbb{H}_c$ by the subtiles $\mathcal{T}(i)$ ($i \in \mathcal{A}$) is given by a *translation set* $\Gamma \subset \mathbb{H}_c \times \mathcal{A}$ such that

(1) $\mathbb{H}_c = \bigcup_{(\gamma,i)\in\Gamma} \mathcal{T}(i) + \gamma$,
(2) each compact subset of $\mathbb{H}_c$ intersects a finite number of tiles,
(3) almost all points in $\mathbb{H}_c$ (w.r.t. the $(d-1)$-dimensional Lebesgue measure) are covered exactly p times for some positive integer p.

When distinct translates of tiles have nonintersecting interiors, *i.e.*, if $p = 1$, then the multiple tiling is a *tiling*.

For subtiles of central tiles, several multiple tilings can be defined. The principle is to project a subset of points of $\mathbb{Z}^n$ on the beta-contracting space $\mathbb{H}_c$. Depending on the properties of this subset, we get different multiple tilings which will be discussed in the subsequent subsections.

3.1. The self-replicating multiple tiling

3.1.1. The self-replicating translation set. A first translation set can be obtained by projecting on the beta-contracting space all the points with integer coordinates that approximate this space. The "discretization" stemming from this approximation corresponds to the notion of an arithmetic space introduced in [**111**]; it consists in approximating the space $\mathbb{H}_c$ by selecting points $\mathbf{x}$ with integral coordinates that are above $\mathbb{H}_c$ and such that the same point shifted down by a canonical base vector $\mathbf{e}_i$, say, is below $\mathbb{H}_c$ [**23**].

DEFINITION 3.2. Let σ be a primitive unit Pisot substitution over the alphabet $\mathcal{A}$. The *self-replicating translation set* is defined as follows.

$$\Gamma_{srs} = \{[\pi(\mathbf{x}), i] \in \pi(\mathbb{Z}^n) \times \mathcal{A}; \quad 0 \le \langle \mathbf{x}, \mathbf{v}_\beta \rangle < \langle \mathbf{e}_i, \mathbf{v}_\beta \rangle\}. \tag{3.1}$$

The pairs $[\pi(\mathbf{x}), i]$ are called *faces*.

REMARK 3.3. In the irreducible case, the term *faces* can be justified as follows. Consider a face $[\gamma, i] \in \Gamma_{srs}$ as defined above. If the substitution is irreducible, the restriction of the mapping π to $\mathbb{Z}^n$ is one-to-one by (2.5). In particular, if we have $[\pi(\mathbf{x}), i], [\pi(\mathbf{y}), i] \in \Gamma_{srs}$ with $\mathbf{x}, \mathbf{y} \in \mathbb{Z}^n$ satisfying $[\pi(\mathbf{x}), i] = [\pi(\mathbf{y}), i]$ then $\mathbf{x} = \mathbf{y}$. Consequently, there exists a unique $\mathbf{x} \in \mathbb{Z}^n$ such that $\gamma = \pi(\mathbf{x})$. Thus we can interpret $[\gamma, i]$ as the set

$$\mathbf{x} + \{\theta_1 e_1 + \cdots + \theta_{i-1} e_{i-1} + \theta_{i+1} e_{i+1} + \cdots + \theta_n e_n \,;\, \theta_j \in [0,1] \text{ for } j \neq i\},$$

which is the face orthogonal to the i-th canonical coordinate in a unit cube located in $\mathbf{x}$. One can show that this set of faces is the discrete approximation of the beta-contracting space $\mathbb{H}_c$ (*cf.* [**23**]). Moreover, the projections of the faces

$$\pi(\mathbf{x}) + \pi(\{\theta_1 e_1 + \cdots + \theta_{i-1} e_{i-1} + \theta_{i+1} e_{i+1} + \cdots + \theta_n e_n) \,;\, \theta_j \in [0,1] \text{ for } j \neq i\}$$

have disjoint interior in $\mathbb{H}_c$ and they provide a polyhedral tiling of $\mathbb{H}_c$.

In the reducible case $\mathbb{H}_c$ is no longer a hyperplane, hence, the notion of discrete approximation by faces of cubes is not well defined in general (for special cases where this is possible even in the reducible case see [**61**]). In this case, the projections of faces do overlap. The restriction of the mapping π to $\mathbb{Z}^n$ is not one-to-one. Nevertheless, if $[\pi(\mathbf{x}), i], [\pi(\mathbf{y}), i] \in \Gamma_{srs}$ with $\mathbf{x}, \mathbf{y} \in \mathbb{Z}^n$ satisfy $[\pi(\mathbf{x}), i] = [\pi(\mathbf{y}), i]$ then $\langle \mathbf{x}, \mathbf{v}_\beta \rangle = \langle \mathbf{y}, \mathbf{v}_\beta \rangle$ so that $\mathbf{y} - \mathbf{x} \in \mathbb{H}_s$.

3.1.2. The dual substitution rule and the geometric property (F). The set Γ_{srs} is named *self-replicating* since it is stabilized by an inflation action on $\pi(\mathbb{Z}^n) \times \mathcal{A}$, obtained as the dual of the one-dimensional realization of σ. This dual is defined as follows.

Definition 3.4. The *dual of a substitution* σ is denoted by $\mathbf{E}_1$. It is defined on the set $\mathbf{P}(\pi(\mathbb{Z}^n) \times \mathcal{A})$ of subsets of $\pi(\mathbb{Z}^n) \times \mathcal{A}$ as follows:

(3.2)

$$\mathbf{E}_1[\gamma, i] = \bigcup_{j \in \mathcal{A}, \sigma(j) = pis} [\mathbf{h}^{-1}(\gamma + \pi\mathbf{l}(p)), j] \in \mathbf{P}(\pi(\mathbb{Z}^n) \times \mathcal{A}) \quad \text{and} \quad \mathbf{E}_1(X_1) \cup \mathbf{E}_1(X_2) = \mathbf{E}_1(X_1 \cup X_2).$$

The stabilization condition for $\mathbf{E}_1$ is contained in the following proposition.

Proposition 3.5 ([**25, 61**]). *Let σ be a primitive unit Pisot substitution. Then the dual substitution rule $\mathbf{E}_1$ maps Γ_{srs} onto Γ_{srs}. Moreover, for all $X_1, X_2 \subseteq \pi(\mathbb{Z}^n) \times \mathcal{A}$ we have*

$$X_1 \cap X_2 = \emptyset \quad \Longrightarrow \quad \mathbf{E}_1(X_1) \cap \mathbf{E}_1(X_2) = \emptyset. \tag{3.3}$$

For abbreviation let $\mathcal{U}$ denote the faces of the unit cube of $\mathbb{R}^n$, *i.e.*,

$$\mathcal{U} := \bigcup_{i \in \mathcal{A}} [\mathbf{0}, i] \subset \Gamma_{srs}. \tag{3.4}$$

A main property of $\mathbf{E}_1$ is that $\mathcal{U}$ is contained in $\mathbf{E}_1(\mathcal{U})$ (*cf.* [**25, 61**]). Hence the sets $\mathbf{E}_1^m(\mathcal{U})$ are increasing subsets of Γ_{srs}.

Definition 3.6 (Geometric property (F)). Let σ be a primitive unit Pisot substitution. When the iterations of $\mathbf{E}_1$ eventually cover the whole self-replicating translation set Γ_{srs}, *i.e.*, if

$$\Gamma_{srs} = \bigcup_{m \geq 0} {\mathbf{E}_1}^m(\mathcal{U}), \tag{3.5}$$

we say that the substitution satisfies the *geometric property (F)*.

By expanding points using the definition of $\mathbf{E}_1$, this means that every point $[\gamma, i] \in \Gamma_{srs}$ has a unique finite $\mathbf{h}$-ary representation

$$\gamma = \mathbf{h}^{-m}\pi\mathbf{l}(p_0) + \cdots + \mathbf{h}^{-1}\pi\mathbf{l}(p_{m-1}) \tag{3.6}$$

where $(p_k, i_k, s_k)_{0 \leq k \leq m-1}$ is the labelling of a finite walk in the prefix-suffix graph that ends at $i = i_m$. Even if the geometric property (F) does not hold, (3.3) implies that if $[\gamma, i] \in \Gamma_{srs}$ has a finite representation of the shape (3.6), then this representation is unique.

This condition was introduced by Frougny and Solomyak [**67**] in the beta-numeration framework and then studied by Akiyama [**6**]. It is stated in the present form in [**38**]. There exist several sufficient conditions for property (F) for specific classes of substitutions related to beta-numeration ([**6, 26, 67**]). In one of our results we will relate the geometric property (F) to topological properties of the central tile.

3.1.3. Definition of the self-replicating multiple tiling. Now, we can use the self-replicating translation set to obtain a multiple tiling, as proved in [**26, 38, 61, 78**]. Before we state the result, recall that a Delauney set is a uniformly discrete and relatively dense set. Moreover, by an aperiodic set we mean a discrete subset of $\mathbb{R}^n$ that is not invariant by n linearly independent translations.

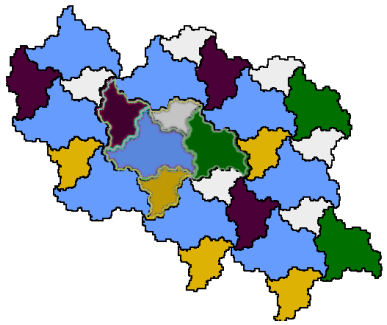

FIGURE 3.1. Self-replicating multiple tiling for the substitution σ_1 defined by $\sigma_1(1) = 12$, $\sigma_1(2) = 3$, $\sigma_1(3) = 4$, $\sigma_1(4) = 5$, $\sigma_1(5) = 1$. We will see in Example 4.2 that the self-replicating multiple tiling induced by σ_1 is a tiling since σ_1 satisfies the super coincidence condition.

PROPOSITION 3.7. *Let σ be a primitive unit Pisot substitution. The self-replicating translation set Γ_{srs} provides a multiple tiling for the subtiles $\mathcal{T}(i)$ $(i \in \mathcal{A})$, that is*

$$\mathbb{H}_c = \bigcup_{[\gamma,i]\in\Gamma_{srs}} (\mathcal{T}(i) + \gamma) \tag{3.7}$$

where almost all points of $\mathbb{H}_c$ are covered p times (p is a positive integer). The translation set Γ_{srs} is an aperiodic Delaunay set.

REMARK 3.8. Such a multiple tiling is called *self-replicating multiple tiling* (see for instance [**83**]). As $\mathcal{T}(i)$ $(i \in \mathcal{A})$ are compact sets this multiple tiling is *locally finite*, *i.e.*, there exists a $P \in \mathbb{N}$ such that each point of $\mathbb{H}_c$ is covered at most P times.

Figure 3.1 contains an example for a self-replicating multiple tiling that is actually a tiling.

3.2. The lattice multiple tiling

Another discrete plane can be defined by considering points with integral coordinates that lie on the *antidiagonal hyperplane* with equation $\langle \mathbf{x}, (1, \dots, 1)\rangle = 0$.

DEFINITION 3.9. Let σ be an irreducible unit Pisot substitution on n letters. The *lattice translation set* is defined by

$$\Gamma_{lat} = \left\{ [\gamma, i] \in \pi(\mathbb{Z}^n) \times \mathcal{A};\ \gamma \in \sum_{k=2}^{n} \mathbb{Z}(\pi(\mathbf{e}_k) - \pi(\mathbf{e}_1)) \right\}. \tag{3.8}$$

The lattice translation set is obviously periodic.

PROPOSITION 3.10 ([**25, 49**]). *Let σ be an irreducible unit Pisot substitution that satisfies the strong coincidence condition. Then the lattice translation set Γ_{lat} is a Delaunay set that provides a multiple tiling for the central subtiles $\mathcal{T}(1), \dots, \mathcal{T}(n)$, that is*

$$\mathbb{H}_c = \bigcup_{[\gamma,i]\in\Gamma_{lat}} (\mathcal{T}(i) + \gamma) \tag{3.9}$$

where almost all points are covered exactly p times by this union ($p \in \mathbb{N}$).

PROOF. Consider the quotient map ϕ from $\mathbb{H}_c$ to the $(d-1)$-dimensional torus $\mathbb{T} = \mathbb{H}_c/\mathcal{L}$, where $\mathcal{L}$ denotes the lattice $\mathcal{L} = \sum_{k=2}^{n} \mathbb{Z}(\pi(\mathbf{e}_k) - \pi(\mathbf{e}_1))$.

We first prove that the union in (3.9) forms a covering of $\mathbb{H}_c$. This is equivalent with proving that the central tile maps to the full torus, that is, $\phi(\mathcal{T}) = \mathbb{T}$. The key point is to notice that the set $\{\phi(\pi(\mathbf{e}_i)); 1 \le i \le n\}$ contains a single point, say $\mathbf{t}$. This follows from the definition of the quotient map ϕ.

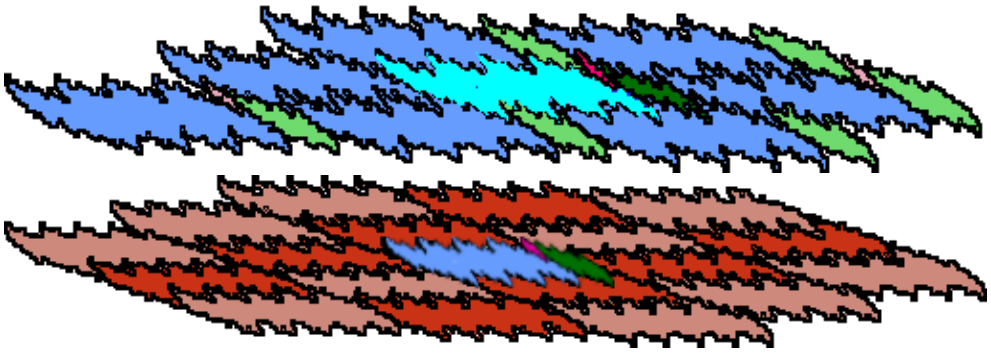

FIGURE 3.2. Self-replicating multiple tiling and lattice tiling for the substitution $\sigma_4(1) = 11112$, $\sigma_4(2) = 11113$ and $\sigma_4(3) = 1$. We will see in Example 4.2 that σ_4 satisfies the super-coincidence condition and that it is irreducible. Thus the self-replicating and lattice multiple tilings are tilings.

Let $u_0 \dots u_k \dots$ denote a periodic point of σ. By the definition of the central tile $\mathcal{T}$, we have $\phi(\mathcal{T}) = \overline{\{\phi(\mathbf{l}(u_0 \dots u_{k-1}));\ k \in \mathbb{N}\}} = \overline{\{k\mathbf{t};\ k \in \mathbb{N}\}}$ in the torus $\mathbb{T}$. To achieve the proof it remains to show by algebraic considerations that the addition of $\mathbf{t}$ on the torus is minimal: to this matter the Kronecker theorem can be applied after a precise study of the dependency between $\mathbf{t}$ and the projection ϕ. Hence $\phi(\mathcal{T}) = \mathbb{T}$ which is equivalent to the covering property in (3.9). The fact that we get actually a multiple tiling follows from the minimality of the rotation by $\mathbf{t}$.

Details can be found in [**25, 49**]; see also the proof of Proposition 3.13 in the Appendix. □

EXAMPLE 3.11. The substitution σ_4 is irreducible. Its self-replicating multiple tiling as well as its lattice multiple tiling which are actually tilings (see Example 4.2) is depicted in Figure 3.2.

To be generalized to the reducible case, this result needs to exhibit a suitable projection ϕ onto a $(d-1)$-dimensional torus such that $\{\phi(\pi(\mathbf{e}_i)); 1 \le i \le n\}$ contains a single point. A sufficient condition is the following one.

DEFINITION 3.12 (Quotient map condition). Let σ be a primitive unit Pisot substitution on n letters. Let d denote the degree of its dominant eigenvalue. We say that σ satisfies the *quotient map condition* if there exist d distinct letters $B(1), \dots, B(d)$ in $\mathcal{A}$ such that

$$\forall i \in \{1, \dots, n\} \quad \langle \mathbf{e}_i - \mathbf{e}_{B(1)}, \mathbf{v}_\beta \rangle \in \sum_{k \in \{2,\dots,d\}} \mathbb{Z}\langle \mathbf{e}_{B(k)} - \mathbf{e}_{B(1)}, \mathbf{v}_\beta \rangle. \tag{3.10}$$

Then, the *lattice translation set* is defined by

$$\Gamma_{lat} = \left\{ [\gamma, i] \in \pi(\mathbb{Z}^n) \times \mathcal{A};\ \gamma \in \sum_{k=2}^{d} \mathbb{Z}(\pi(\mathbf{e}_{B(k)}) - \pi(\mathbf{e}_{B(1)})) \right\}. \tag{3.11}$$

Under this condition the results of Proposition 3.10 hold.

PROPOSITION 3.13. *Let σ be a primitive unit Pisot substitution that satisfies the strong coincidence condition and the quotient map condition. Then the lattice translation set Γ_{lat} is a Delaunay set that provides a multiple tiling for the central subtiles $\mathcal{T}(1), \dots, \mathcal{T}(n)$, that is* (3.9) *is satisfied where almost all points are covered exactly p times by this union ($p \in \mathbb{N}$).*

PROOF. If the quotient map condition is satisfied, the following relation holds for all i:

$$\pi(\mathbf{e}_i) = \pi(\mathbf{e}_{B(1)}) \pmod{\sum_{k=1}^{d-1} \mathbb{Z}(\pi(\mathbf{e}_{B(k)}) - \pi(\mathbf{e}_{B(1)}))}.$$

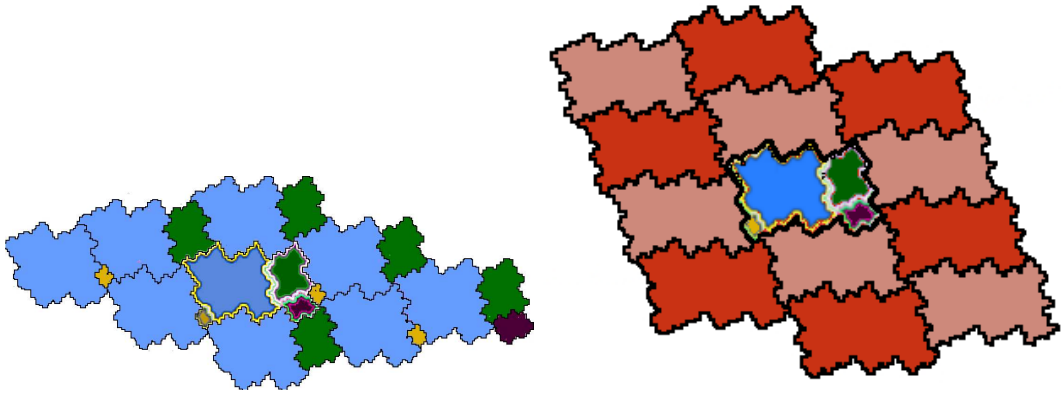

FIGURE 3.3. Self-replicating and lattice multiple tilings for the substitution σ_0. In the lattice tiling, the subtiles are shown only in the central tile. Subdivision in subtiles is omitted in the other copies of the central tile.
Since σ_0 satisfies the super-coincidence condition, the self-replicating multiple tiling is a tiling. The same is true for the lattice multiple tiling (see Example 4.2).

Hence the quotient map from $\mathbb{H}_c$ to $\mathbb{H}_c/\mathcal{L}$ maps $\{\phi(\pi(\mathbf{e}_i)); 1 \le i \le n\}$ to a single point $\mathbf{t}$. The condition also implies that $\langle \mathbf{v}_\beta, \mathbf{e}_{B(1)}\rangle$, $\langle \mathbf{v}_\beta, \mathbf{e}_{B(2)}\rangle$, $\ldots$, $\langle \mathbf{v}_\beta, \mathbf{e}_{B(d)}\rangle$ are rationally independent so that the addition of $\mathbf{t}$ is minimal, which yields the result. A detailed proof is given in the Appendix. □

EXAMPLE 3.14. The substitution $\sigma_1(1) = 12$, $\sigma_1(2) = 3$, $\sigma_1(3) = 4$, $\sigma_1(4) = 5$, $\sigma_1(5) = 1$ does not satisfy the quotient map condition. Indeed, if the condition is satisfied, the elements $\langle \mathbf{v}_\beta, \mathbf{e}_{B(1)}\rangle$, $\langle \mathbf{v}_\beta, \mathbf{e}_{B(2)}\rangle$ and $\langle \mathbf{v}_\beta, \mathbf{e}_{B(3)}\rangle$ are rationally independent. In this example we have $\mathbf{v}_\beta = (1, \beta - 1, \beta^2 - \beta, -\beta^2 + \beta + 1, \beta^2 - 1)$. Then $\langle \mathbf{v}_\beta, -\mathbf{e}_1 + \mathbf{e}_3 + \mathbf{e}_4\rangle = 0$ and $\langle \mathbf{v}_\beta, \mathbf{e}_2 + \mathbf{e}_3 - \mathbf{e}_5\rangle = 0$. The first relation yields $\langle \mathbf{v}_\beta, \mathbf{e}_4\rangle = \langle \mathbf{v}_\beta, \mathbf{e}_1\rangle - \langle \mathbf{v}_\beta, \mathbf{e}_3\rangle$. Hence, if $\{B(1), B(2), B(3)\}$ contains $\{1, 3\}$ we deduce that $\langle \mathbf{v}_\beta, \mathbf{e}_4\rangle$ belongs to the set on the right hand side of (3.10). Since the quotient map condition holds this set must contain also $\langle \mathbf{v}_\beta, \mathbf{e}_4 - \mathbf{e}_1\rangle$. Hence, also $\langle \mathbf{v}_\beta, \mathbf{e}_1\rangle$ belongs to this set. But this implies that there must be a rational dependency between the vectors in $\{B(1), B(2), B(3)\}$, a contradiction. With similar arguments we prove that $\{1, 4\}$, $\{2, 5\}$ and $\{3, 5\}$ cannot be subsets of $\{B(1), B(2), B(3)\}$. Thus the only possibility is $\{B(1), B(2), B(3)\} = \{2, 3, 4\}$. However, if the quotient map condition is satisfied for this set then $\beta - 2 = \langle \mathbf{v}_\beta, \mathbf{e}_2\rangle - \langle \mathbf{v}_\beta, \mathbf{e}_1\rangle$ is an integer combination of $\langle \mathbf{v}_\beta, \mathbf{e}_3 - \mathbf{e}_2\rangle = \beta^2 - 2\beta + 1$ and $\langle \mathbf{v}_\beta, \mathbf{e}_4 - \mathbf{e}_2\rangle = -\beta^2 + 2$ which is impossible. Hence, the condition is not satisfied for σ_1.

EXAMPLE 3.15. The substitution $\sigma_0(1) = 112$, $\sigma_0(2) = 113$, $\sigma_0(3) = 4$, $\sigma_0(4) = 1$ satisfies the quotient map condition. Indeed, we have $\mathbf{v}_\beta = (1, \beta - 2, \beta^2 - 2\beta - 2, \beta^2 - 3\beta + 1)$. Hence $\langle \mathbf{v}_\beta, \mathbf{e_4} - \mathbf{e_1}\rangle = \beta^2 - 3\beta = \beta^2 - 2\beta - 2 - (\beta - 2) = \langle \mathbf{v}_\beta, \mathbf{e_3} - \mathbf{e_1}\rangle - \langle \mathbf{v}_\beta, \mathbf{e_2} - \mathbf{e_1}\rangle$. Then a suitable basis is given by $B(1) = 1$, $B(2) = 2$, $B(3) = 3$. The self-replicating multiple tiling and the lattice multiple tiling which are actually tilings (see Example 4.2)are depicted in Figure 3.3.

REMARK 3.16. It remains to characterize all reducible primitive unit Pisot substitutions that satisfy the quotient map condition. We are not sure whether this is possible by means of a simple criterion.

3.3. The Pisot conjecture and the super-coincidence condition

A fundamental question is whether the multiple tilings defined in the previous subsections are indeed tilings. A combinatorial condition appeared for self-replicating tilings, the so-called *super-coincidence condition*, defined first in [**26, 78**] in the irreducible case and then generalized

to the reducible case in [**61**]. Since we will not use it explicitly in this monograph, we refer to the original papers for a precise definition. The main result is the following.

THEOREM 3.17 ([**26, 61, 78**]). *Let σ be a primitive unit Pisot substitution. Then the self-replicating multiple tiling is a tiling if and only if σ satisfies the super-coincidence condition.*

If σ is irreducible, the lattice multiple tiling is a tiling if and only if σ satisfies the super-coincidence condition.

The Pisot conjecture states that as soon as σ is an irreducible Pisot substitution, then the self-replicating and the lattice multiple tilings are tilings. In the reducible case, the Pisot conjecture states that the self-replicating multiple tiling is a tiling. In each case, no counter-example has been found yet.

The coincidence conjecture cannot be properly stated by means of lattice tilings in the reducible case, since there exist examples of reducible substitutions for which the lattice multiple-tiling cannot be properly defined (when they do not satisfy the quotient map condition detailed in Definition 3.12). A generalization of the Pisot conjecture to the reducible case could then be that if a substitution satisfies the quotient map condition, then the lattice multiple tiling is a tiling.

In the irreducible case, the multiple lattice tiling has been widely studied and presents many interesting features, related to the symbolic dynamical system associated with the substitution [**25, 66, 110**]. As a consequence of the proof of Proposition 3.10, if the lattice multiple tiling is a tiling, then the substitutive dynamical system associated with σ has a pure discrete spectrum, since it is measure theoretically conjugate to a toral translation.

CHAPTER 4

Statement of the main results: topological properties of central tiles

In this chapter we will state our main results in a slightly informal way. All details will be given in Chapter 6 where we also give the full proofs of all results. We do it that way in order to provide those readers who want to apply our results a way to use them without having to go into technical details.

4.1. A description of specific subsets of the central tile

We start with some notions and definitions needed in order to state the results. In all what follows we assume that σ is a primitive unit Pisot substitution. We build several graphs to describe with GIFSs the intersections of tiles. Technical details and precise definitions will be given in Chapter 5. The main idea is the following: we intend to describe the intersection between two tiles $\mathcal{T}(i)$ and $\mathcal{T}(j)+\gamma$. To do so, we consider the GIFS decomposition of each tile, that is $\mathcal{T}(i)=\bigcup_{\sigma(i_1)=p_1is_1}\mathbf{h}\mathcal{T}(i_1)+\pi\mathbf{l}(p_1)$ and $\mathcal{T}(j)=\bigcup_{\sigma(j_1)=p_2js_2}\mathbf{h}\mathcal{T}(j_1)+\pi\mathbf{l}(p_2)$. Then we write a decomposition of the intersection as

$$\mathcal{T}(i)\cap(\mathcal{T}(j)+\gamma)=\bigcup_{\substack{\sigma(i_1)=p_1is_1\\ \sigma(j_1)=p_2js_2}}(\mathbf{h}\mathcal{T}(i_1)+\pi\mathbf{l}(p_1))\cap(\mathbf{h}\mathcal{T}(j_1)+\pi\mathbf{l}(p_2)+\gamma).$$

We express each element of this decomposition as the image by $\mathbf{h}$ of a translated intersection of tiles

$$\mathcal{T}(i)\cap(\mathcal{T}(j)+\gamma)=\bigcup_{\substack{\sigma(i_1)=p_1is_1\\ \sigma(j_1)=p_2js_2}}\mathbf{h}\left(\mathcal{T}(i_1)\cap(\mathcal{T}(j_1)+\underbrace{\mathbf{h}^{-1}\pi\mathbf{l}(p_2)-\mathbf{h}^{-1}\pi\mathbf{l}(p_1)+\mathbf{h}^{-1}\gamma)}_{=\gamma_1}\right)+\pi\mathbf{l}(p_1). \tag{4.1}$$

This equation means that the intersection between two tiles can be expressed as the union of intersections between other tiles. Let us denote by $B[i,\gamma,j]$ the intersection $\mathcal{T}(i)\cap(\mathcal{T}(j)+\gamma)$. Then we have

$$B[i,\gamma,j]=\bigcup_{\substack{\sigma(i_1)=p_1is_1,\sigma(j_1)=p_2js_2\\ \gamma_1=\mathbf{h}^{-1}\pi\mathbf{l}(p_2)-\mathbf{h}^{-1}\pi\mathbf{l}(p_1)+\mathbf{h}^{-1}\gamma}}\mathbf{h}B[i_1,\gamma_1,j_1]+\pi\mathbf{l}(p_1).$$

Now we build a graph with nodes $[i,\gamma,j]$ such that there exists and edge between $[i,\gamma,j]$ and $[i_1,\gamma_1,j_1]$ if the latter node appears in the decomposition of the former. Starting from a finite set of nodes, we will prove that this graph is finite. Hence, a node $[i,\gamma,j]$ is the starting point of an infinite walk in this graph if and only if the intersection $B[i,\gamma,j]=\mathcal{T}(i)\cap(\mathcal{T}(j)+\gamma)$ is nonempty.

Depending on the purpose, we use different sets of initial nodes, and we use a similar process to describe intersections of more than two tiles, so that we finally define several different graphs. Besides these graphs, several other types of graphs will be used. We want to give a short survey over all these graphs in the following list.

***Zero-expansion graph*:** The nodes of the *zero-expansion graph* correspond to tiles $\mathcal{T}(i)+\gamma$ in the self-replicating tiling that contain $\mathbf{0}$.

***Connectivity graphs*:** The *tile-connectivity graph* contains an edge between two letters $i, j \in \mathcal{A}$ if and only if $\mathcal{T}(i)$ and $\mathcal{T}(j)$ intersect.
For each letter i, the *tile-refinement-connectivity graph* of $\mathcal{T}(i)$ exhibits intersections between the subtiles that appear in the GIFS decomposition of $\mathcal{T}(i)$.
Similarly, the *boundary-connectivity graph* of $\mathcal{T}(i)$ contains a node for each piece $\mathcal{T}(i) \cap (\mathcal{T}(j)+\gamma)$ that is nonempty and an edge between each two pieces that have nonempty intersection.
Moreover, the *boundary-refinement-connectivity graph* of a piece $\mathcal{T}(i) \cap (\mathcal{T}(j) + \gamma)$ of $\partial\mathcal{T}(i)$ exhibits intersections between the pieces that appear in the GIFS decomposition of $\mathcal{T}(i) \cap (\mathcal{T}(j) + \gamma)$.

***Self-replicating (SR) and lattice boundary graph*:** A point is called a *double point* if it is contained in a subtile of the central tile and in at least one other tile of a multiple tiling (self-replicating tiling or lattice tiling). The structure of the double-points in each of the above-mentioned tilings can be described by a GIFS governed by a graph. This graph is called *SR-boundary graph* and *lattice boundary graph*, respectively.

***Contact graph*:** The boundary of the tiles $\mathcal{T}(i)$ ($i \in \mathcal{A}$) can be written as a GIFS. We call *contact graph* the graph directing this GIFS.

***Triple point and quadruple point graph*:** A point is called *triple point* (*quadruple point*, respectively) if it is contained in a subtile of the central tile as well as in at least two (respectively three) other tiles of a multiple tiling. The triple (quadruple, respectively) points of the above mentioned self-replicating multiple tiling are the solutions of a GIFS directed by the so-called *triple point graph* (*quadruple point graph*, respectively).

Now we are ready to state our main results.

4.2. Tiling properties of the central tile and its subtiles

The contact graph and the lattice boundary graph allow to check that the self-replicating or lattice multiple tilings are indeed tilings.

THEOREM 4.1 (*cf.* [**119**]). *Let σ be a primitive unit Pisot substitution over the alphabet $\mathcal{A}$. Let β be the dominant eigenvalue of its incidence matrix. Then the following assertions hold.*

1. *The self-replicating multiple tiling is a tiling if and only if the largest eigenvalue in modulus of the SR-boundary graph*[4.1] *is strictly less than β. This is equivalent to the super-coincidence condition.*
2. *When the quotient map condition is satisfied, the lattice multiple tiling is a tiling if and only if the largest eigenvalue in modulus of the lattice boundary graph is strictly less than β.*

The interest of the first point of the theorem is the following. Usually, one checks whether the self-replicating multiple tiling is a tiling by considering the super-coincidence condition. More precisely, the super-coincidence condition cannot be checked directly but the so called *balanced pair algorithm* (*cf.* [**86**]) terminates if and only if this condition is satisfied; and this is the criterion that is usually used. However, this algorithm does not allow to test whether a substitution *does not* satisfy the super-coincidence condition. Theorem 4.1, however, is effective for checking both super-coincidence and not-super-coincidence, since the SR-boundary graph as well as the contact graph[4.2] can be constructed in finite time for each primitive unit Pisot substitution.

The second part of the theorem is not needed in the irreducible case because the lattice tiling property is equivalent to the self-replicating tiling property. The interest of this part lies

[4.1] It is possible to use the contact graph instead of the SR-boundary graph here. The contact graph is often much smaller than the SR-boundary graph and therefore more convenient for calculations. However, the contact graph does not exist for some reducible substitutions (see Section 5.4).

[4.2] See footnote 4.1.

in the reducible case. Ea and IO [**60**] have provided examples of computations of lattice tilings for some substitutions. Here we provide a general criterion for lattice tilings in the reducible case.

EXAMPLE 4.2. The example substitutions of Section 2.4 have the following tiling properties.

- The substitution σ_0 generates both, a self-replicating and a lattice tiling. Both tilings are shown in Figure 3.3. A detailed treatment of the tiling properties of σ_0 is given in Example 5.11.
- The substitution $\sigma_1(1) = 12$, $\sigma_1(2) = 3$, $\sigma_1(3) = 4$, $\sigma_1(4) = 5$, $\sigma_1(5) = 1$ generates an self-replicating tiling (see Figure 3.1) but not a lattice tiling. It does not satisfy the quotient map condition. To prove the self-replicating tiling property, details can be done in the same way as in the case of σ_0.
- Each of the substitutions $\sigma_2, \ldots, \sigma_6$ induces an self-replicating and a lattice tiling. This can be shown in the same way as it is shown for σ_0 in Example 5.11.

4.3. Dimension of the boundary of central tiles

A natural question is now to compute the Hausdorff and box counting dimension of the boundary of $\mathcal{T}(a)$ (for a definition of these notions of dimension see *e.g.* Falconer [**63**]). This question was handled for the Tribonacci substitution in [**74, 97**]. Moreover, in [**64**] an upper bound of the Hausdorff dimension is computed for a class of substitutions. Finally, [**124**] exhibits a formula for the box-counting dimension of a central tile in the irreducible case. This box counting dimension coincides with the Hausdorff dimension when the contraction $\mathbf{h}$ on the contracting plane $\mathbb{H}_c$ is a similarity, that is, when the conjugates of β all have the same modulus. If this is not the case, the calculation of the Hausdorff dimension of the boundary seems to be a very hard problem.

We include a slightly more general version of [**124**, Proposition 5.7 and Theorem 5.9]. Indeed, our version also contains the case of reducible substitutions.

THEOREM 4.3. *Let σ be a primitive unit Pisot substitution over the alphabet $\mathcal{A}$. Let β be the dominant eigenvalue of its incidence matrix and β' be one of the smallest conjugates of β in modulus. Let μ denote the largest eigenvalue in modulus of the SR-boundary graph*[4.3] *of σ.*

Suppose that the SR-boundary graph of σ is strongly connected and $\mu < \beta$. Then the box counting dimension of the boundary of $\mathcal{T}$ satisfies

$$\forall i = 1, \ldots, n, \qquad \dim_B(\partial\mathcal{T}) = \dim_B(\partial\mathcal{T}(i)) = d - 1 + \frac{\log\beta - \log\mu}{\log|\beta'|}. \tag{4.2}$$

If all the conjugates of β have the same modulus, then the box counting dimensions in (4.2) *agree with the associated Hausdorff dimensions.*

EXAMPLE 4.4. In this example we deal with the box counting dimension of the boundaries of $\mathcal{T}$ as well as $\mathcal{T}(i)$ ($i \in \mathcal{A}$) for the examples in Section 2.4. For $\sigma_0, \sigma_1, \sigma_2, \sigma_4$ and σ_6 all conjugates of β have the same modulus. Thus for these examples the box counting dimension is equal to the Hausdorff dimension. We calculate the following values.

- For σ_0 we have $\dim_B(\partial\mathcal{T}) = \dim_B(\partial\mathcal{T}(i)) = 1.196510420\ldots$
- For σ_1 we have $\dim_B(\partial\mathcal{T}) = \dim_B(\partial\mathcal{T}(i)) = 1.100263385\ldots$
- For σ_2 we have $\dim_B(\partial\mathcal{T}) = \dim_B(\partial\mathcal{T}(i)) = 1.946434603\ldots$
- For σ_3 we have $\dim_B(\partial\mathcal{T}) = \dim_B(\partial\mathcal{T}(i)) = 1.630544213\ldots$
- For σ_4 we have $\dim_B(\partial\mathcal{T}) = \dim_B(\partial\mathcal{T}(i)) = 1.563995213\ldots$
- For σ_5 we have $\dim_B(\partial\mathcal{T}) = \dim_B(\partial\mathcal{T}(i)) = 1.744561766\ldots$
- For σ_6 we have $\dim_B(\partial\mathcal{T}) = \dim_B(\partial\mathcal{T}(i)) = 1.791903475\ldots$

In the case of σ_0 the dimension calculations are detailed in Example 5.11. For all the other examples the calculations are similar to this case.

[4.3] See Footnote 4.1.

4.4. Exclusive inner points and the geometric property (F)

As mentioned in Definition 3.6, the well-known finiteness property (F) for beta-expansions invented by Frougny and Solomyak [**67**] can be extended to number systems associated to a substitution and expressed in geometrical terms. In the context of beta-numeration, Akiyama [**7**] proved that property (F) has consequences for the topology of the tile $\mathcal{T}$ since it is equivalent with $\mathbf{0}$ to be an exclusive inner point of $\mathcal{T}$. Notice that an *exclusive point* of a patch of finitely many tiles in a multiple tiling is a point that is contained exclusively in this patch and in no other tile of the multiple tiling.

We generalize Akiyama's result to every substitution by giving a geometric proof.

THEOREM 4.5. *Let σ be a primitive unit Pisot substitution with strong coincidence. Then σ satisfies the geometric property (F) (see Definition 3.6) if and only if $\mathbf{0}$ is an exclusive inner point of the patch $\mathcal{T} = \mathcal{T}(1) \cup \ldots \cup \mathcal{T}(n)$ in the self-replicating multiple tiling. If the geometric property (F) holds, the self-replicating multiple tiling is a tiling.*

Hence, the geometric property (F) implies super-coincidence, but the converse is not true (see Example 4.7).

The geometric property (F) cannot be checked directly since it implies infinite iterations. We provide an algorithm to check (F) in terms of boundary graph, by considering the tiles containing $\mathbf{0}$ in the self-replicating multiple tiling.

THEOREM 4.6. *Let σ be a primitive unit Pisot substitution over the alphabet $\mathcal{A}$ that satisfies the strong coincidence condition. Then σ satisfies the geometric property (F) if and only if the zero-expansion graph contains only nodes of the shape $[\mathbf{0}, i]$ ($i \in \mathcal{A}$).*

EXAMPLE 4.7. For the substitutions in Section 2.4 we have the following situation.

- The substitutions σ_0, σ_1 and σ_4 satisfy the geometric property (F).
- The substitutions σ_2, σ_3, σ_5, σ_6 do not satisfy the geometric property (F). For σ_3 for instance, $\mathbf{0}$ belongs to four different tiles $[0, 2]$, $[0, 3]$, $[(1, 1, 0), 3]$ and $[(-1, -1, 1), 3]$. The same holds for σ_5.

For σ_0 and σ_2 details are given in Example 5.3. The zero-expansion graph of σ_0 contains only one node with a loop, while the zero expansion graph of σ_2 contains 8 nodes and is depicted in Figure 5.1. This means that $\mathbf{0}$ is contained in 8 subtiles of the self-replicating tiling associated to σ_2. Thus σ_2 does not satisfy the geometric property (F) despite it satisfies the super-coincidence condition. Thus the geometric property (F) is strictly stronger than the super-coincidence condition.

4.5. Connectivity properties of the central tile

Apart from the Tribonacci substitution [**110**], sufficient conditions for connectivity appear in [**48**], but they are not algorithmic. We provide an effective checking of the connectivity condition.

THEOREM 4.8. *Let σ be a primitive unit Pisot substitution over the alphabet $\mathcal{A}$. The subtiles $\mathcal{T}(i)$ ($i \in \mathcal{A}$) are locally connected continua if and only if the tile-refinement-connectivity graph of $\mathcal{T}(j)$ is connected for each $j \in \mathcal{A}$.*

The central tile $\mathcal{T}$ is a locally connected continuum if the tile-connectivity graph as well as each tile-refinement-connectivity graph is connected.

Notice that it is not easy to provide a necessary and sufficient condition for the full connectivity of the central tile. The reason is that the central tile $\mathcal{T}$ may be connected even if some of the subtiles are disconnected. However, we were not able to find an example with this constellation.

EXAMPLE 4.9. We will use this theorem in Example 5.15 to prove that the central tile of $\sigma_3(1) = 3$, $\sigma_3(2) = 23$, $\sigma_3(3) = 31223$ is not connected. Indeed the tile-connectivity graph is

connected for this substitution, however, the tile-refinement-connectivity graph of $\mathcal{T}(2)$ is not connected (the tile is depicted in Figure 2.2).

For all the other substitutions given in Section 2.4 the central tiles as well as all their subtiles are connected. For σ_0 this is proved in Example 5.14. The proofs for all the other examples runs along the same lines.

4.6. Disklikeness of the central tile and its subtiles

Next we turn to the question whether a given tile $\mathcal{T}$ or one of its subtiles $\mathcal{T}(a)$ is homeomorphic to a closed disk. This implies that the dominant eigenvalue β has degree 3.

Examples of central tiles being homeomorphic to a closed disk are given in [**90, 97, 98**], where a parametrization of the boundary is given for a class of substitution related to the Tribonacci substitution. Here, we start by proving the following criterion for $\mathcal{T}$ to be homeomorphic to a closed disk.

THEOREM 4.10. *Let σ be a primitive unit Pisot substitution such that the dominant eigenvalue of its incidence matrix has degree 3. Suppose that the substitution satisfies the quotient map condition and that the lattice multiple tiling is a tiling (see Theorem 4.1).*

Assume further that the associated central tile $\mathcal{T}$ is homeomorphic to a closed disk. Then there exist at most eight values γ with $[\gamma, i] \in \Gamma_{lat}$ and

$$\mathcal{T} \cap (\mathcal{T} + \gamma) \neq \emptyset. \tag{4.3}$$

Among these eight values of γ there are at most six ones for with the intersection in (4.3) *contains more than one point.*

These "neighbor constellations" of $\mathcal{T}$ can be checked algorithmically by checking the nodes of the lattice boundary graph of σ.

The previous result can often be used in order to prove that a given tile $\mathcal{T}$ is *not* homeomorphic to a disk by exhibiting *too many* "neighbors" $\mathcal{T} + \gamma$ of $\mathcal{T}$ in the induced lattice tiling.

EXAMPLE 4.11. We discuss the theorem for two examples from Section 2.4.

The central tile of $\sigma_4(1) = 11112$, $\sigma_4(2) = 11113$ and $\sigma_4(3) = 1$ is not homeomorphic to a disk (see the tile in its induced tilings in Figure 3.2). Indeed, in the lattice tiling the tile $\mathcal{T}$ has 10 neighbors (for details see Example 5.13 and the lattice boundary graph depicted in Figure 5.3).

Notice that the criterion is very precise: indeed, for the substitution σ_0, the (disk-like) central tile $\mathcal{T}$ has eight neighbors, but four of the intersections are single points. Thus Theorem 4.10 cannot be used (see the tiling in Figure 3.3, the lattice boundary graph in Figure 5.4 and Example 5.13 for further details).

We will also prove the following criterion for the subtiles $\mathcal{T}(i)$ ($i \in \mathcal{A}$) to be homeomorphic to a closed disk.

THEOREM 4.12. *Let σ be a primitive unit Pisot substitution such that the dominant eigenvalue of its incidence matrix has degree 3. Suppose that the self-replicating multiple tiling is a tiling (see Theorem 4.1).*

Then each $\mathcal{T}(i)$ ($i \in \mathcal{A}$) is homeomorphic to a closed disk if the following assertions hold.

1. *Each boundary-connectivity graph is a simple loop.*
2. *Each boundary-refinement connectivity graph is either empty or a single node or a line.*
3. *Each intersection between three distinct tiles of the self-replicating tiling is either empty or a single point.*

REMARK 4.13. If a boundary-connectivity graph is a single node and the associated boundary-refinement-connectivity graph is a unique loop then the theorem is also true. The proof of

this variant runs along the same lines as the proof of the theorem. As we could not construct a single example with this property we omit the details.

It is also possible to give a condition for the central tile $\mathcal{T}$ to be homeomorphic to a closed disk. This is the case for instance if all the subtiles $\mathcal{T}(i)$ ($i \in \mathcal{A}$) are closed disks and if they intersect each other in a point or in a simple arc in a way that no holes occur. All this can be checked by means of our graphs.

EXAMPLE 4.14. The subtiles of the central tile of the substitutions σ_0 and σ_1 are homeomorphic to a closed disk. Details are given in Examples 5.34 and 5.35, respectively. All the other examples contained in Section 2.4 are not homeomorphic to a closed disk.

4.7. The fundamental group of the central tile and its subtiles

Finally, we are able to say something about the fundamental group of $\mathcal{T}(a)$ ($a \in \mathcal{A}$).

THEOREM 4.15. *Let σ be a primitive unit Pisot substitution such that the dominant eigenvalue of its incidence matrix has degree 3. Suppose that the substitution satisfies the supercoincidence condition.*

Then there exists a criterion which guarantees that each subtile $\mathcal{T}(i)$ ($i \in \mathcal{A}$) has an uncountable fundamental group which is not free.

The detailed statement of this result is contained in Theorem 6.21 (see also Theorem 6.18 which contains a criterion for the fundamental group of $\mathcal{T}(i)$ ($i \in \mathcal{A}$) to be nontrivial).

EXAMPLE 4.16. Four of the examples of Section 2.4 have uncountable fundamental group.

The subtiles of the central tile of the substitution $\sigma_5(1) = 123$, $\sigma_5(2) = 1$, $\sigma_5(3) = 31$ has an uncountable fundamental group which is not free. Details are given in Example 6.24.

The subtiles of the central tile for the flipped Tribonacci substitution $\sigma_6(1) = 12$, $\sigma_6(2) = 31$, $\sigma_6(3) = 1$ has an uncountable fundamental group which is not free. Details are given in Example 6.23.

Also for σ_2 and σ_4 one can prove in a similar way as for σ_5 and σ_6 that the fundamental group of each of the subtiles of their central tiles has uncountable and not free fundamental group.

CHAPTER 5

Several graphs that contain topological information on the central tile

We intend to describe topological properties of a central tile $\mathcal{T}$ and its subtiles $\mathcal{T}(i)$ ($i \in \mathcal{A}$) by using the self-affinity of $\mathcal{T}(i)$ and information on the intersections of tiles in the induced tilings.

In all what follows σ is a primitive unit Pisot substitution over the alphabet $\mathcal{A}$ with dominant eigenvalue β.

5.1. The graph detecting expansions of zero

Let us start our definitions by building a graph that permits to decide whether the origin $\mathbf{0}$ is contained in a given tile of the self-replicating tiling.

DEFINITION 5.1 (Zero-expansion graph). The *zero-expansion graph* $\mathcal{G}^{(\mathbf{0})}$ of σ is the largest[5.1] graph such that the following conditions hold.

(1) The nodes $[\gamma, i]$ of the graph belong to the self-replicating translation set Γ_{srs} and satisfy

$$||\gamma|| \leq \frac{\max\{||\pi\mathbf{l}(p)||; (p,a,s) \in \mathcal{P}\}}{1 - \max\{|\beta^{(j)}|; j = 2, \ldots, d\}}, \tag{5.1}$$

where $\beta^{(j)}$, $j = 2, \ldots, d$ denote the algebraic conjugates of β.

(2) There is an edge between two nodes $[\gamma_1, i_1]$ and $[\gamma_2, i_2]$, if and only if there exists $(p_1, i_1, s_1) \in \mathcal{P}$ such that

$$p_1 i_1 s_1 = \sigma(i_2) \qquad \text{and} \qquad \mathbf{h}\gamma_2 = \gamma_1 + \pi\mathbf{l}(p_1).$$

(3) Every node belongs to an infinite path.

PROPOSITION 5.2. *The zero-expansion graph $\mathcal{G}^{(\mathbf{0})}$ of a primitive unit Pisot substitution is well defined and finite. A pair $[\gamma, i]$ is a node of this graph if and only if $\mathbf{0} \in \mathcal{T}(i) + \gamma$.*

This type of graph first appeared in more specific settings in [**7, 110, 119**]. For the sake of clarity, we detail the proof of Proposition 5.2 in the Appendix.

EXAMPLE 5.3. In this example we give the details for Example 4.7.

- The zero-expansion graph for the substitution $\sigma_0(1) = 112$, $\sigma_0(2) = 113$, $\sigma_0(3) = 4$, $\sigma_0(4) = 1$ is equal to the node $[\mathbf{0}, 1]$ together with a self-loop. Thus the origin $\mathbf{0}$ only belongs to one subtile of the central tile in the self-replicating tiling. Hence, σ_0 satisfies the geometric property (F).
- The zero-expansion graph for the substitution $\sigma_2(1) = 2$, $\sigma_2(2) = 3$, $\sigma_2(3) = 12$ is shown in Figure 5.1. It consists of eight states which are grouped in two independent cycles. Hence, $\mathbf{0}$ belongs to eight tiles of the self-replicating tiling: it belongs to the three subtiles $\mathcal{T}(1)$, $\mathcal{T}(2)$ and $\mathcal{T}(3)$ as well as to the translated subtiles $\mathcal{T}(1) + \pi(1,1,-1)$, $\mathcal{T}(2) + \pi(-1,1,0)$, $\mathcal{T}(2) + \pi(-1,0,1)$, $\mathcal{T}(3) + \pi(1,0,0)$, $\mathcal{T}(3) + \pi(0,-1,1)$. Thus σ_2 does not satisfy the geometric property (F).

[5.1] By "largest" we mean that every set of nodes that satisfies the condition has to be included in $\mathcal{G}^{(\mathbf{0})}$. We will prove that such a set exists.

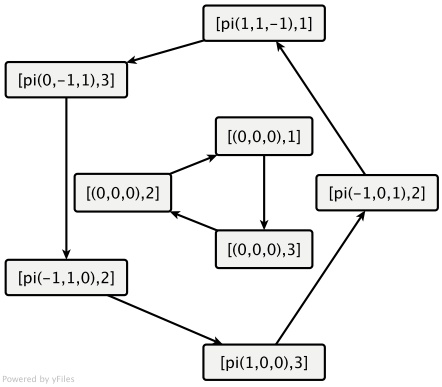

FIGURE 5.1. Zero-expansion graph for the substitution $\sigma_2(1) = 2$, $\sigma_2(2) = 3$, $\sigma_2(3) = 12$. "pi" stands for the projection map π.

5.2. Graphs describing the boundary of the central tile

Our aim here is to investigate the intersections between the central tile and some translated subtiles (corresponding to the self-replicating tiling or the lattice tiling). We introduce the following terminology. We will say that $\mathcal{T}(i) + \gamma_1$ and $\mathcal{T}(j) + \gamma_2$ with $[\gamma_1, i], [\gamma_2, j] \in \Gamma_{srs}$ are *neighbors* if they have nonempty intersection.

In this setting, the intersection between $\mathcal{T}(i)$ and $\mathcal{T}(j)+\gamma$ is described by the node $[i, \gamma, j] \in \mathcal{A} \times \pi(\mathbb{Z}^n) \times \mathcal{A}$. However, $[i, \gamma, j]$ and $[j, -\gamma, i]$ will then stand for the same intersection. To avoid redundancy in boundary graphs, we reduce the set of admissible nodes to

$$\mathfrak{D} = \{[i, \gamma, j] \in \mathcal{A} \times \pi(\mathbb{Z}^n) \times \mathcal{A};\ \gamma = \pi(\mathbf{x}),\ (\langle \mathbf{x}, \mathbf{v}_\beta \rangle > 0) \text{ or } (\gamma = \mathbf{0} \text{ and } i \leq j)\}.$$

We are now going to define graphs whose set of nodes are finite subsets of $\mathfrak{D}$.

DEFINITION 5.4 (Boundary graph). Let $\mathcal{S} \subset \mathfrak{D}$ be a finite set. The *boundary graph* of $\mathcal{S}$ is denoted by $\mathcal{G}^{(B)}(\mathcal{S})$. It is the largest[5.2] graph such that the following conditions hold.

(1) If $[i, \gamma, j]$ is a node of $\mathcal{G}^{(B)}(\mathcal{S})$ then $[i, \gamma, j] \in \mathfrak{D}$ and

$$||\gamma|| \leq \frac{2 \max\{||\pi \mathbf{l}(p)||; (p, a, s) \in \mathcal{P}\}}{1 - \max\{|\beta^{(j)}|; j = 2, \ldots, d\}} \tag{5.2}$$

where $\beta^{(j)}$ are the algebraic conjugates of β.

(2) There is an edge between two nodes $[i, \gamma, j]$ and $[i', \gamma', j']$, if and only if there exist $[\overline{i}, \overline{\gamma}, \overline{j}] \in \mathcal{A} \times \pi(\mathbb{Z}^n) \times \mathcal{A}$ and $[(p_1, a_1, s_1), (p_2, a_2, s_2)] \in \mathcal{P} \times \mathcal{P}$ such that

$$\begin{cases} [i', \gamma', j'] = [\overline{i}, \overline{\gamma}, \overline{j}] \text{ (type 1) or } [i', \gamma', j'] = [\overline{j}, -\overline{\gamma}, \overline{i}] \text{ (type 2)} \\ a_1 = i \text{ and } p_1 a_1 s_1 = \sigma(\overline{i}) \\ a_2 = j \text{ and } p_2 a_2 s_2 = \sigma(\overline{j}) \\ \mathbf{h}\overline{\gamma} = \gamma + \pi(\mathbf{l}(p_2) - \mathbf{l}(p_1)). \end{cases} \tag{5.3}$$

The edge is labelled by $\mathbf{e} \in \{\pi \mathbf{l}(p_1), \pi \mathbf{l}(p_2) + \gamma\}$ such that

$$\langle \mathbf{e}, \mathbf{v}_\beta \rangle = \min\{\langle \mathbf{l}(p_1), \mathbf{v}_\beta \rangle, \langle \mathbf{l}(p_2) + \mathbf{x}, \mathbf{v}_\beta \rangle\}, \qquad \pi(\mathbf{x}) = \gamma,\ \mathbf{x} \in \mathbb{Z}^n.$$

(3) Each node belongs to an infinite path starting from a node $[i, \gamma, j] \in \mathcal{S}$.

Definitions of edges in this graph are directly deduced from (4.1).

PROPOSITION 5.5. *The boundary graph associated with a finite subset of $\mathfrak{D}$ is well defined and finite.*

[5.2]The meaning of "largest" is explained in Definition 5.1.

We give the full proof of this proposition in the Appendix. It implies that a boundary graph can be algorithmically computed as soon as the set $\mathcal{S}$ is known. Indeed, start with the set of nodes $\mathcal{S}$. Then recursively increase this set with nodes $[i', \gamma', j']$ that satisfy conditions (1) and (2). The finiteness property in Proposition 5.5 ensures that this procedure will eventually stabilize the set of nodes. From this final set, nodes with no outgoing edges have to be removed recursively, so that condition (3) is also fulfilled.

THEOREM 5.6. *Let $\mathcal{S}$ be a finite subset of $\mathfrak{D}$. Let $[i, \gamma, j] \in \mathcal{S}$. The intersection between $\mathcal{T}(i)$ and $\mathcal{T}(j) + \gamma$ is nonempty if and only if $[i, \gamma, j]$ is a node of the boundary graph $\mathcal{G}^{(B)}(\mathcal{S})$.*

The proof is given in the Appendix.

Depending on the set $\mathcal{S}$, we build several boundary graphs that have certain useful properties.

5.2.1. The self-replicating boundary graph. The self-replicating tiling is based on the set Γ_{srs} (see Definition 3.2), that is, the condition $0 \leq \langle \gamma, \mathbf{v}_\beta \rangle < \langle \mathbf{e}_j, \mathbf{v}_\beta \rangle$. Hence, the set of points in Γ_{srs} that satisfy condition (5.2) is finite (the proof is similar to the proof of Proposition 5.5).

$$\mathcal{S}_{srs} = \left\{ [i, \gamma, j] \in \mathfrak{D}; \quad \left| \begin{array}{l} \gamma = \pi(\mathbf{x}),\ \mathbf{x} \in \mathbb{Z}^n,\ 0 \leq \langle \mathbf{x}, \mathbf{v}_\beta \rangle < \langle \mathbf{e}_j, \mathbf{v}_\beta \rangle \\ \gamma \neq \mathbf{0} \text{ or } i \neq j \\ \gamma \text{ satisfies condition (5.2)} \end{array} \right. \right\}. \tag{5.4}$$

The *self-replicating boundary graph* (SR-boundary graph, for short) is the boundary graph of this set, *i.e.*,

$$\mathcal{G}^{(B)}_{srs} = \mathcal{G}^{(B)}\left(\mathcal{S}_{srs}\right).$$

By its definition, this graph describes tiles of the self-replicating tiling that intersect the central tile.

THEOREM 5.7. *Let σ be a primitive unit Pisot substitution and let $[i, \gamma, j] \in \mathcal{S}_{srs}$. Let $B[i, \gamma, j]$ denote the nonempty compact set that is uniquely defined by the GIFS*

$$B[i, \gamma, j] = \bigcup_{[i,\gamma,j] \xrightarrow{\mathbf{e}} [i_1,\gamma_1,j_1] \text{ in } \mathcal{G}^{(B)}_{srs}} \mathbf{h} B[i_1, \gamma_1, j_1] + \mathbf{e}. \tag{5.5}$$

which is directed by the graph $\mathcal{G}^{(B)}_{srs}$.

Then the following assertions are true.

- *If $[i, \gamma, j]$ is a node of the SR-boundary graph $\mathcal{G}^{(B)}_{srs}$, then $[\gamma, j]$ belongs to the self-replicating translation set Γ_{srs} so that $\mathcal{T}(j)+\gamma$ is a piece of the self-replicating multiple tiling.*
- *The intersections between two tiles are solutions of (5.5), since the solutions $B[i, \gamma, j]$ of the GIFS equation satisfy*[5.3]

$$B[i, \gamma, j] = \mathcal{T}(i) \cap (\mathcal{T}(j) + \gamma).$$

- *If the self-replicating multiple tiling is a tiling, then the boundary of the subsets of the central tile is described by the sets $B[i, \gamma, j]$, in particular,*

$$\partial\mathcal{T}(i) := \bigcup_{\substack{[i,\gamma,j] \in \mathcal{G}^{(B)}_{srs} \\ [i,\gamma,j] \neq [i,0,i]}} B[i, \gamma, j] \cup \bigcup_{\substack{[j,\mathbf{0},i] \in \mathcal{G}^{(B)}_{srs} \\ j < i}} B[j, \mathbf{0}, i]. \tag{5.6}$$

The proof of this theorem is given in the Appendix. Note that the first part of Theorem 4.1 is a direct consequence of this result.

LEMMA 5.8. *If $B[i, \gamma, j]$ contains only one point it can be omitted in the representation of $\partial\mathcal{T}$ in (5.6).*

[5.3] This justifies the notation $B[i, \gamma, j]$ in (5.5).

PROOF. Suppose that $B[i,\gamma,j]$ contains a single point. If this single point is not isolated in $\partial\mathcal{T}(i)$ then $B[i,\gamma,j]$ has to be contained in another intersection $B[i',\gamma',j']$ because each of these intersections is compact. So let us assume that $B[i,\gamma,j]$ is an isolated point of $\partial\mathcal{T}(i)$. Then, as $\mathcal{T}(i)$ is the closure of its interior, each point in a small neighborhood of $B[i,\gamma,j]$ belongs to $\mathrm{Int}(\mathcal{T}(i))$ (note that each two points in this neighborhood are not separated by $\partial\mathcal{T}(i)$). Thus $B[i,\gamma,j]$ is an inner point of $\mathcal{T}(i)$, a contradiction. □

From the GIFS equation (5.5) we deduce that each point in $\mathcal{T}(i)\cap(\mathcal{T}(j)+\gamma)$ can be expanded through $\mathbf{h}$ by following edges labels in the SR-boundary graph.

COROLLARY 5.9. *Let $[i,\gamma,j]\in\mathfrak{D}$. A point $\mathbf{x}$ belongs to the intersection $\mathcal{T}(i)\cap(\gamma+\mathcal{T}(j))$ if and only if there exists an infinite path in $\mathcal{G}^{(B)}(\mathcal{S})$, starting from $[i,\gamma,j]$ and labelled by $(\mathbf{e}^{(k)})_{k\geq 0}$ such that*

$$\mathbf{x}=\sum_{k\geq 0}\mathbf{h}^k\mathbf{e}^{(k)}.$$

This is an immediate consequence of (5.5) (it is proved analogously to Corollary 2.7).

Note that Theorem 5.7 and Corollary 5.9 can be used to draw boundaries of central tiles and their subtiles. They were used to draw the boundaries of the tiles in the figures of the present monograph.

We need the following definition.

DEFINITION 5.10. Two infinite paths in a boundary graph $\mathcal{G}^{(B)}$ are called *essentially different* if their labelling $(\mathbf{e}_1^{(k)})_{k\geq 0}$ and $(\mathbf{e}_2^{(k)})_{k\geq 0}$ give rise to two different expansions, *i.e.*, if

$$\sum_{k\geq 0}\mathbf{h}^k\mathbf{e}_1^{(k)}\neq\sum_{k\geq 0}\mathbf{h}^k\mathbf{e}_2^{(k)}.$$

According to Proposition 5.30 we can check algorithmically whether a given node of the SR-boundary graph is the starting point of one or more essentially different paths. This is equivalent to the fact that the associated intersection contains one or more points.

EXAMPLE 5.11. The SR-boundary graph for $\sigma_0(1)=112$, $\sigma_0(2)=113$, $\sigma_0(3)=4$, $\sigma_0(4)=1$ is depicted in Figure 5.2. We deduce that the central tile $\mathcal{T}=\mathcal{T}(1)\cup\mathcal{T}(2)\cup\mathcal{T}(3)\cup\mathcal{T}(4)$ intersects 11 tiles in the self-replicating tiling, corresponding to the different pairs $[\gamma,j]$ with $\gamma\neq 0$ appearing in a node $[i,\gamma,j]$ of the SR-boundary graph.

As mentioned in the caption of Figure 5.2 the boundary of $\mathcal{T}(1)$ consists of eight intersections: three intersections with tiles inside the full central tile and five intersections with tiles outside the central tile. In particular,

$$\begin{aligned}\partial\mathcal{T}(1) &= B[1,\mathbf{0},2]\cup B[1,\mathbf{0},3]\cup B[1,\mathbf{0},4]\cup B[1,\pi(0,0,1,0),1]\cup B[1,\pi(0,0,1,0),2]\\ &\quad\cup B[1,\pi(0,1,-1,0),1]\cup B[1,\pi(0,1,0,0),1]\cup B[1,\pi(1,-1,1),1].\end{aligned}$$

Note that in the boundary graph a unique path goes out from each of the nodes $[1,\mathbf{0},3]$ and $[1,\pi(0,0,1,0),1]$. This means that each of the pieces $\mathcal{T}(1)\cap\mathcal{T}(3)$ and $\mathcal{T}(1)\cap(\mathcal{T}(1)+\pi(1,-1,1,0))$ consists of a single point. Therefore by Lemma 5.8 these pieces can be omitted in the description of the boundary of $\mathcal{T}(1)$. Thus

$$\begin{aligned}\partial\mathcal{T}(1) &= B[1,\mathbf{0},2]\cup B[1,\mathbf{0},4]\cup B[1,\pi(0,0,1,0),1]\\ &\quad\cup B[1,\pi(0,0,1,0),2]\cup B[1,\pi(0,1,-1,0),1]\cup B[1,\pi(0,1,0,0),1].\end{aligned}$$

As we know the SR-boundary graph of σ_0 we can easily calculate the dominant eigenvalue $\mu=1.839286755\ldots$ of its incidence matrix. Since μ is strictly less than the dominant eigenvalue $\beta=2.769292354\ldots$ of the incidence matrix of σ_0, Theorem 4.1 shows that the self-replicating multiple tiling as well as the lattice tiling induced by σ_0 are actually tilings. Moreover, the knowledge of μ, β and $|\beta'|=0.6009185307\ldots$ yields in view of Theorem 4.3 that

$$\dim_B(\partial\mathcal{T})=\dim_B(\partial\mathcal{T}(i))=1.196510420\ldots$$

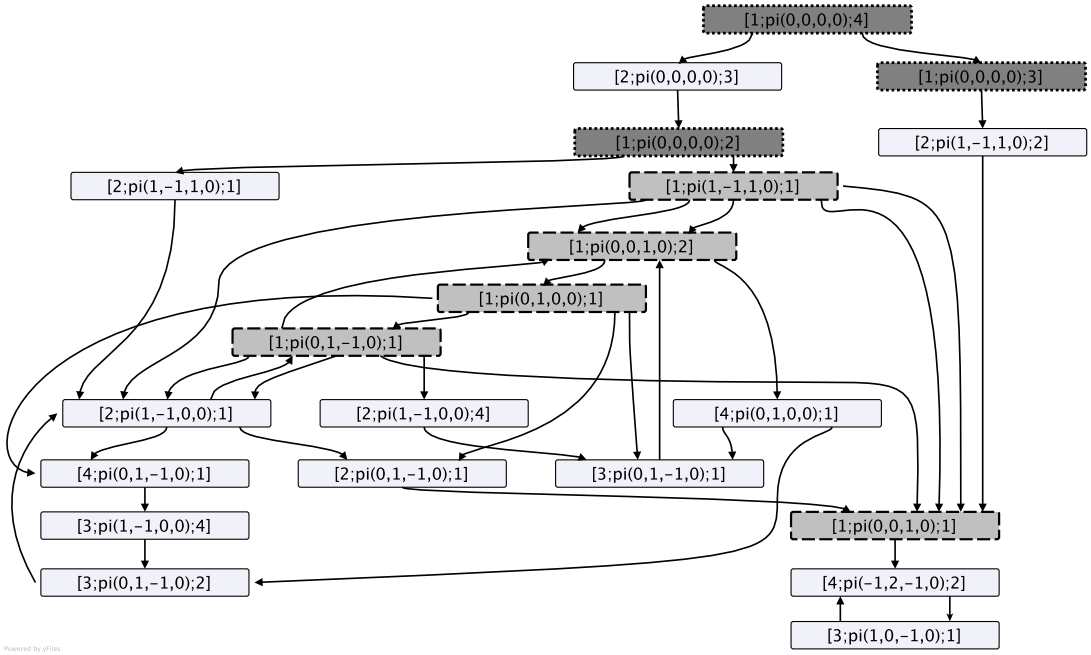

FIGURE 5.2. The SR-boundary graph for the substitution $\sigma_0(1) = 112$, $\sigma_0(2) = 113$, $\sigma_0(3) = 4$, $\sigma_0(4) = 1$. Labels of edges are omitted, "pi" stands for the projection map π. A node $[i, \gamma, j]$ occurs in this graph if and only if $\mathcal{T}(i)$ intersects the tile $\mathcal{T}(j) + \gamma$ in the self-replicating tiling.
For instance, the tile $\mathcal{T}(1)$ intersects the three other subtiles $\mathcal{T}(2)$, $\mathcal{T}(3)$ and $\mathcal{T}(4)$ since the nodes $[1, \mathbf{0}, 2]$, $[1, \mathbf{0}, 3]$ and $[1, \mathbf{0}, 4]$ appear in the graph (nodes with dotted frame). The tile $\mathcal{T}(1)$ also intersects five tiles outside the central tile, namely $\mathcal{T}(1)+\pi(0, 0, 1, 0)$, $\mathcal{T}(2)+\pi(0, 0, 1, 0)$, $\mathcal{T}(1)+\pi(0, 1, -1, 0)$, $\mathcal{T}(1)+\pi(0, 1, 0, 0)$ and $\mathcal{T}(1) + \pi(1, -1, 1, 0)$, since the corresponding nodes appear in the graph. These are $[1, \pi(0, 0, 1, 0), 1]$, $[1, \pi(0, 0, 1, 0), 2]$, $[1, \pi(0, 1, -1, 0), 1]$, $[1, \pi(0, 1, 0, 0), 1]$, $[1, \pi(1, -1, 1, 0), 1]$ (nodes with dashed frame).

Since the conjugates of β have all the same modulus the Hausdorff dimension of the boundaries $\partial\mathcal{T}(i)$ is the same as their box counting dimension in this case.

5.2.2. The lattice boundary graph. Here we suppose that σ satisfies the quotient map condition (see Definition 3.12). Then the points of the lattice translation set that satisfy condition (5.2) is finite. The *lattice boundary graph* is the boundary graph of this set, *i.e.*,

$$\mathcal{G}_{lat}^{(B)} = \mathcal{G}^{(B)}(\mathcal{S}_{lat})$$

with

$$\mathcal{S}_{lat} := \left\{ [i, \gamma, j] \in \mathfrak{D}; \quad \left| \begin{array}{l} \gamma \in \Gamma_{lat} \setminus \{\mathbf{0}\} \\ \gamma \text{ satisfies condition (5.2)} \end{array} \right. \right\}.$$

As in Theorem 5.7 the definition implies that the graph describes tiles of the lattice tiling that intersect the central tile. In particular, we have the following result.

PROPOSITION 5.12. *Assume that σ satisfies the quotient map condition. Let $[\gamma, i] \in \Gamma_{lat} \setminus \{\mathbf{0}\}$. The intersection between the subtile $\mathcal{T}(i)$ and the subtile $\mathcal{T}(j) + \gamma$ in the lattice tiling is nonempty if and only $[i, \gamma, j]$ or $[j, -\gamma, i]$ is a node of the lattice boundary graph.*

This graph is used in Theorem 4.10 to obtain a sufficient condition for non-dislikeness of $\mathcal{T}$. Contrarily to the set Γ_{srs} in the SR-boundary graph, the lattice translation set Γ_{lat} is not

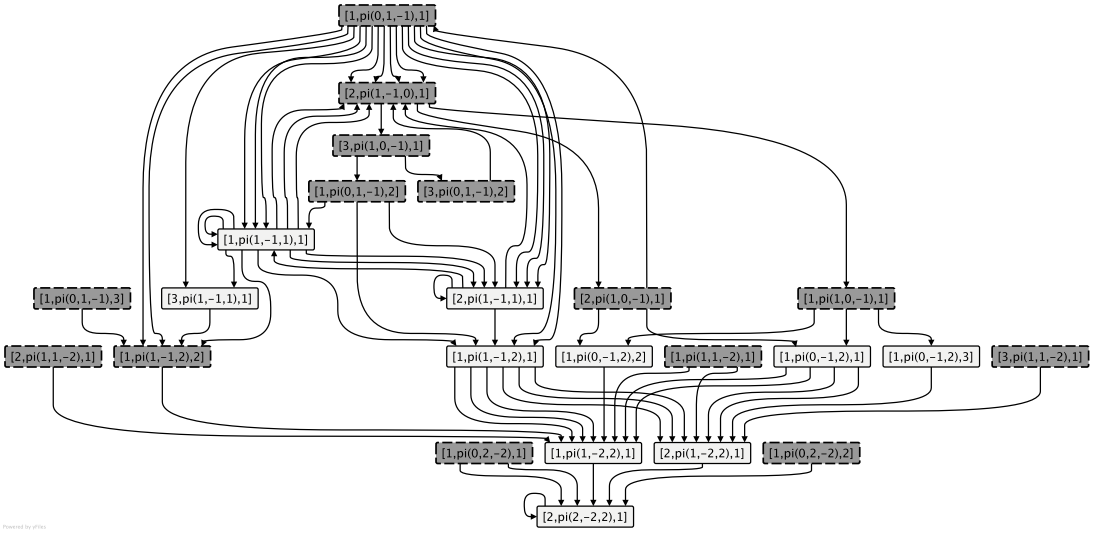

FIGURE 5.3. Lattice boundary graph for the substitution $\sigma_4(1) = 11112$, $\sigma_4(2) = 11113$, $\sigma_4(3) = 1$. Nodes with dashed frame correspond to intersections in the lattice tiling, that is, $\gamma \in \mathcal{S}_{lat}$.

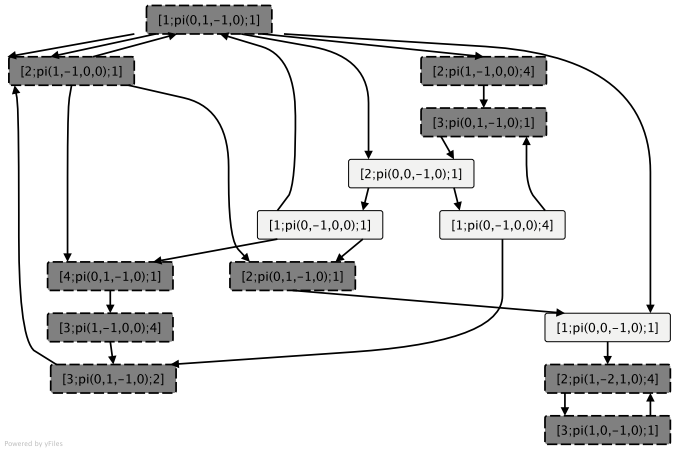

FIGURE 5.4. Lattice boundary graph for the substitution $\sigma_0(1) = 112$, $\sigma_0(2) = 113$, $\sigma_0(3) = 4$, $\sigma_0(4) = 1$. Nodes with dashed frame correspond to intersections in the lattice tiling, that is, $\gamma \in \mathcal{S}_{lat}$.

stable by the edge condition (5.3). Thus there may well exist nodes in the lattice boundary graph that correspond to elements not belonging to Γ_{lat}.

EXAMPLE 5.13. In Figure 5.3 the lattice boundary graph of σ_4 is depicted. From this figure we deduce that $\mathcal{T} \cap (\mathcal{T} + \gamma) \neq \emptyset$ if and only if $\gamma \in \pm\{\pi(1,-1,0,0),\ \pi(0,1,-1,0),\ \pi(1,0,-1,0),\ \pi(0,2,-2,0),\ \pi(1,1,-2,0)\}$. Thus the central tile has 10 neighbors and, hence, Theorem 4.10 applies to deduce that the central tile associated to σ_4 is not homeomorphic to a closed disk (the tile together with its neighbors in the induced tilings is depicted in Figure 3.2).

In Figure 5.4 the lattice boundary graph of σ_0 is depicted. From this figure we deduce that $\mathcal{T} \cap (\mathcal{T} + \gamma) \neq \emptyset$ if and only if $\gamma \in \pm\{\pi(1,-1,0,0),\ \pi(1,0,-1,0),\ \pi(0,1,-1,0),\ \pi(1,1,-2,0\}$. Notice that a unique infinite path starts from the node $[3;\pi(1,0,-1,0);1]$ and from the node

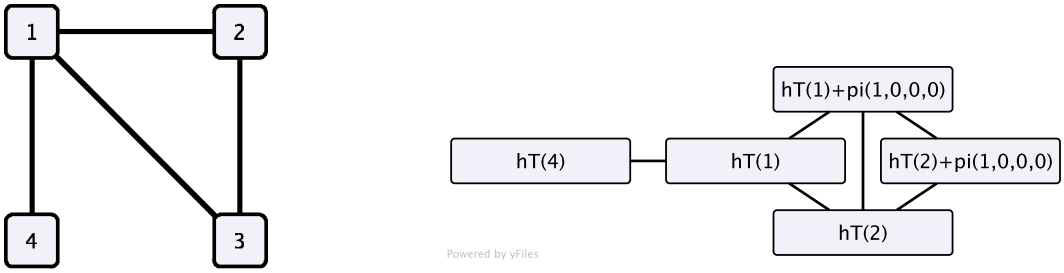

FIGURE 5.5. The tile-connectivity graph (left side) and the tile-refinement-connectivity graph of $\mathcal{T}(1)$ (right side) for the substitution σ_0. The notation "pi" stands for π in the labelling. Additionally, we check that for each of the subtiles $\mathcal{T}(2)$, $\mathcal{T}(3)$ and $\mathcal{T}(4)$ the tile-refinement-connectivity graph is equal to a single node. Therefore, all the tile-refinement-connectivity graphs and the tile-connectivity graph are connected; from this we deduce that the central tile is connected (see Figure 2.1 for a picture of the tile).

$[2;\pi(1,-2,1,0);4]$. This implies that each of the intersections $\mathcal{T} \cap (\mathcal{T} + \pi(1,0,-1,0))$ and $\mathcal{T} \cap (\mathcal{T} + \pi(1,1,-2,0))$ is equal to a single point. Thus Theorem 4.10 cannot be applied.

5.3. Graphs related to the connectivity of the central tile

The following graphs make it possible to decide whether certain sets are connected or not.

Tile-connectivity graph: This non-oriented graph encodes intersections between tiles in the central tile. Its nodes are the elements of $\mathcal{A}$. There is an edge from i to j if and only if $\mathcal{T}(i)$ and $\mathcal{T}(j)$ intersect.
Concretely, There is an edge from i to j if $[i,\mathbf{0},j]$ or $[j,\mathbf{0},i]$ belongs to the SR-boundary graph.

Tile-refinement-connectivity graph: According to Theorem 2.6, the tiles $\mathcal{T}(i)$ ($i \in \mathcal{A}$) are the solutions of a GIFS governed by the prefix-suffix graph. Thus each $\mathcal{T}(i)$ can be represented as

$$\mathcal{T}(i) = \bigcup_{i \xrightarrow{(p,i,s)} j} \mathbf{h}\mathcal{T}(j) + \pi\mathbf{l}(p).$$

Denote the sets in the union on the right hand side by $T_{i1},\dots,T_{i\ell}$. These sets are the nodes of the tile-refinement-connectivity graph of $\mathcal{T}(i)$. Each two of them are connected by an edge if and only if they have a nonempty intersection.
Therefore, there is an edge between $\mathbf{h}\mathcal{T}(j_1)+\pi\mathbf{l}(p_1)$ and $\mathbf{h}\mathcal{T}(j_2)+\pi\mathbf{l}(p_2)$ if and only if $[j_1,\mathbf{h}^{-1}\pi(\mathbf{l}(p_2)-\mathbf{l}(p_1)),j_2]$ or $[j_2,\mathbf{h}^{-1}\pi(\mathbf{l}(p_1)-\mathbf{l}(p_2)),j_1]$ is a node of the SR-boundary graph.

EXAMPLE 5.14. The central tile of σ_0 is depicted in Figure 2.1 together with its GIFS decomposition. We now prove that this tile as well as each of its subtiles is connected.

We first use the SR-boundary graph of σ_0 (see Figure 5.2) to build the global-connectivity graph. We check that $[1,\mathbf{0},2]$, $[1,\mathbf{0},3]$, $[1,\mathbf{0},4]$, $[2,\mathbf{0},3]$ are nodes of the SR-boundary graph. Thus we obtain the tile connectivity graph depicted in Figure 5.5. It means that the largest tile $\mathcal{T}(1)$ intersects all the tiles, while the second and third tiles $\mathcal{T}(2)$ and $\mathcal{T}(3)$ intersect each other and the smallest tile $\mathcal{T}(4)$ only intersect the largest one $\mathcal{T}(1)$. Therefore the $\mathcal{T}$-connectivity graph is connected.

The tile-refinement-connectivity graphs for $\mathcal{T}(2)$, $\mathcal{T}(3)$ and $\mathcal{T}(4)$ are equal to a single node since only one subset appears in their GIFS decomposition (see details in Section 2.4). The last graph to compute is the tile-refinement-connectivity graph of $\mathcal{T}(1)$: it has five nodes,

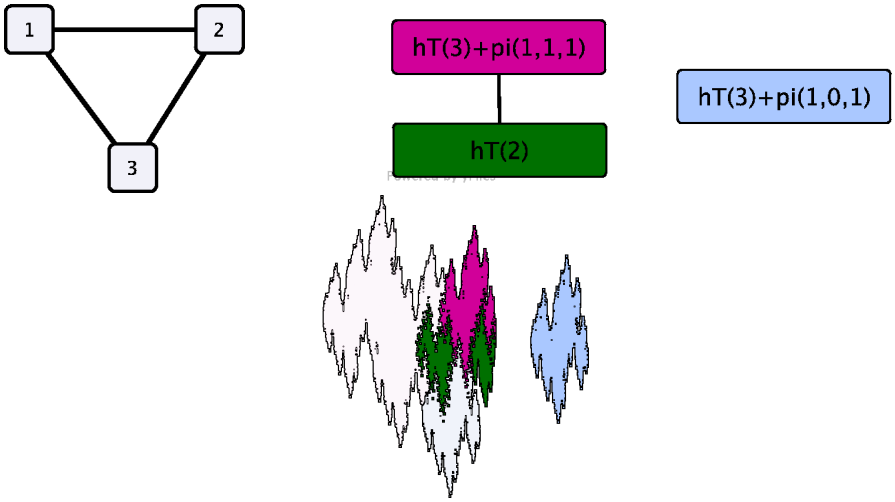

FIGURE 5.6. The global-connectivity graph (upper left side) and the tile-refinement-connectivity graph of $\mathcal{T}(2)$ (upper right side) for the substitution $\sigma_3(1) = 3$, $\sigma_3(2) = 23$, $\sigma_3(3) = 31223$. The prefix-suffix equation shows that $\mathcal{T}(2)$ can be decomposed into three pieces. The tile-refinement-connectivity graph shows that the piece $\mathbf{h}\mathcal{T}(3) + \pi(1,0,1)$ is disconnected from the other pieces appearing in the decomposition of $\mathcal{T}(2)$. The subdivision of $\mathcal{T}(2)$ is indicated by the three dark tiles in the figure. The light tiles correspond to $\mathcal{T}(1)$ and $\mathcal{T}(3)$ (these are drawn without subdivision). We deduce that the central tile is not connected.

corresponding to the tiles that appear in the decomposition of $\mathcal{T}(1)$, namely $\mathbf{h}\mathcal{T}(1)$, $\mathbf{h}\mathcal{T}(1) + \pi(1,0,0,0)$, $\mathbf{h}\mathcal{T}(2)$, $\mathbf{h}\mathcal{T}(2) + \pi(1,0,0,0)$, $\mathbf{h}\mathcal{T}(4)$.

We use the boundary graph to check intersections between these tiles, that is, to check whether the SR-boundary graph contains the nodes $[1, \mathbf{h}^{-1}\pi(1,0,0,0), 1]$, $[1, \mathbf{0}, 2]$, $[1, \mathbf{0}, 4]$, $[1, \mathbf{h}^{-1}\pi(1,0,0,0), 2]$, $[2, \mathbf{h}^{-1}\pi(1,0,0,0), 1]$, $[2, \mathbf{h}^{-1}\pi(1,0,0,0), 2]$, $[2, \mathbf{0}, 4]$, $[4, \mathbf{h}^{-1}\pi(1,0,0,0), 2]$, or their symmetric nodes. We deduce that the tile-refinement-connectivity graph of $\mathcal{T}(1)$ is connected (it is depicted in Figure 5.5).

By Theorem 4.8, we conclude that all the tiles $\mathcal{T}(1)$, $\mathcal{T}(2)$, $\mathcal{T}(3)$, $\mathcal{T}(4)$ as well as the central tile $\mathcal{T}$ of σ_0 are connected, as suggested by Figure 2.1.

EXAMPLE 5.15. The central tile of σ_3 is depicted in Figure 5.6. We use the SR-boundary graph (which contains 29 nodes) to build the tile-connectivity graph, it turns out that it is a complete graph, meaning that each subtile intersects all the other subtiles.

The SR-boundary graph is also used to build the tile-refinement-connectivity graph of $\mathcal{T}(2)$. This graph contains three nodes corresponding to the GIFS decomposition of $\mathcal{T}(2)$, namely $\mathbf{h}\mathcal{T}(2)$, $\mathbf{h}\mathcal{T}(3) + \pi(1,0,1)$, $\mathbf{h}\mathcal{T}(3) + \pi(1,1,1)$. We check that $[2, \mathbf{h}^{-1}\pi(1,1,1), 3]$ is a node of the boundary graph, leading to an edge in the tile-refinement-connectivity graph between $\mathbf{h}\mathcal{T}(2)$ and $\mathbf{h}\mathcal{T}(3) + \pi(1,1,1)$. Meanwhile, $[2, \mathbf{h}^{-1}\pi(1,0,1), 3]$ and its symmetric $[3, -\mathbf{h}^{-1}\pi(1,0,1), 1]$ are not nodes of the SR-boundary graph, hence, there is no edge in the tile-refinement-connectivity graph between $\mathbf{h}\mathcal{T}(2)$ and $\mathbf{h}\mathcal{T}(3) + \pi(1,1,1)$.

Similarly, neither $[3, \mathbf{h}^{-1}\pi(0,1,0), 3]$ nor $[3, -\mathbf{h}^{-1}\pi(0,1,0), 3]$ is a node in the SR-boundary graph, hence, there is no edge between $\mathbf{h}\mathcal{T}(3) + \pi(1,0,1)$ and $\mathbf{h}\mathcal{T}(3) + \pi(1,1,1)$ in the tile-refinement-connectivity graph. We conclude that tile-refinement-connectivity graph of $\mathcal{T}(2)$ contains an isolated node $\mathbf{h}\mathcal{T}(3) + \pi(1,0,1)$. By Theorem 4.8, this proves that $\mathcal{T}(2)$ is not connected, as suggested by the picture in Figure 5.6. The same figure also contains the tile-connectivity graph as well as the tile-refinement-connectivity graph of $\mathcal{T}(2)$.

5.4. Contact graphs

In the present section we have to assume that the faces $[\pi(\mathbf{x}), i]$ have a geometric interpretation as polyhedra that induce a tiling of $\mathbb{H}_c$. If σ is irreducible this is always true in view of Remark 3.3. Indeed, in this case the union of the faces contained in the set Γ_{srs} forms a tiling related to a discrete approximation of the beta-contracting space $\mathbb{H}_c$ (see for instance [**38**]). In the case of reducible substitutions it is not known whether such a geometric interpretation is always possible (see [**61**]). Only for some special instances like for the substitution σ_1 such an interpretation is known (see [**60**]). In particular, for these examples we can associate a certain polyhedron to each of the faces $[\pi(\mathbf{x}), i]$. However, in the reducible case there is no universal construction known to obtain such polyhedra. They have to be constructed by separate considerations for each of the known instances (*cf.* [**60, 61**]). So in this section we confine ourselves to irreducible unit Pisot substitutions as well as reducible ones admitting a geometric interpretation of their faces.

If the elements of Γ_{srs} can be viewed as polyhedra then images of these faces under the dual substitution $\mathbf{E}_1$ can be regarded as finite unions of such polyhedra which form a subset of the discrete approximation of $\mathbb{H}_c$ mentioned before. Indeed, the dual substitution can be used to define natural approximations of the central tile $\mathcal{T}$ and its subtiles $\mathcal{T}(i)$ $(i \in \mathcal{A})$ in this case. In particular, we set

$$\mathcal{T}_m(i) := \mathbf{h}^m \mathbf{E}_1{}^m[\mathbf{0}, i] \qquad (i \in \mathcal{A}).$$

Comparing the definition of $\mathbf{E}_1$ with the set equation (2.6) we conclude from the theory of GIFS (see Definition 2.3 and the remarks after it) that

$$\mathcal{T}(i) = \lim_{m\to\infty} \mathcal{T}_m(i) \qquad (i \in \mathcal{A}) \tag{5.7}$$

holds in Hausdorff metric. For this reason we call $\mathcal{T}_m(i)$ the (natural) *m-th approximation of* $\mathcal{T}(i)$.

Contact graphs describe intersections between these approximations of tiles in the self-replicating multiple tiling. Indeed, if the approximations $\mathcal{T}_m(i) + \gamma_1$ and $\mathcal{T}_m(j) + \gamma_2$ have non-empty intersection for arbitrarily large m then we say that they have *contact*.

Definition 5.16 (Pre-contact graph). Let $\mathcal{S} \subset \mathfrak{D}$ be finite. The *pre-contact graph* of $\mathcal{S}$ is denoted by $\tilde{\mathcal{G}}^{(C)}(\mathcal{S})$. It the largest[5.4] graph such that

(1) The nodes of $\tilde{\mathcal{G}}^{(C)}(\mathcal{S})$ belong to $\mathfrak{D}$.
(2) There is an edge between two nodes $[i_1, \gamma_1, i_2]$ and $[j_1, \gamma_2, j_2]$, labelled by $\mathbf{e}$ if and only if the relation (5.3) is satisfied.
(3) Every node belongs to a path *ending* in a node in $\mathcal{S}$.

Proposition 5.17. *For every finite $\mathcal{S} \subset \mathfrak{D}$, the pre-contact graph is finite.*

This is proved in [**124**]. We give a sketch of the proof in the Appendix.

Now we can state the main properties of contact graphs. The first result is proved in [**124**]. We recall the proof in the Appendix.

Proposition 5.18. *Let $\tilde{\mathcal{G}}^{(C)}(\mathcal{S})$ be a pre-contact graph and $[i, \gamma, j] \in \mathcal{S}$. $[i, \gamma, j]$ is a node of $\tilde{\mathcal{G}}^{(C)}(\mathcal{S})$ which is the starting point of an infinite path if and only if the approximations $\mathcal{T}_n(i)$ and $\mathcal{T}_n(j) + \gamma$ have nonempty intersection for arbitrarily large n. As a consequence, $\mathcal{T}(i)$ and $\mathcal{T}(j) + \gamma$ have nonempty intersection, so that $[i, \gamma, j]$ is also a node of the boundary graph $\mathcal{G}^{(B)}(\mathcal{S})$.*

For a directed graph G denote by $\mathrm{Red}(G)$ the graph emerging from G by successively removing all nodes which are not the starting point of an infinite walk.

[5.4] The meaning of "largest" is explained in Definition 5.1.

DEFINITION 5.19 (Contact graph). Let $\tilde{\mathcal{G}}^{(C)}(\mathcal{S})$ be the pre-contact graph of $\mathcal{S}$. Then the *contact graph* of $\mathcal{S}$ is defined by

$$\mathcal{G}^{(C)}(\mathcal{S}) := \mathrm{Red}(\tilde{\mathcal{G}}^{(C)}(\mathcal{S})).$$

Proposition 5.18 now implies that when $[i,\gamma,j]$ is a node of the contact graph, not only the tiles $\mathcal{T}(i)$ and $\mathcal{T}(j)+\gamma$ do intersect, but this intersection can already be "seen" in their approximation. We say in this case that $\mathcal{T}(i)$ and $\mathcal{T}(j)+\gamma$ have *contact* instead of being only *neighbors* in the tiling.

Let

$$\mathcal{S}_{cont} := \{[i,\gamma,j] \in \mathfrak{D};\ \mathcal{L}_{d-2}([0,i]\cap[\gamma,j]) > 0\}$$

($\mathcal{L}_k$ denotes the k-dimensional Lebesgue measure; $[\gamma,j]$ stands for a polygonal face as in Definition 3.2). We define the *self-replicating contact graph* (SR-contact graph for short) as the contact graph with respect to this set, *i.e.*,

$$\mathcal{G}_{srs}^{(C)} = \mathcal{G}^{(C)}\left(\mathcal{S}_{cont}\right).$$

THEOREM 5.20. *Let σ be an irreducible primitive unit Pisot substitution.*

Let $[i,\gamma,j] \in \mathcal{S}_{cont}$. Let $C[i,\gamma,j]$ denote the non-empty compact sets that are uniquely defined by the GIFS

$$C[i,\gamma,j] = \bigcup_{[i,\gamma,j]\xrightarrow{\mathbf{e}}[i_1,\gamma_1,j_1] \text{ in } \mathcal{G}_{srs}^{(C)}} \mathbf{h}C[i_1,\gamma_1,j_1]+\mathbf{e}$$

which is directed by the contact graph $\mathcal{G}_{srs}^{(C)}$.

If the self-replicating multiple tiling is a tiling, then the boundary of the subsets of the central tile is described by the sets $C[i,\gamma,j]$, i.e.,

$$\partial\mathcal{T}(i) := \bigcup_{\substack{[i,\gamma,j]\in\mathcal{G}_{srs}^{(C)}\\ [i,\gamma,j]\neq[i,0,i]}} C[i,\gamma,j] \cup \bigcup_{\substack{[j,\mathbf{0},i]\in\mathcal{G}_{srs}^{(C)}\\ j<i}} B[j,\mathbf{0},i].$$

The proof of this result in given in [**124**] for the irreducible case. The remaining cases mentioned at the beginning of the present section can be treated in the same way. We can understand better the structure of the subset $C[i,\gamma,j]$ in this theorem.

PROPOSITION 5.21. *Suppose that σ is an irreducible primitive unit Pisot substitution that satisfies the super-coincidence condition. Let $C[i,\gamma,j]$ be the nonempty compact sets that are defined in Theorem 5.20. Then for every $[i,\gamma,j]$, we have $C[i,\gamma,j] \subset \mathcal{T}(i)\cap(\mathcal{T}(j)+\gamma)$.*

PROOF. (SEE [**124**, Section 4]). In Proposition 5.18 we saw that the nodes of the contact graph $\mathcal{G}_{srs}^{(C)}$ form a subgraph of the boundary graph $\mathcal{G}_{srs}^{(B)}$. Thus

$$C[i,\gamma,j] \subset B[i,\gamma,j] = \mathcal{T}(i)\cap(\mathcal{T}(j)+\gamma)$$

and we are done. □

Despite the SR-contact graph is not always defined it is often more convenient to apply this graph rather than the SR-boundary graph. Note that all nodes in the SR-contact graph correspond to intersections of the shape $\mathcal{T}_m(i)\cap\mathcal{T}_m(j)+\gamma$ which are nonempty for m large enough. However, if this intersection is nonempty for $m \geq m_0$ then $\mathcal{T}(i)\cap T(j)+\gamma$ is also nonempty. This follows from Proposition 5.21 together with the definition of the Hausdorff limit.

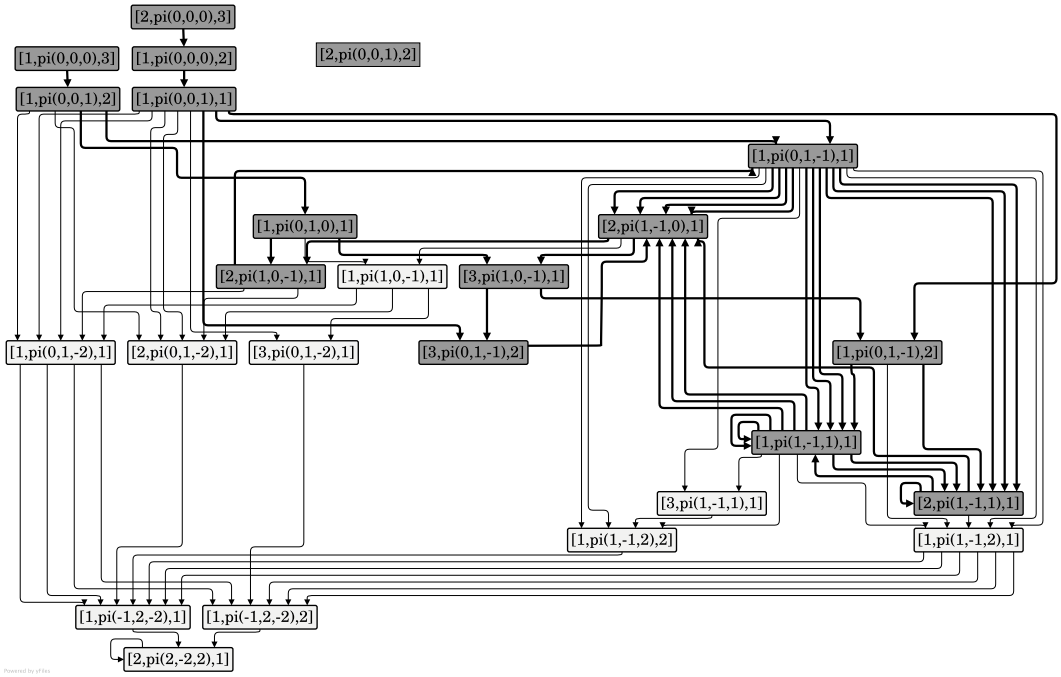

FIGURE 5.7. The dark nodes in the graph depicted in this figure shows the SR-contact graph of the substitution σ_4. The whole graph is the SR-boundary graph. In this example the SR-contact graph is a proper subgraph of the SR-boundary graph.

Thus the SR-contact graph is a subgraph of the SR-boundary graph. In [**124**] the SR-contact graphs of the class ($b \geq a \geq 1$)

$$\begin{aligned} \sigma(1) &= \underbrace{1\dots1}_{b \text{ times}}\, 2 \\ \sigma(2) &= \underbrace{1\dots1}_{a \text{ times}}\, 3 \\ \sigma(3) &= 1 \end{aligned}$$

of irreducible Pisot substitutions have been calculated. The number of their nodes is uniformly bounded by 20. On the other hand, numerical evidence suggests that the number of nodes of the associated SR-boundary graphs becomes arbitrarily large within this class. This is due to the fact that approximations of central tiles often behave much more nicely than the central tiles themselves. Taking the limit may increase the number of neighbors considerably.

In the following example we deal with the choice $a = b = 4$ of the above class. This corresponds to our example σ_4.

EXAMPLE 5.22. Consider the substitution σ_4. Its SR-contact as well as SR-boundary graph is depicted in Figure 5.7. One can see that the contact graph without one isolated node is a proper subgraph of the SR-contact graph.

5.5. Triple points and connectivity of the boundary

We generalize the definition of boundary graphs to describe intersections between three tiles. We will restrict to the self-replicating tiling, but the definition also holds in the lattice tiling setting. We are interested in intersections of three distinct tiles of a tiling. Hence, we set

$$\mathfrak{T} = \{[i, \gamma_1, j, \gamma_2, k] \in \mathcal{A} \times \pi(\mathbb{Z}^n) \times \mathcal{A} \times \pi(\mathbb{Z}^n) \times \mathcal{A}; \quad [\mathbf{0}, i],\, [\gamma_1, i],\, [\gamma_2, k] \text{ are all distinct}\}.$$

We first reduce the set of all the possible intersections.

$$\overline{\mathfrak{T}} = \left\{ \begin{array}{l} [i,\gamma_1,j,\gamma_2,k] \in \mathfrak{T} \\ \gamma_1 = \pi(\mathbf{x}_1),\ \gamma_2 = \pi(\mathbf{x}_2)\ ; \\ \mathbf{x}_1, \mathbf{x}_2 \in \mathbb{Z}^n \end{array} \middle| \begin{array}{l} 0 \le \langle \mathbf{x}_1, \mathbf{v}_\beta\rangle \le \langle \mathbf{x}_2, \mathbf{v}_\beta\rangle \\ \text{if } \gamma_1 = 0 \text{ then } i < j \\ \text{if } \gamma_2 = \gamma_1 \text{ then } j < k \end{array} \right\}.$$

We need to prove that the set $\overline{\mathfrak{T}}$ is enough to describe all the possible intersections of three tiles in a tiling. The proof is a case study, it is done in the Appendix.

LEMMA 5.23. *We define an equivalence relation on $\mathfrak{T}$ by: $[i,\gamma_1,j,\gamma_2,k] \simeq_t [i',\gamma_1',j',\gamma_2',k']$ if and only if the sets $\{\mathbf{e}_i, \mathbf{e}_j+\gamma_1, \mathbf{e}_k+\gamma_2\}$ and $\{\mathbf{e}_{i'}, \mathbf{e}_{j'}+\gamma_1', \mathbf{e}_{k'}+\gamma_2'\}$ are equal up to a translation vector. Then the set $\overline{\mathfrak{T}}$ is a quotient set for the equivalence relation $\simeq_t$: for every $[i,\gamma_1,j,\gamma_2,k]$, there exists a unique element in $\overline{\mathfrak{T}}$, denoted by $\phi_{\overline{\mathfrak{T}}}([i,\gamma_1,j,\gamma_2,k])$ such that $[i,\gamma_1,j,\gamma_2,k] \simeq_t \phi_{\overline{\mathfrak{T}}}([i,\gamma_1,j,\gamma_2,k])$.*

We denote by $\mathbf{e}([i,\gamma_1,j,\gamma_2,k]) \in \{\mathbf{0},\gamma_1,\gamma_2\}$ the translation difference between $[i,\gamma_1,j,\gamma_2,k]$ and its representant. This vector satisfies:

$$\langle \mathbf{e}([i,\gamma_1,j,\gamma_2,k]), \mathbf{v}_\beta\rangle = \min\{\mathbf{0}, \langle \mathbf{x}_1, \mathbf{v}_\beta\rangle, \langle \mathbf{x}_2, \mathbf{v}_\beta\rangle\} \qquad (\pi(\mathbf{x}_k) = \gamma_k,\ \mathbf{x}_k \in \mathbb{Z}^n,\ k = 1,2).$$

Coming back to the intersection between three tiles, let $T[i,\gamma_1,j,\gamma_2,k]$ denote the intersection

$$T[i,\gamma_1,j,\gamma_2,k] = \mathcal{T}(i) \cap (\mathcal{T}(j)+\gamma_1) \cap (\mathcal{T}(k)+\gamma_2)\,.$$

The previous lemma implies that intersections for equivalent triples are equal up to a translation vector, in particular

$$T[i,\gamma_1,j,\gamma_2,k] = T\phi_{\overline{\mathfrak{T}}}([i,\gamma_1,j,\gamma_2,k]) + \mathbf{e}([i,\gamma_1,j,\gamma_2,k]). \tag{5.8}$$

Then we can reduce the study of triple intersections to the set $\overline{\mathfrak{T}}$.

DEFINITION 5.24 (Triple point graph). The *triple point graph* of σ is denoted by $\mathcal{G}^{(T)}$. It is the largest[5.5] graph such that

(1) If $[i,\gamma_1,j,\gamma_2,k]$ is a node of $\mathcal{G}^{(T)}$, then $[i,\gamma_1,j,\gamma_2,k] \in \overline{\mathfrak{T}}$ and

$$\max\{||\gamma_1||, ||\gamma_2||\} \le \frac{2\max\{||\pi\mathbf{l}(p)||; (p,a,s) \in \mathcal{P}\}}{1-\max\{|\beta^{(j)}|; j = 2\dots d\}}. \tag{5.9}$$

(2) There is an edge between two nodes $[i,\gamma_1,j,\gamma_2,k]$ and $[i',\gamma_1',j',\gamma_2',k']$ if and only if there exists $[\bar{i},\overline{\gamma_1},\bar{j},\overline{\gamma_2},\bar{k}] \in \mathfrak{T}$ and $(p_0,a_0,s_0),(p_1,a_1,s_1),(p_2,a_2,s_2) \in \mathcal{P}$ such that

$$\left\{ \begin{array}{l} [i',\gamma_1',j',\gamma_2',k'] = \Phi_{\overline{\mathfrak{T}}}[\bar{i},\overline{\gamma_1},\bar{j},\overline{\gamma_1},\bar{k}] \\ a_0 = i \text{ and } p_0a_0s_0 = \sigma(\bar{i}) \\ a_1 = j \text{ and } p_1a_1s_1 = \sigma(\bar{j}) \\ a_2 = k \text{ and } p_2a_2s_2 = \sigma(\bar{k}) \\ \mathbf{h}\overline{\gamma_1} = \gamma_1 + \pi\mathbf{l}(p_1) - \pi\mathbf{l}(p_0) \\ \mathbf{h}\overline{\gamma_2} = \gamma_2 + \pi\mathbf{l}(p_2) - \pi\mathbf{l}(p_0). \end{array} \right.$$

The edge is labelled by $\mathbf{e} \in \{\pi\mathbf{l}(p_0), \pi\mathbf{l}(p_1)+\gamma_1, \pi\mathbf{l}(p_2)+\gamma_2\}$ defined so that

$$\langle \mathbf{e}, \mathbf{v}_\beta\rangle = \min\{\langle \mathbf{l}(p_0), \mathbf{v}_\beta\rangle, \langle \mathbf{l}(p_1)+\mathbf{x}_1, \mathbf{v}_\beta\rangle, \langle \mathbf{l}(p_2)+\mathbf{x}_2, \mathbf{v}_\beta\rangle\},\ \text{with } \pi(\mathbf{x}_{1,2}) = \gamma_{1,2},\ \mathbf{x}_{1,2} \in \mathbb{Z}^n.$$

(3) Every node belongs to an infinite path starting from a node $[i,\gamma_1,j,\gamma_2,k]$ such that $[\gamma_1,j] \in \Gamma_{srs}$ and $[\gamma_2,k] \in \Gamma_{srs}$.

With a treatment similar to the boundary graph, we prove that this graph is finite and identifies triple points in the self-replicating multiple tiling (see the proof in the Appendix).

[5.5] The meaning of "largest" is explained in Definition 5.1.

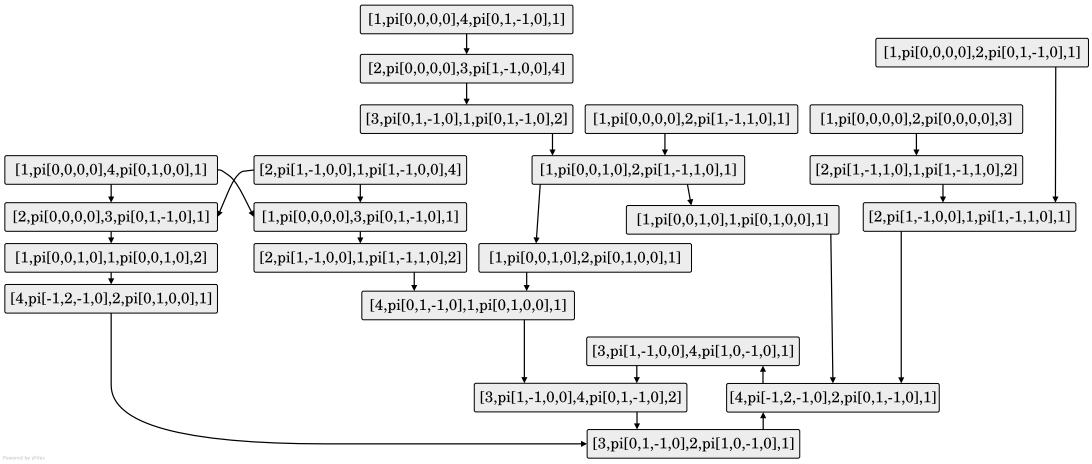

FIGURE 5.8. The triple point graph for the substitution σ_0. There are 23 nodes, with the shape $[i, \gamma_1, j, \gamma_2, k]$, corresponding to an intersection between $\mathcal{T}(i)$, $\mathcal{T}(j) + \gamma_1$ and $\mathcal{T}(k) + \gamma_2$. In this case there are 23 infinite paths in the triple point graph. However, notice that some triple intersections might coincide (see Example 5.27 and Remark 5.30).

THEOREM 5.25. *The triple point graph is finite.*

Let $[i, \gamma_1, j, \gamma_2, k] \in \mathfrak{T}$ be such that $[\gamma_1, j] \in \Gamma_{srs}$ and $[\gamma_2, k] \in \Gamma_{srs}$. The tiles $\mathcal{T}(i)$, $\mathcal{T}(j)+\gamma_1$ and $\mathcal{T}(k) + \gamma_2$ have a nonempty intersection if and only if $\phi_{\overline{\mathfrak{T}}}([i, \gamma_1, j, \gamma_2, k])$ is a node of the triple point graph.

A point $\mathbf{x}$ belongs to the intersection $\mathcal{T}(i) \cap (\mathcal{T}(j) + \gamma_1) \cap (\mathcal{T}(k) + \gamma_2)$ if and only if there exists an infinite path starting from $\phi_{\overline{\mathfrak{T}}}([i, \gamma_1, j, \gamma_2, k])$ and labelled by $(\mathbf{e}^{(k)})_{k\geq 0}$ such that

$$\mathbf{x} = \mathbf{e}([i, \gamma_1, j, \gamma_2, k]) + \sum_{k\geq 0} \mathbf{h}^k \mathbf{e}^{(k)}. \tag{5.10}$$

As in the case of boundary graphs (see Definition 5.10) we need to define essentially different paths in a triple point graph.

DEFINITION 5.26. Two infinite paths in the triple point graph are called *essentially different* if their labels correspond to different points in their $\mathbf{h}$-ary expansion (5.10).

EXAMPLE 5.27. The triple point graph for the substitution σ_0 is depicted in Figure 5.8. It contains 23 nodes. However, the tiling depicted in Figure 3.3 suggests that there are only 12 triple intersections. The difference between observation and computation comes from the existence of quadruple points: if four pairwise distinct tiles $T(i_1)$, $T(i_2) + \gamma_2$, $T(i_3) + \gamma_3$, $T(i_4) + \gamma_4$ intersect in the same point $\mathbf{x}$, with $\gamma_2, \gamma_3, \gamma_4 \neq 0$, then three different nodes in the triple point graph correspond to this intersection, namely $\phi_{\overline{\mathfrak{T}}}[i_1, \gamma_2, i_2, \gamma_3, i_3]$, $\phi_{\overline{\mathfrak{T}}}[i_1, \gamma_2, i_2, \gamma_4, i_4]$, $\phi_{\overline{\mathfrak{T}}}[i_1, \gamma_3, i_3, \gamma_4, i_4]$. Moreover, from each of these nodes there leads away an infinite walk corresponding to $\mathbf{x}$ so that there are also three walks corresponding to $\mathbf{x}$.

In the next section, the computation of the quadruple point graph will confirm that this phenomenon explains why there are 23 nodes in the graph but only 12 visible triple points in the tiling.

The triple point graph is useful to detect intersections between the parts of the boundary of a tile $\mathcal{T}(i)$: according to Theorem 5.7, $\partial\mathcal{T}(i)$ can be represented as a finite union of pieces of the shape $\mathcal{T}(j_1) \cap (\mathcal{T}(j_2) + \gamma)$. The boundary-connectivity graph contains information about intersections between these pieces.

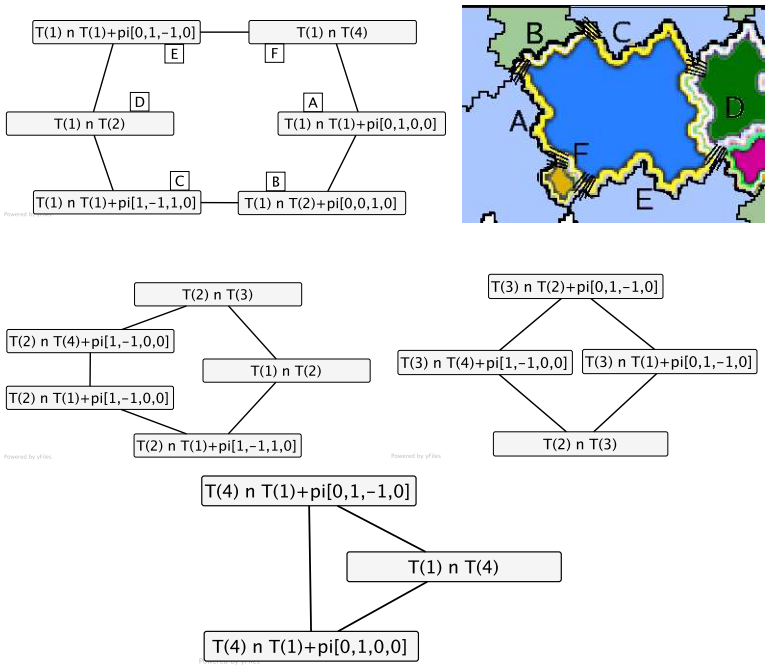

FIGURE 5.9. The boundary connectivity graphs for the tiles $\mathcal{T}(1)$, $\mathcal{T}(2)$, $\mathcal{T}(3)$, $\mathcal{T}(4)$ associated to the substitution σ_0. Each node corresponds to an intersection $\mathcal{T}(i) \cap T(j) + \gamma$ that appears in the decomposition of the boundary of $\mathcal{T}(i)$. An edge between two nodes means that the two corresponding pieces in the boundary intersect. Therefore, the first graph confirms that $\mathcal{T}(1)$ can be described with 6 pieces that each have two adjacent pieces, as suggested in the picture of the tile.

DEFINITION 5.28 (Boundary-connectivity graph). Let $i \in \mathcal{A}$. The *boundary-connectivity graph* of $\mathcal{T}(i)$ admits for nodes the sets of the shape $\mathcal{T}(i) \cap (\mathcal{T}(j_2) + \gamma)$ that are not reduced to a single point and that appear in the decomposition of the boundary of $\mathcal{T}(i)$ according to Theorem 5.7. Each two of them are connected by an edge if and only if they have nonempty intersection.

According to Theorem 5.7, the nodes of the boundary-connectivity graph of $\mathcal{T}(i)$ are the nodes of the shape $[i, \gamma, j] \in \mathcal{G}_{srs}^{(B)}$ or $[j, \mathbf{0}, i] \in \mathcal{G}_{srs}^{(B)}$, with $j > i$. We remove from this set the nodes from which there is a unique outgoing path in the SR-boundary graph. To determine whether there is an edge between $[i_1, \gamma_1, j_1]$ and $[i_2, \gamma_2, j_2]$, we notice that among the four pairs $[\mathbf{0}, i_1]$, $[\gamma_1, j_1]$, $[\mathbf{0}, i_2]$, $[\gamma_2, j_2]$, there are exactly three different pairs, $[\mathbf{0}, i]$, $[\gamma_1', j_1']$ and $[\gamma_2', j_2']$, say. Then we put an edge between the two nodes if and only if the triple point graph contains the node $\phi_{\overline{\mathfrak{T}}}[i, \gamma_1', j_1', \gamma_2', i_2']$.

EXAMPLE 5.29. Let us consider again the substitution σ_0. According to Example 5.11, the boundary $\partial\mathcal{T}(1)$ is the union of six different pieces that are not reduced to a single point. Their intersections are checked by using the triple point graph, issuing in the boundary-connectivity graph of $\mathcal{T}(1)$ depicted in Figure 5.9 together with the boundary-connectivity graphs for $\mathcal{T}(2)$, $\mathcal{T}(3)$ and $\mathcal{T}(4)$.

It is often necessary to decide whether a given intersection $B[i, \gamma, j]$ contains at least two points or not. This is equivalent to the existence of two essentially different paths leading away from the node $[i, \gamma, j]$ in the SR-boundary graph. In practice, this can often be decided very

easily (see for instance in Example 5.34). However, we want to show that it can always be done algorithmically.

PROPOSITION 5.30. *Consider a node $\mathcal{N}$ in the SR-boundary graph, the triple point graph or the quadruple point graph.*

- *If an infinite number of paths lead away from the node $\mathcal{N}$, then the intersection of tiles associated with the node $\mathcal{N}$ contains an infinite number of different points.*
- *If from the node $\mathcal{N}$ there lead away only a finite number of paths, then each of these paths is ultimately periodic. Consequently, the point described by each path can be explicitly computed and compared to the others. This allows to decide in a finite time whether the corresponding intersection is a single point or not.*

The proof is given in the Appendix.

5.6. Quadruple points and connectivity of pieces of the boundary

We build a new graph to describe quadruple intersections in the self-replicating tiling. As mentioned in Example 5.27 and in Proposition 5.30 this graph is useful in order to decide whether two paths in the triple point graph are essentially different. Moreover, it will be used for checking the sufficient condition for the disklikeness of subtiles of $\mathcal{T}$ and in the description of their fundamental group. In order to proceed, we need a description of intersections between four tiles in the self-replicating tiling. We set

$$\begin{aligned}\mathfrak{Q} \;=\; \{[i,\gamma_1,j,\gamma_2,k,\gamma_3,l] \in \mathcal{A}\times\pi(\mathbb{Z}^n)\times\mathcal{A}\times\pi(\mathbb{Z}^n)\times\mathcal{A}\times\pi(\mathbb{Z}^n)\times\mathcal{A};\\ [\mathbf{0},i],\,[\gamma_1,i],\,[\gamma_2,k]\,[\gamma_3,l] \text{ are all distinct}\}.\end{aligned}$$

Similar to the triple point graph, we reduce the set of all possible intersections to a set of unique representants (up to a translation) $\overline{\mathfrak{Q}}$. The mapping from an intersection to its representant is denoted by $\phi_{\mathfrak{Q}}$. After that we define a *quadruple point graph* $\mathcal{G}^{(Q)}$ that allows to describe intersections between four distinct tiles in the self-replicating tiling. Precise definitions and proofs are given in the Appendix.

THEOREM 5.31. *The quadruple point graph is finite. Let $[i,\gamma_1,j,\gamma_2,k,\gamma_3,l]\in\mathfrak{Q}$. Then the tiles $\mathcal{T}(i)$, $\mathcal{T}(j)+\gamma_1$, $\mathcal{T}(k)+\gamma_2$ and $\mathcal{T}(l)+\gamma_3$ have a nonempty intersection if and only if the quadruple point graph contains the node $\phi_{\mathfrak{Q}}[i,\gamma_1,j,\gamma_2,k,\gamma_3,l]$.*

Each point of the intersection $\mathcal{T}(i)\cap(\mathcal{T}(j)+\gamma_1)\cap(\mathcal{T}(k)+\gamma_2)\cap(\mathcal{T}(l)+\gamma_3)$ corresponds to an infinite path starting in one of these nodes.

EXAMPLE 5.32. The quadruple point graph for the substitution σ_0 is depicted in Figure 5.10. There are 5 quadruple intersections, as suggested by the tiling illustration in this figure. Since a unique path starts from each node, each node corresponds to an intersection of four tiles which contains one single point. It is easy to see that each infinite path in the quadruple point graph corresponds to a point that is different from the others. The quadruple points are depicted in Figure 5.10.

We use the quadruple point graph in order to decompose the pieces of the boundary of each tile: by (5.5) the intersections $B[i,\gamma,j]=\mathcal{T}(i)\cap(\mathcal{T}(j)+\gamma)$ are the solutions of a GIFS.

DEFINITION 5.33 (Boundary-refinement connectivity graph). Let $[i,\gamma,j]$ be a node of the SR-boundary graph such that $\mathcal{T}(i)\cap(\mathcal{T}(j)+\gamma)$ is not equal to a single point. The *boundary-refinement connectivity graph* of $\mathcal{T}(i)\cap(\mathcal{T}(j)+\gamma)$ admits for nodes the sets in the union on the right hand side of (5.5) that are not equal to a single point. Each two of them are connected by an edge if and only if they have nonempty intersection.

Concretely, the nodes of the graphs have the shape $\mathbf{e}^{(1)}+\mathbf{h}(\mathcal{T}(i_1)\cap(\mathcal{T}(j_1)+\gamma_1))$, where $[i,\gamma,j]\xrightarrow{\mathbf{e}^{(1)}}[i_1,\gamma_1,j_1]$ is an edge in the SR-boundary graph. There is an edge between $\mathbf{e}^{(1)}+\mathbf{h}(\mathcal{T}(i_1)\cap(\mathcal{T}(j_1)+\gamma_1))$ and $\mathbf{e}^{(2)}+\mathbf{h}(\mathcal{T}(i_2)\cap(\mathcal{T}(j_2)+\gamma_2))$ if and only if $\phi_{\mathfrak{Q}}[i_1,\gamma_1,j_1,\mathbf{h}^{-1}(\mathbf{e}^{(2)}-$

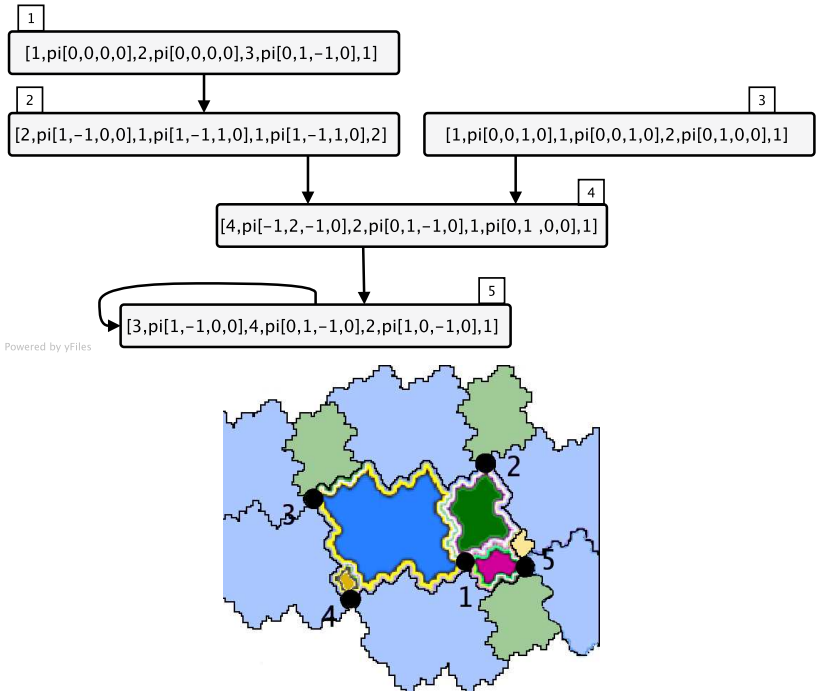

FIGURE 5.10. The quadruple point graph for the substitution σ_0. There are 5 nodes, with the shape $[i, \gamma_1, j, \gamma_2, k, \gamma_3, l]$, corresponding to an intersection between $\mathcal{T}(i)$, $\mathcal{T}(j) + \gamma_1$, $\mathcal{T}(k) + \gamma_2$ and $\mathcal{T}(l) + \gamma_3$. In this case there are 5 quadruple intersections. Since a unique path goes out from each node, quadruple intersections are single points. They are all different and marked by black dots on the tiling picture on the left hand side.

$\mathbf{e}^{(1)}), i_2, \gamma_2 + \mathbf{h}^{-1}(\mathbf{e}^{(2)} - \mathbf{e}^{(1)}), j_2)]$ is a node of the quadruple point graph (or the triple point graph if two of the pairs $[\mathbf{0}, i_1]$, $[\gamma_1, j_1]$, $[\mathbf{h}^{-1}(\mathbf{e}^{(2)} - \mathbf{e}^{(1)}), i_2]$, $[\gamma^{(2)} + \mathbf{h}^{-1}(\mathbf{e}^{(2)} - \mathbf{e}^{(1)}, j_2]$ coincide).

5.7. Application of the graphs to the disklikeness criterion

According to Theorem 4.12, checking whether the tile $\mathcal{T}(i)$ is homeomorphic to a disk amounts to checking the following three conditions.

(1) Each boundary-connectivity graph is a simple loop.
(2) Each boundary-refinement connectivity graph is either empty or a single node or a line.
(3) Each intersection between three distinct tiles of the self-replicating tiling is either empty or a single point.

EXAMPLE 5.34. Let us consider again the substitution $\sigma_0(1) = 112$, $\sigma_0(2) = 113$, $\sigma_0(3) = 4$, $\sigma_0(4) = 1$. We want to show in this example that each subtile $\mathcal{T}(i)$ $(1 \leq i \leq 4)$ of the central tile $\mathcal{T}$ of σ_0 is homeomorphic to a closed disk. To this matter we have to check the Items (1), (2) and (3) above.

***Checking (1)*:** The boundary-connectivity graphs of $\mathcal{T}(i)$ $(1 \leq i \leq 4)$ are depicted in Figure 5.9. Since they are all simple loops Item (1) is satisfied.

***Checking(2)*:** Checking the SR-boundary graph depicted in Figure 5.2 we verify the following assertions.

- The SR-boundary graph has 6 nodes having a unique outgoing path. Each of the corresponding intersection is therefore a single point. Thus the boundary-refinement connectivity graph is empty.
- The SR-boundary graph has 7 additional nodes having a single outgoing edge leading to several paths some of which are pairwise different. Their boundary-refinement connectivity graph is thus a single node.
- The SR-boundary graph has 4 nodes having two outgoing edges. Their boundary-refinement connectivity graph is either a pair of nodes linked by a single edge, or a single node (depending on whether the paths are essentially different or not).
- The SR-boundary graph has 4 remaining nodes that have at least three outgoing edges. These are the nodes $[1, \pi(0,1,-1,0),1]$, $[1, \pi(1,-1,1,0),1]$, $[2, \pi(1,-1,0,0),1]$ and $[1, \pi(0,1,0,0),1]$. Following (5.5), we obtain the GIFS decomposition of the boundary piece corresponding to the first node. It reads

$$\begin{aligned} B[1,\pi(0,1,-1,0),1] &= \mathbf{h}B[2,\pi(1,-1,0,0),1] \cup \mathbf{h}B[2,\pi(1,-1,0,0),1] + \pi(1,0,0,0) \\ &\quad \cup \mathbf{h}B[2,\pi(1,-1,0,0),4] \cup \mathbf{h}B[1,\pi(0,0,1,0),2] + \pi(0,1,-1,0) \\ &\quad \cup \mathbf{h}B[1,\pi(0,0,1,0),1] + \pi(0,1,-1,0). \end{aligned}$$

  In this decomposition, the last piece $\mathbf{h}B[1,\pi(0,0,1,0),1] + \pi(0,1,-1,0)$ is a single point. Therefore, we do not take it into account in the boundary-refinement connectivity graph. This latter graph thus contains 4 nodes. Intersections between the corresponding pieces of the central tile are checked by using the triple point graph and the quadruple point graph. The result is shown in Figure 5.11. Similarly, $B[1,\pi(1,-1,1,0),1]$ is made of 5 distinct pieces by the GIFS equation; 2 pieces among these 5 correspond to single points and are not relevant to the boundary-refinement connectivity graph. Finally $B[1,\pi(0,1,0,0),1]$ and $B[2,\pi(1,-1,0,0),1]$ have a GIFS decomposition in three pieces each; in each case, one piece of the three pieces is reduced to a single point). Their boundary-refinement graphs are depicted in Figure 5.11.

Summing up we get that all the boundary-refinement graphs are either empty or single points or lines. Thus Item (2) is satisfied.

***Checking (3)*:** In order to apply Theorem 4.12, we finally have to check that each intersection between three distinct tiles is empty or equal to a single point. Although the triple point graph will be our main tool, we will also use quadruple intersections as an auxiliary tool to show that this item is satisfied by σ_0. Observe that each quadruple intersection is a single point as a unique path leads away from each node of the quadruple point graph (see Figure 5.10).

We only have to check intersections which correspond to nodes of the triple point graph, as all the other triple intersections are empty. In the triple point graph, all nodes but three have a unique outgoing path. These exceptional nodes are $[1,\mathbf{0},4, \pi(0,1,0,0),1]$, $[1,\pi(0,0,1,0),2,\pi(1,-1,1,0),1]$ and $[2,\pi(1,-1,0,0),1,\pi(1,-1,0,0),4]$. As outlined in Proposition 5.30 we show that each of these intersections is a single point by inspecting the quadruple point graph. Indeed, for these three nodes, we write the GIFS decomposition of the corresponding intersection and get the following equations.

$$\begin{aligned} T[1,\mathbf{0},4,\pi(0,1,0,0),1] &= \mathbf{h}T[1,\mathbf{0},3,\pi(0,1,-1,0),1] \\ &\quad \cup \mathbf{h}T[2,\mathbf{0},3,\pi(0,1,-1,0),1], \\ T[2,\pi(1,-1,0,0),1,\pi(1,-1,0,0),4] &= \mathbf{h}T[1,\mathbf{0},3,\pi(0,1,-1,0),1] + \pi(0,1,-1,0) \\ &\quad \cup \mathbf{h}T[2,\mathbf{0},3,\pi(0,1,-1,0),1] + \pi(0,1,-1,0), \\ T[1,\pi(0,0,1,0),2,\pi(1,-1,1,0),1] &= \mathbf{h}T[1,\pi(0,0,1,0),2,\pi(0,1,0,0,1] \\ &\quad \cup \mathbf{h}T[1,\pi(0,0,1,0),1,\pi(0,1,0,0,1]. \end{aligned}$$

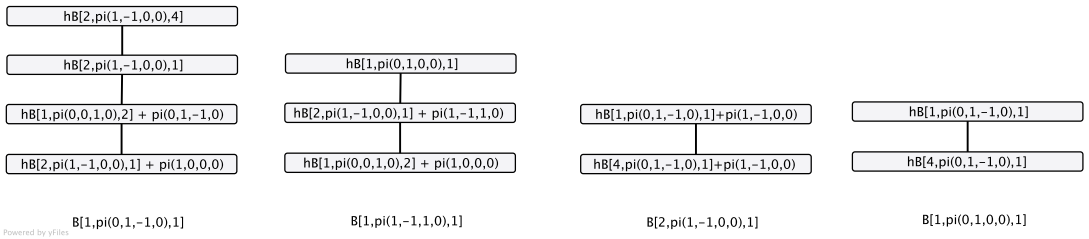

FIGURE 5.11. Nontrivial boundary-refinement connectivity graphs for the substitution σ_0. We considered the graph for the nodes of the SR-boundary graph that have at least three targets in the graph.

Here we remark that each piece appearing in the right part of the equations is equal to a single point, since a unique path leaves away from the corresponding node in the triple point graph. Additionally, we have

$$T[1,\mathbf{0},3,\pi(0,1,-1,0),1]\cap T[2,\mathbf{0},3,\pi(0,1,-1,0),1]=Q[1,\mathbf{0},2,\mathbf{0},3,\pi(0,1,-1,0),1],$$

and this node appears in the quadruple point graph.
Hence the intersections $T[1,\mathbf{0},3,\pi(0,1,-1,0),1]$ and $T[2,\mathbf{0},3,\pi(0,1,-1,0),1]$ are equal and correspond to the quadruple intersection $Q[1,\mathbf{0},2,\mathbf{0},3,\pi(0,1,-1,0),1]$. However, as from each node in the quadruple point graph there leads away only one single path, $Q[1,\mathbf{0},2,\mathbf{0},3,\pi(0,1,-1,0),1]$ is a single point. Thus also the intersection $T[1,\mathbf{0},4,\pi(0,1,0,0),1]$ is a single point. One checks in the same way that the same is true for the two others triple intersections that have more than one outgoing walk in the triple point graph. Thus Item (3) is satisfied.

Summing up we see that the conditions for disklikeness are satisfied. Therefore, each of the subtiles $\mathcal{T}(1),\dots,\mathcal{T}(4)$ of σ_0 is homeomorphic to a closed disk. It is not hard to check that the same is true for the central tile $\mathcal{T}$.

EXAMPLE 5.35. For σ_1 a similar reasoning leads to the conclusion that each of the subtiles $\mathcal{T}(1),\dots,\mathcal{T}(5)$ as well as $\mathcal{T}$ is homeomorphic to a closed disk. From Figure 3.1 we see that in this case there exist even 5-tuple points. Even if, according to Proposition 5.30 the 5-tuple graph would be needed in order to check that the triple intersections are single points, this can be proved in practice much easier by inspecting the different representations derived from the (finitely many) infinite paths of the triple point graph.

CHAPTER 6

Exact statements and proofs of the main results

In this chapter we give the exact statements of the main results of the present monograph that were already announced in Chapter 4. Moreover, we provide full proofs of all the results.

6.1. Tiling properties

Theorem 4.1 is proved in [**119**] for the SR-boundary graph. The proof of the analogous result using the contact graph runs along the same lines.

6.2. Dimension of the boundary of the subtiles $\mathcal{T}(i)$ $(i \in \mathcal{A})$

The GIFS description of the boundaries $\partial\mathcal{T}(i)$ $(i \in \mathcal{A})$ contained in Theorems 5.7 and 5.20 allow to compute its box counting dimension as proved for the irreducible case in [**124**, Proposition 5.7 and Theorem 5.9]. This directly implies Theorem 4.3 for the contact graph in the irreducible case. By arguing in the same way as in [**124**, Section 5] one can easily see that we can substitute the contact graph by the SR-boundary graph $\mathcal{G}_{SR}^{(B)}$ in Theorem 4.3. The reducible case is shown in exactly the same way. All we need in the proof is a GIFS decomposition of the boundary. This is given by the SR-boundary graph in the irreducible as well as in the reducible case. The formula of the box counting dimension including the contact graph works in the reducible cases only if the contact graph is defined (see Section 5.4 for details).

6.3. Inner points of $\mathcal{T}$ and the geometric property (F)

We have introduced in Chapter 3.1.2 the so-called *geometric property (F)*. Now we want to dwell upon the relation of this property to the localization of $\mathbf{0}$ in the central tile. In particular, we shall give the proofs of Theorems 4.5 and 4.6.

Let $\mathrm{Int}^*(\mathcal{T})$ be the set of exclusive inner points of the patch $\mathcal{T} = \mathcal{T}(1) \cup \ldots \cup \mathcal{T}(n)$ in the self-replicating tiling.

Proof of Theorem 4.5. Suppose first that the geometric property (F) holds: for all $[\gamma, i] \in \Gamma_{srs}$, γ has a finite $\mathbf{h}$-ary representation $\gamma = \mathbf{h}^{-m}\pi\mathbf{l}(p_{-m}) + \cdots + \mathbf{h}^{-1}\pi\mathbf{l}(p_{-1})$, where $(p_k, i_k, s_k)_{-m \le k < 0}$ is a finite walk in the prefix-suffix graph that ends at $i = i_0$.

Suppose now that $\alpha \in \mathcal{T}(i) + \gamma$ with $[\gamma, i] \in \Gamma_{srs}$. Then, by considering the $\mathbf{h}$-ary representation of $\alpha - \gamma$ given in (2.7), we obtain

$$\alpha \in \mathcal{T}(i) + \gamma \quad \Longleftrightarrow \quad \alpha = \sum_{k=-m}^{\infty} \mathbf{h}^k \pi\mathbf{l}(p_k) \tag{6.1}$$

where $(p_k, i_k, s_k)_{k \ge -m}$ is the labelling of a walk in the prefix-suffix graph such that $i_0 = i$.

Suppose that $\mathbf{0} \notin \mathrm{Int}^*(\mathcal{T})$. Then $\mathbf{0}$ is not an exclusive point of the patch $\mathcal{T} = \mathcal{T}(1) \cup \ldots \cup \mathcal{T}(n)$. Indeed, if it was an exclusive point of this patch then $\mathbf{0} \notin \mathrm{Int}^*(\mathcal{T})$. Thus $\mathbf{0} \in \partial\mathcal{T}$. But since $\mathcal{T}$ is a patch of the self-replicating multiple tiling there exists $[\gamma, i] \in \Gamma_{srs}$ with $\gamma \neq \mathbf{0}$ such that $\mathbf{0} \in \mathcal{T}(i) + \gamma$.

In view of (6.1) the existence of $[\gamma, i] \in \Gamma_{srs}$ with $\gamma \neq \mathbf{0}$ and $\mathbf{0} \in \mathcal{T}(i) + \gamma$ is equivalent to the existence of a representation of the shape

$$\mathbf{0} = \sum_{j=-m}^{\infty} \mathbf{h}^j \pi\mathbf{l}(p_j).$$

Multiplying this equation by $\mathbf{h}^{-k}$ yields $\mathbf{0} = \sum_{j=-m}^{\infty} \mathbf{h}^{j-k}\pi\mathbf{l}(p_j)$. Applying (6.1) again this implies that $\mathbf{0} \in \mathcal{T}(i_k) + \sum_{\ell=1}^{m+k} \mathbf{h}^{-\ell}\pi\mathbf{l}(p_{k-\ell})$ holds for each $k \in \mathbb{N}$, a contradiction to the local finiteness of self-replicating multiple-tiling Γ_{srs} (note that the representations in (3.6) are unique; thus each k yields a different value of the sum).

Now suppose on the contrary that the geometric property (F) does not hold. This implies that there exists

$$[\gamma_0, i_0] \in \Gamma_{srs} \setminus \bigcup_{m\geq 0} \mathbf{E}_1^m(\mathcal{U}).$$

Note that this assures that $\gamma_0 \neq \mathbf{0}$. Since Proposition 3.5 implies that $\mathbf{E}_1(\Gamma_{srs}) = \Gamma_{srs}$ we can define a sequence $([\gamma_k, i_k])_{k\geq 1}$ of elements of Γ_{srs} with

$$[\gamma_k, i_k] \in \mathbf{E}_1([\gamma_{k+1}, i_{k+1}]) \qquad (k \geq 0).$$

By the definition of $\mathbf{E}_1$ (recall in particular the contraction ratio (2.2) of the mapping $\mathbf{h}$) this yields

$$||\gamma_{k+1}|| \leq \max\{|\beta^{(j)}|;\, j = 2, \ldots, d\}||\gamma_k|| + \max\{\pi\mathbf{l}(p);\, (p, a, s) \in \mathcal{P}\}.$$

Since Γ_{srs} is a Delauney set by Proposition 3.7 there exists a $K \in \mathbb{N}$ such that

$$||\gamma_k|| \leq \frac{\max\{\pi\mathbf{l}(p);\, (p, a, s) \in \mathcal{P}\}}{1 - \max\{|\beta^{(j)}|;\, j = 2, \ldots, d\}} \qquad \text{for } k \geq K \tag{6.2}$$

(note that without the Delauney property we would get a slightly weaker bound). Again because Γ_{srs} is a Delauney set there exist only finitely many $[\gamma, i] \in \Gamma_{srs}$ satisfying the inequality in (6.2). For the sequence $([\gamma_k, i_k])_{k\geq 0}$ this means that there is a $K' > K$ and a $p > 0$ such that

$$[\gamma_{K'}, i_{K'}] = [\gamma_{K'+p}, i_{K'+p}]. \tag{6.3}$$

Now observe the following facts. Firstly, the definition of $\mathbf{E}_1$ implies that γ_0 admits a representation of the shape

$$\gamma_0 = \mathbf{h}^{-K'}\gamma_{K'} + \mathbf{h}^{-K'}p_0 + \cdots + \mathbf{h}^{-1}p_{K'-1}.$$

Note that $\gamma_{K'} \neq 0$ because otherwise $\gamma_0 \in \bigcup_{m\geq 0} \mathbf{E}_1^m(\mathcal{U})$ would hold contrary to our assumption. Secondly, the (nonzero) element $\gamma_{K'}$ admits by (6.3) and by the definition of $\mathbf{E}_1$ the representation

$$\gamma_0 = \mathbf{h}^{-p}\gamma_{K'} + \mathbf{h}^{-p}p_{K'} + \cdots + \mathbf{h}^{-1}p_{K'+p-1}.$$

However, by the definition of the zero-expansion graph $\mathcal{G}^{(\mathbf{0})}$ this is equivalent to the existence of a loop

$$\gamma_{K'} \to \gamma_{K'+p-1} \to \cdots \to \gamma_{K'+1} \to \gamma_{K'}$$

in $\mathcal{G}^{(\mathbf{0})}$. In view of Proposition 5.2 this implies that $\mathbf{0} \in \mathcal{T}(i_{K'}) + \gamma_{K'}$. Since $\gamma_{K'} \neq \mathbf{0}$ this yields $\mathbf{0} \notin \mathrm{Int}^*(\mathcal{T})$ and we are ready.

□

Proof of Theorem 4.6. The fact that the zero-expansion graph only contains nodes of the shape $[0, i]$ ($i \in \mathcal{A}$) is equivalent to $\mathbf{0} \in \mathrm{Int}^*(\mathcal{T})$ by Proposition 5.2. But by Theorem 4.5, $\mathbf{0} \in \mathrm{Int}^*(\mathcal{T})$ is equivalent to the geometric property (F) and we are done. □

6.4. Connectivity

We need the following definitions.

Definition 6.1. Let $\{Q_1, \ldots, Q_\nu\}$ be a finite collection of subsets.

- We say that $\{Q_1, \ldots, Q_\nu\}$ ($\nu \geq 1$) forms a *finite chain* joining Q_1 and Q_ν if $Q_i \cap Q_{i+1} \neq \emptyset$ for each $i \in \{1, \ldots, \nu - 1\}$.
- We say that $\{Q_1, \ldots, Q_\nu\}$ ($\nu \geq 1$) forms a *regular chain*, if $|Q_i \cap Q_{i+1}| = 1$ for each $i \in \{1, \ldots, \nu + 1\}$ and $Q_i \cap Q_j = \emptyset$ if $|i - j| \geq 2$.
- We say that $\{Q_1, \ldots, Q_\nu\}$ ($\nu \geq 2$) forms a *circular chain*, if $|Q_i \cap Q_{i+1}| = 1$ for each $i \in \{1, \ldots, \nu + 1\}$, $|Q_\nu \cap Q_1| = 1$ and $Q_i \cap Q_j = \emptyset$ if $2 \leq |i - j| \leq \nu - 2$.

In [**91**] the following result on the connectivity of GIFS was shown.

LEMMA 6.2 ([**91**, Theorem 4.1]). *Let $S = S_1 \cup \ldots \cup S_q$ be a GIFS with graph $G(V, E)$ and contractions F_e ($e \in E$) and set*

$$\mathcal{E}_i := \{F_e(S_j)\,;\, e \text{ is an edge from } i \text{ to } j \text{ in } G(V, E)\}.$$

Then S_j is a locally connected continuum (or a single point) for each $j \in \{1, \ldots, q\}$ if and only if for each $i \in \{1, \ldots, q\}$ and each pair $X_1, X_2 \in \mathcal{E}_i$ there exists a finite chain $\mathcal{C}$ in $\mathcal{E}_i$ joining X_1 and X_2.

We can use Lemma 6.2 in order to derive the criterion given in Chapter 3 for the connectivity of $\mathcal{T}(a)$.

PROOF OF THEOREM 4.8. Let $i \in \mathcal{A}$ and let E_i be the set of all tiles whose union is equal to $\mathbf{h}^{-1}\mathcal{T}(i)$, *i.e.*,

$$E_i = \{\mathcal{T}(j) + \gamma;\, \exists\,(p, s),\, \sigma(j) = pis \text{ and } \gamma = \mathbf{h}^{-1}\pi(\mathbf{l}(p))\}.$$

By its definition, every pair of tiles $\mathcal{T}(j_1) + \gamma_1$, $\mathcal{T}(j_2) + \gamma_2 \in E_i$ do intersect if and only if the $\mathcal{T}(i)$-connectivity graph contains an edge between $\mathbf{h}\mathcal{T}(j_1) + \gamma_1$ and $\mathbf{h}\mathcal{T}(j_2) + \gamma_2$.

Hence, a sequence of tiles $\mathcal{T}(c_\ell) + \alpha_\ell \in E_i$ ($1 \le \ell \le k$) is a finite chain in E_i if and only if the $\mathcal{T}(i)$-connectivity graph is connected. The part concerning the sets $\mathcal{T}(i)$ of Theorem 4.8 follows from Lemma 6.2 (note that the single point case is excluded since $\mathcal{T}(i)$ is the closure of its interior).

The part concerning $\mathcal{T}$ is now easy. What we proved until now ensures that the $\mathcal{T}(i)$ are connected. The connectivity of the $\mathcal{T}$-connectivity graph ensures that the connected sets $\mathcal{T}(i)$ ($i \in \mathcal{A}$) form a finite chain. Thus their union is connected by standard plane topology. □

6.5. Homeomorphy to a closed disk

6.5.1. Necessary condition coming from the lattice tiling property. We start with a very simple criterion that allows to conclude that a certain central tile $\mathcal{T}$ is not homeomorphic to a closed disk. Suppose that $\mathcal{T}$ is homeomorphic to a closed disk. Suppose further that $\mathcal{T}$ admits a tiling of $\mathbb{R}^2$ with respect to a lattice Γ. In Bandt and Gelbrich [**27**, Section 5] it is shown in a more general context[6.1] that under these conditions the intersections $(\mathcal{T}+\gamma)\cap(\mathcal{T}+\gamma')$ ($\gamma \neq \gamma'$) are either empty or a single point or a simple arc. To identify such intersections, we use the lattice boundary graph $\mathcal{G}_{lat}^{(B)}$ defined in Chapter 5.2 and Proposition 5.12. More precisely, [**27**, Lemma 5.1] implies the following result.

LEMMA 6.3. *Let σ be a primitive unit Pisot substitution whose dominant eigenvalue has degree 3. Suppose that the lattice multiple tiling is a tiling (see Theorem 4.1). Suppose further that the associated central tile $\mathcal{T}$ is homeomorphic to a closed disk. Then the central tile $\mathcal{T}$ has at most eight neighbors. Moreover, it has at most six neighbors γ with the property*

$$|\mathcal{T} \cap (\mathcal{T} + \gamma)| > 1.$$

Now we may apply Proposition 5.12 in order to get the following simple criterion for a central tile to be not homeomorphic to a closed disk.

THEOREM 6.4. *Let σ be a primitive unit Pisot substitution whose dominant eigenvalue has degree 3. Suppose that the lattice multiple tiling is a tiling (see Theorem 4.1).*

The central tile $\mathcal{T}$ is not homeomorphic to a closed disk as soon as at least one of the following assertions is true.

- *There exist pairwise disjoint $\gamma_1, \ldots, \gamma_9$ such that the lattice boundary graph contains states of the shape $[i_k, \gamma_k, j_k]$ with $[\gamma_k, j_k] \in \Gamma_{lat}$.*

[6.1] In fact the arguments there are a bit heuristic. However, they can be made exact with little effort.

- *There exist pairwise disjoint $\gamma_1, \ldots, \gamma_7$ each of which satisfies the following property: there exist at least two essentially different walks in the lattice boundary graph that start in nodes of the shape $[i, \gamma_k, j]$ with $[\gamma_k, j] \in \Gamma_{lat}$.*

These conditions can obviously be checked algorithmically. Theorem 4.10 follows naturally. Examples of application are given in Example 5.13. Note that in general Remark 5.30 is needed in order to decide whether a given intersection contains more than one point.

6.5.2. Preliminary results on GIFS. In a next step we wish to give a criterion for a GIFS to be homeomorphic to a closed disk. To this matter we need some preparations.

Let $S_1, \ldots, S_q$ be solutions of a GIFS directed by a graph $G(V, E)$ with $V := \{1, \ldots, q\}$. To each edge $e \in E$ there is associated a contraction F_e. By $W_i(\nu)$ ($i \in V$, $\nu \in \mathbb{N}$) we denote the set of walks in G starting at i and having length ν. Let $w = e_1 \ldots e_\nu \in W_i(\nu)$. Then we set

$$F_w := F_{e_1} \circ \cdots \circ F_{e_\nu}.$$

We start with a variant of [**71**, Theorem 5.3] for GIFS.

LEMMA 6.5. *Let $S_1, \ldots, S_q$ be solutions of a GIFS with injective contractions directed by a graph G with set of vertices $\{1, \ldots, q\}$ and set of edges E. Let E_i be the set of edges in G starting at i. Then*

$$S_i = \bigcup_{e : i \xrightarrow{\ell} j \in E_i} F_e(S_j)$$

with some injective contractions F_e ($e \in E$). Assume that the collection

$$\mathcal{C}_i := \left\{ F_e(S_j)\,;\, e : i \xrightarrow{\ell} j \in E_i \right\}$$

forms a regular chain for each $i \in V$. Then S_i does not separate the plane.

PROOF. Suppose that S_i separates the plane for some $i \in V$. Since by Lemma 6.2 the set S_i is a locally connected continuum, there exists a simple closed curve $C \subset S_i$ which separates the plane (*cf.* [**82**, §62, VI, Theorem 1]). Since C has positive diameter, there exists a maximal $\nu \in \mathbb{N}$ such that $C \subset F_w(S_j)$ for some $w \in W_i(\nu)$. Fix this w. Since F_w is injective, we conclude that $D := F_w^{-1}(C)$ is a simple closed curve satisfying

$$D \subset S_j.$$

By the assumptions we know that

$$S_j = \bigcup_{e \in E_j} F_e(S_k)$$

where the sets in the union form a regular chain. However, by the maximality of ν there exist two different sets $F_{e_1}(S_{k_1})$ and $F_{e_2}(S_{k_2})$ with the property that

$$D \cap (F_{e_1}(S_{k_1}) \setminus F_{e_2}(S_{k_2})) \neq \emptyset \quad \text{and} \quad D \cap (F_{e_2}(S_{k_2}) \setminus F_{e_1}(S_{k_1}) \neq \emptyset)\,.$$

Thus there exist two different paths leading from a point in $F_{e_1}(S_{k_1})$ to a point in $F_{e_2}(S_{k_2})$ contradicting the fact that $\mathcal{C}_j$ forms a regular chain. □

Furthermore, we need the following simple result about the refinement of circular chains.

LEMMA 6.6. *Let $\{Q_1, \ldots, Q_\nu\}$ be a circular chain. Suppose that Q_1 can be represented as*

$$Q_1 = R_1 \cup \ldots \cup R_m, \tag{6.4}$$

where $\{R_1, \ldots, R_m\}$ is a regular chain.

Then (possibly after reverting the order of the R_i) there exist $1 \leq i \leq j \leq m$ such that

$$\{R_i, \ldots, R_j, Q_2, \ldots, Q_\nu\} \tag{6.5}$$

forms a circular chain. Moreover, if $i > 1$ then

$$|R_1 \cap (R_2 \cup \ldots \cup R_m \cup Q_2 \cup \ldots \cup Q_\nu)| = 1 \tag{6.6}$$

and if $j < m$ then

$$|R_m \cap (R_1 \cup \ldots \cup R_{m-1} \cup Q_2 \cup \ldots \cup Q_\nu)| = 1.$$

PROOF. From (6.4) we conclude that

$$\exists i, j \in \{1, \ldots, m\} : R_i \cap Q_\nu \neq \emptyset,\ R_j \cap Q_2 \neq \emptyset.$$

If i and j are not unique choose them in a way such that the subchain $\{R_i, \ldots, R_j\}$ is as short as possible. Furthermore, assume that $\{R_1, \ldots, R_m\}$ is ordered in a way that $i \leq j$ holds.

It is now a routine matter to check that (6.5) is a circular chain. Firstly, it is clear that $R_i \cap Q_\nu$, $R_\ell \cap R_{\ell+1}$ $(1 \leq \ell \leq m-1)$, $R_j \cap Q_2$ and $Q_\ell \cap Q_{\ell+1}$ each contain exactly one point. Furthermore, the unions $R_k \cap R_\ell$ and $Q_k \cap Q_\ell$ are empty if the indices differ by more than 1. Since $R_k \subset Q_1$ holds for each $k \in \{1, \ldots, m\}$ we have $Q_\ell \cap R_k = \emptyset$ for $\ell \notin \{2, \nu\}$. It remains to check

$$Q_2 \cap R_\ell = \emptyset \quad (\ell \neq j) \quad \text{and} \quad Q_\nu \cap R_\ell = \emptyset \quad (\ell \neq i).$$

If one of these unions were nonempty, this would contradict the fact that we have chosen i and j in a way that the subchain $\{R_i, \ldots, R_j\}$ is as small as possible.

For the second assertion assume that $i > 1$. Then, since $\{R_1, \ldots, R_m\}$ forms a regular chain, $R_1 \cap R_2 = \{p\}$ and $R_1 \cap R_\ell = \emptyset$ for $\ell > 2$. Because $R_1 \subset Q_1$ we conclude that $R_1 \cap Q_\ell = \emptyset$ if $\ell \in \{3, \ldots \nu - 1\}$. It remains to check the intersections $R_1 \cap Q_2$ and $R_1 \cap Q_\nu$.

Suppose that the intersection $R_1 \cap Q_2$ is nonempty. Then it can contain at most one point q, say. Because $R_i \cap Q_2 \neq \emptyset$ for some $i > 1$ and $|(R_1 \cup R_i) \cap Q_2| \leq |Q_1 \cap Q_2| = 1$ we must have

$$q \in (R_1 \cap Q_2) \cap (R_i \cap Q_2).$$

Thus $R_1 \cap R_i \neq \emptyset$ which implies that $i = 2$. Hence, $q \in R_1 \cap R_2$ and thus $q = p$ because this intersection contains only one point. The intersection $R_1 \cap Q_\nu$ is treated likewise by observing that $j \geq i > 1$. Thus p is the only point contained in the intersection (6.6).

Finally, the third assertion is proved in the same way as the first one. □

We now establish a criterion for the solution of a GIFS to be a simple closed curve. To this matter we will use regular and circular chains, already used in [**92, 94**]. We will use the following results from topology.

LEMMA 6.7 (Janiszewski's first theorem, see [**82**, §61, I, Theorem 7]). *Suppose that M_1 and M_2 are two subsets of $\mathbb{R}^2$ with $|M_1 \cap M_2| = 1$. If $M_1 \cup M_2$ separates the plane then the same is true for M_1 or M_2.*

LEMMA 6.8 (*cf.* [**82**, §52, IV, Theorem 1]). *If $X \subset \mathbb{R}^2$ is a locally connected continuum containing no separating point and no θ-curve, then X is a simple closed curve (unless it is a single point).*

6.5.3. A sufficient condition for the subtiles $\mathcal{T}(i)$ $(i \in \mathcal{A})$ to be homeomorphic to a disk. We first give some preliminaries on GIFS. Because $\mathbb{R}^2$ is a Janiszewski Space (this follows immediately from [**82**, §61, I, Theorem 2]) we get the following result.

LEMMA 6.9. *Let $T \subset \mathbb{R}^2$ be a set having the following properties.*

- *T is the closure of its interior.*
- *$\partial T = S_1 \cup \ldots \cup S_q$ where $S_1, \ldots, S_Q$ $(Q \geq q)$ are the solution of a GIFS directed by a graph $G(V, E)$ with $V = \{1, \ldots, Q\}$.*
- *$\{S_1, \ldots, S_q\}$ is a circular chain.*
- *The elements of the union*

$$S_i = \bigcup_{e : i \xrightarrow{\ell} j} F_e(S_j) \qquad (1 \leq i \leq Q) \tag{6.7}$$

form a regular chain.

Then

$$K_{\nu_1,\ldots,\nu_q} := \{F_w(S_i)\,;\, i \in V,\, w \in W_{\nu_i}(i)\}$$

is a circular chain.

REMARK 6.10. Note that iteration of the GIFS equation for $S_1, \ldots, S_q$ yields

$$\partial T := \bigcup_{Z \in K_{\nu_1,\ldots,\nu_q}} Z.$$

PROOF. The proof is done by induction on $\nu := \sum_{i=1}^{q} \nu_i$. Let

$$\mathcal{K}_\nu := \left\{ K_{\nu_1,\ldots,\nu_q}\,;\, \sum_{i=1}^{q} \nu_i = \nu \right\}.$$

The induction start is simple as the assertion is true for the only element $\{S_1, \ldots, S_q\}$ of $\mathcal{K}_0$ by assumption.

To perform the induction step assume from now that the assertion has already been proved for all elements of $\mathcal{K}_\nu$. We need to show that it is also true for all elements of $\mathcal{K}_{\nu+1}$. Note that each element $K \in \mathcal{K}_{\nu+1}$ emerges from a circular chain $K' \in \mathcal{K}_\nu$ by replacing an

$$F_w(S_i) \in K'$$

by the collection

$$\{F_{w\circ e}(S_j)\,;\, e : i \xrightarrow{\ell} j \text{ is an edge in } G(V,E)\}. \tag{6.8}$$

In view of Lemma 6.6 there are two possibilities for K.

(i) K is a circular chain. In this case we are ready.

(ii) There is a set $X := F_{w\circ e_0}(S_{j_0})$ in the collection (6.8) such that, setting $Y := \bigcup_{Z \in K\setminus\{X\}} Z$ we have

$$\partial T = X \cup Y$$

with $X \cap Y = \{p\}$, a single point. Let $x \in X \setminus Y$. Since Y is a compact set there exists $\varepsilon > 0$ such that

$$B_\varepsilon(x) \cap Y = \emptyset. \tag{6.9}$$

Because T is the closure of its interior, $x \in \partial T$ implies the existence of $x_1, x_2 \in B_\varepsilon(x)$ with $x_1 \in \mathrm{int}(T)$ and $x_2 \in \mathbb{R}^2 \setminus T$. Thus ∂T separates x_1 and x_2. Lemma 6.7 now implies that X or Y separates x_1 and x_2. From (6.9) we immediately see that X separates x_1 and x_2.

On the other hand, $X \subset S_i$ holds for some $i \in V$. Since the union in (6.7) forms a regular chain, Lemma 6.5 implies that S_i does not separate the plane. Thus also X does not separate the plane, a contradiction.

So only case (i) can occur and, hence, $\mathcal{K}_{\nu+1}$ contains only circular chains. This concludes the induction proof. □

The following proposition is of interest in its own right. It provides a criterion for the homeomorphy to a disk that is usable for large classes of IFS tiles as well as GIFS tiles. We will use it to derive a criterion for the homeomorphy to a disk of the subtiles $\mathcal{T}(i)$ $(i \in \mathcal{A})$ which can be checked algorithmically by using the graphs we introduced in the previous chapter.

PROPOSITION 6.11. *Let $T \subset \mathbb{R}^2$ be a set having the following properties.*

- *T is the closure of its interior.*
- *$\partial T = S_1 \cup \ldots \cup S_q$ where $S_1, \ldots, S_Q$ $(Q \geq q)$ are the solution of a GIFS directed by a graph $G(V,E)$ with $V = \{1, \ldots, Q\}$.*
- *$\{S_1, \ldots, S_q\}$ is a circular chain.*

- *The elements of the union*

$$S_i = \bigcup_{e:i\xrightarrow{\ell}j} F_e(S_j) \qquad (1 \le i \le Q)$$

form a regular chain.

Then ∂T is a simple closed curve and T is homeomorphic to a closed disk.

REMARK 6.12. Let $\mathcal{C}'$ be the subcollection of $\mathcal{C} = \{S_1, \dots, S_q\}$ consisting of all S_i with $\#S_i > 1$. Lemma 6.11 and Proposition 6.9 remain true if we replace the condition $\mathcal{C}$ *forms a circular chain* by the condition $\mathcal{C}'$ *forms a circular chain.* This is true by the same arguments as in the proof of Lemma 5.8.

PROOF. We prove the result in three steps.

(i) S_i is a locally connected continuum for each $i \in V$. This is a consequence of Lemma 6.2.

(ii) $\partial T = S_1 \cup \ldots \cup S_q$ contains no separating point. To see this assume on the contrary that there exist $p_1, p_2 \in \partial T$ which are separated by $s \in \partial T$. According to Lemma 6.9 there is a circular chain $K \in \mathcal{K}_\nu$ such that

$$\operatorname{diam} C < \varepsilon$$

holds for each $C \in K$ with

$$\varepsilon < \frac{1}{2}\min(|p_1 - p_2|, |p_1 - s|, |p_2 - s|).$$

Thus there exist different sets $C_{p_1}, C_{p_2}, C_s \in K$ with

$$p_1 \in C_{p_1} \setminus (C_{p_2} \cup C_s), \quad p_2 \in C_{p_2} \setminus (C_{p_1} \cup C_s), \quad s \in C_s \setminus (C_{p_1} \cup C_{p_2}).$$

Since K is a circular chain, C_{p_1} and C_{p_2} can be connected by elements of $K \setminus \{C_s\}$. Because all elements of K are locally connected continua this implies that p and q can be connected by an arc avoiding C_s and, hence, avoiding s, a contradiction.

(iii) ∂T contains no θ-curve. Let a_1, a_2, a_3 be the simple arcs that form the θ-curve and let $p_i \in \operatorname{int} a_i$ and $s \in a_1 \cap a_2 \cap a_3$. Choose

$$\varepsilon < \frac{1}{2}\min_{i\neq j}(|p_i - p_j|, |p_i - s|).$$

By Lemma 6.9 there is a circular chain $K \in \mathcal{K}_\nu$ with

$$\operatorname{diam} C < \varepsilon \quad \text{for all } C \in K.$$

Choose $C_1, C_2, C_3, D \in K$ such that $p_i \in C_i$ and $s \in D$ (by the choice of ε the sets C_1, C_2, C_3, D have pairwise empty intersection). Since K is a circular chain there exist the subchains

$$C_1 = E_1 \hookleftarrow E_2 \hookleftarrow \cdots \hookleftarrow E_{\ell_1} \hookleftarrow D,$$
$$C_2 = F_1 \hookleftarrow F_2 \hookleftarrow \cdots \hookleftarrow F_{\ell_2} \hookleftarrow D,$$
$$C_3 = G_1 \hookleftarrow G_2 \hookleftarrow \cdots \hookleftarrow G_{\ell_3} \hookleftarrow D.$$

Suppose first that E_i, F_j, G_k are pairwise distinct elements of K. Then D has nonempty intersection with each of the sets $E_{\ell_1}, F_{\ell_2}, G_{\ell_3}$ which is impossible for the elements of a circular chain.

If these elements are not pairwise distinct elements of K we may assume w.l.o.g. that there exist $j, k > 1$ minimal, such that $E_j = F_k$. In this case the set E_j has (setting $E_{\ell_1+1} := D$ if necessary)

$$E_{j-1} \cap E_j \neq \emptyset, \quad F_{k-1} \cap E_j \neq \emptyset, \quad E_{j+1} \cap E_j \neq \emptyset.$$

By the minimality of j and k this means that E_j intersects three distinct elements of K, a contradiction to the fact that K is a circular chain. Thus ∂T contains no θ-curve.

By (i), (ii) and (iii) we conclude from Lemma 6.8 that ∂T is a simple closed curve. The fact that T is homeomorphic to a closed disk now follows from the Jordan Curve Theorem (*cf.* [**82**, §61, II, Theorem 1]). □

From this result we deduce the following algorithmic criterion for the subtiles $\mathcal{T}(i)$ to be homeomorphic to a disk.

THEOREM 6.13. *Let σ be a primitive unit Pisot substitution whose dominant eigenvalue has degree 3. Suppose that the self-replicating multiple tiling is a tiling (see Theorem 4.1). Then each of the subtiles $\mathcal{T}(i)$ ($i \in \mathcal{A}$) are homeomorphic to a closed disk as soon as the following conditions are satisfied.*

1. *The boundary-connectivity graph of $\mathcal{T}(i)$ is either a single node or a circle for each $i \in \mathcal{A}$.*
2. *For each $i \in \mathcal{A}$ each edge of the boundary-connectivity graph of $\mathcal{T}(i)$ corresponds to an intersection containing exactly one point.*
3. *For each node $[i, \gamma, j]$ of $\mathcal{G}_{srs}^{(B)}$, the boundary-refinement connectivity graph of $B[i, \gamma, j]$ is either empty or a line (that may degenerate to a single node).*
4. *For each node $[i, \gamma, j]$ of $\mathcal{G}_{srs}^{(B)}$ each edge of the boundary-refinement connectivity graph of $B[i, \gamma, j]$ corresponds to an intersection containing exactly one point.*

REMARK 6.14. If we consider also the case contained in Remark 4.13 one could show with some effort that the above criterion is necessary and sufficient for the subtiles to be homeomorphic to a closed disk.

PROOF. The proof follows immediately from Proposition 6.11 and Remark 6.12 after it. The first two conditions of this proposition are fulfilled by each subtile $\mathcal{T}(i)$. The third condition follows from (1) and (2) and the forth condition is true because of (3) and (4). □

It remains to explain how to check the conditions of Theorem 6.13 algorithmically using the graphs we have at our disposal.

Checking (1) and (3): corresponds to building the boundary-connectivity graph and the boundary-refinement connectivity graph.

Checking (2) and (4): We successively consider each edge of the boundary-connectivity graph and the boundary-refinement connectivity graph. We consider the node of the triple of quadruple point graph that was computed in order to check that the considered edge did exist. And we check that the walks leading away from this node are pairwise not essentially different (see Remark 5.30). This is especially true when the node and all its successors have degree 1 (see Theorem 5.25).

6.6. The fundamental group

In this section we want to establish criteria that allow to conclude that a given central tile has nontrivial or even uncountable fundamental group. The proof of these criteria relies on the following topological lemmas.

LEMMA 6.15 ([**93**, Lemma 6.1]). *Let $B_0, B_1, B_2 \subset \mathbb{R}^2$ be locally connected continua with the following properties.*

(i) $\operatorname{int}(B_i) \cap \operatorname{int}(B_j) = \emptyset$ *for* $i \neq j$.
(ii) B_i *is the closure of its interior* ($0 \leq i \leq 2$).
(iii) $\mathbb{S}^2 \setminus \operatorname{int}(B_i)$ *is a locally connected continuum* ($0 \leq i \leq 2$).
(iv) *There exist* $x_1, x_2 \in B_0 \cap B_1 \cap B_2$ *with* $x_1 \in \operatorname{int}(B_0 \cup B_1 \cup B_2)$.

Then there is an $i \in \{0, 1, 2\}$ such that $B_i \cup B_{i+1}$ has a bounded complementary component U with $U \cap \operatorname{int}(B_{i+2}) \neq \emptyset$ (the indices are to be taken modulo 3).

LEMMA 6.16. [**93**, Proposition 4.1] *Let $K \subset \mathbb{S}^2$ be a locally arcwise connected set. If $\mathbb{S}^2 \setminus K$ is disconnected then K contains a non-trivial loop.*

LEMMA 6.17. [**93**, Proposition 4.2] *Let $K \subset \mathbb{S}^2$ be a locally arcwise connected continuum. Suppose that $\mathbb{S}^2 \setminus K$ has infinitely many components. Then the following assertions hold.*

(i) *$\pi_1(K)$ is not free.*
(ii) *$\pi_1(K)$ is uncountable.*
(iii) *K is not locally simply connected.*
(iv) *K has no universal cover.*

We now state the first result on the fundamental group. After that we discuss how it can be checked by using the graphs we defined in Chapter 5.

THEOREM 6.18. *Suppose that σ is a primitive unit Pisot substitution whose dominant eigenvalue has degree 3. Suppose that $\mathcal{T}(j)$ is connected for each $j \in \mathcal{A}$ and that the self-replicating multiple tiling associated to σ is a tiling (see Theorem 4.1). Then the subtile $\mathcal{T}(i)$ ($i \in \mathcal{A}$) has nontrivial fundamental group as soon as there exist $[\gamma_1, i_1]$, $[\gamma_2, i_2] \in \Gamma_{srs}$ such that $[0, i]$, $[\gamma_1, i_1]$, $[\gamma_2, i_2]$ are pairwise disjoint and the following conditions are satisfied.*

(1) *The intersection $\mathcal{T}(i) \cap (\mathcal{T}(i_1)+\gamma_1) \cap (\mathcal{T}(i_2)+\gamma_2)$ contains at least two elements $\mathbf{x}_1, \mathbf{x}_2$. The point $\mathbf{x}_1$ is contained in $\operatorname{int}(\mathcal{T}(i) \cup (\mathcal{T}(i_1)+\gamma_1) \cup (\mathcal{T}(i_2)+\gamma_2))$.*
(2) *Let $[\gamma_0, i_0] := [0, i]$ for convenience. Then there exists an integer N such that for all $\ell \in \{0, 1, 2\}$ one can find $\mathbf{v}_\ell \in \pi(\mathbb{Z}^d)$ such that $[\gamma_\ell + \mathbf{v}_\ell, i_\ell] \in \Gamma_{srs}$ and (indices are to be taken* mod 3*)*

$$[\gamma_\ell + \mathbf{v}_\ell, i_\ell] \notin \mathbf{E}_1^N[0, i], \qquad [\gamma_{\ell+1} + \mathbf{v}_\ell, i_{\ell+1}] \in \mathbf{E}_1^N[0, i], \qquad [\gamma_{\ell+2} + \mathbf{v}_\ell, i_{\ell+2}] \in \mathbf{E}_1^N[0, i].$$

SEE [**93**, Proposition 6.2] FOR THE LATTICE TILE ANALOGUE. We first prove that $B_0 := \mathcal{T}(i)$, $B_1 := \mathcal{T}(i_1) + \gamma_1$ and $B_2 := \mathcal{T}(i_2) + \gamma_2$ satisfy the conditions of Lemma 6.15. Indeed all are locally connected continua by Theorem 4.8 (connectivity of each $\mathcal{T}(i)$ implies the local connectivity of each of them).

Condition (i) of Lemma 6.15 is true because we assume the tiling property in the statement of the theorem and Condition (ii) follows because each tile $\mathcal{T}(j)$, $j \in \mathcal{A}$, as well as each of their translates is the closure of its interior by Theorem 2.6. Condition (iii) is true because the closed connected set $\mathbb{R}^2 \setminus \operatorname{int}(\mathcal{T}(j))$ can be written as a locally finite union of translates of the tiles by the tiling property. Thus it is also locally connected and its closure in $\mathbb{S}^2$, the set $\mathbb{S}^2 \setminus \operatorname{int}(\mathcal{T}(j))$, is a locally connected continuum. The same holds for each translate of $\mathcal{T}(j)$. Condition (iv) of Lemma 6.15 is just the same as condition (1) of the theorem.

Thus we may apply Lemma 6.15 and therefore assume that for some $\ell \in \{0, 1, 2\}$ there is a point $\mathbf{z} \in \operatorname{int}(\mathcal{T}(i_\ell) + \gamma_\ell)$ which is contained in a bounded complementary component of $(\mathcal{T}(i_{\ell+1}) + \gamma_{\ell+1}) \cup (\mathcal{T}(i_{\ell+2}) + \gamma_{\ell+2})$. In view of condition (2) we know that $\mathcal{T}(i_\ell) + \gamma_\ell + \mathbf{v}_\ell$ is a piece of the self-replicating tiling but it is not a piece of $\mathbf{h}^{-N}\mathcal{T}(i)$ since

$$\mathbf{h}^{-N}\mathcal{T}(i) = \bigcup_{[\gamma,k] \in \mathbf{E}_1^N[0,i]} (\mathcal{T}(k) + \gamma).$$

By the tiling assumption, we deduce that $\operatorname{int}(\mathcal{T}(i_\ell) + \gamma_\ell + \mathbf{v}_\ell)$ has nonempty intersection with $\mathbf{h}^{-N}\mathcal{T}(i)$. This means that $\mathbf{z} + \mathbf{v}_\ell$ is contained in a complementary component of $\mathbf{h}^{-N}\mathcal{T}(i)$.

But condition (2) also implies that both $(\mathcal{T}(i_{\ell+1}) + \mathbf{v}_\ell + \gamma_{\ell+1})$ and $(\mathcal{T}(i_{\ell+2}) + \mathbf{v}_\ell + \gamma_{\ell+2})$ are subsets of $\mathbf{h}^{-N}\mathcal{T}(i)$. We deduce that the complementary component of $\mathbf{h}^{-N}\mathcal{T}(i)$ that contains $\mathbf{z}+\mathbf{v}_\ell$ is included in the bounded complementary component of $(\mathcal{T}(i_{\ell+1})+\mathbf{v}_\ell+\gamma_{\ell+1}) \cup (\mathcal{T}(i_{\ell+2})+\mathbf{v}_\ell+\gamma_{\ell+2})$ that contains $\mathbf{z} + \mathbf{v}_\ell$; therefore it is bounded.

Thus $\mathbf{h}^{-N}\mathcal{T}(i)$ and therefore also $\mathcal{T}(i)$ has a least one bounded complementary component. The result now follows from Lemma 6.16. □

It remains to explain how to check the conditions of Theorem 6.18 algorithmically using the graphs we have at our disposal.

Checking (1) algorithmically: The existence of at least two points $\mathbf{x}_1, \mathbf{x}_2 \in \mathcal{T}(i) \cap (\mathcal{T}(i_1)+\gamma_1) \cap (\mathcal{T}(i_2)+\gamma_2)$ can be checked with help of the triple point graph by using Theorem 5.25 and Proposition 5.30.

The fact that the point $\mathbf{x}_1$ is contained in $\mathrm{int}(\mathcal{T}(i) \cup (\mathcal{T}(i_1) + \gamma_1) \cup (\mathcal{T}(i_2) + \gamma_2))$ means that $\mathbf{x}$ is a triple point but not a quadruple point. Thus in view of Theorems 5.25 and 5.31 such a point exists if a certain infinite walk which exists in the triple point graph does not exist in the quadruple point graph.

Checking (2): This is done by exhaustively checking the composition of $\mathbf{E}_1^N[0, i]$ for increasing N. More precisely, we consider $[0, i]$, $[\gamma_1, i_1]$, $[\gamma_2, i_2]$ that satisfy (1). We fix N. For every $\mathbf{v}$ whose modulus is bounded by the sum of the maximal modulus of a vector in $\mathbf{E}_1^N[0, i]$ $(\ell = 1, 2, 3)$ and the maximal modulus of the vectors γ_ℓ, we shift the three faces $[\gamma_\ell, i_\ell]$ $(0 \le \ell \le 2)$ by $\mathbf{v}$ and check whether the condition is satisfied for a given $\ell = 0, 1, 2$. If this is possible for all three ℓ's we are done. If not, it may help to repeat the procedure for a different choice of N. We will illustrate this procedure in two examples (see Examples 6.19 and 6.20 below).

EXAMPLE 6.19. We consider the substitution $\sigma_5(1) = 123$, $\sigma_5(2) = 1$, $\sigma_5(3) = 31$. Our goal is to show that $\mathcal{T}(2)$ has nontrivial fundamental group for this example. We will prove Conditions (1) and (2) of Theorem 6.18 for the elements $[\mathbf{0}, 2], [\mathbf{0}, 3], [\pi(1, 0, -1), 1]$ of Γ_{srs}.

Checking Condition (1): First observe that $[2, \mathbf{0}, 3, \pi(1, 0, -1), 1]$ is a node of the triple point graph from which there start infinitely many infinite walks (this can be checked easily by looking at the loop structure of the triple point graph in Figure 6.2). Thus the intersection

$$T(2) \cap \mathcal{T}(3) \cap (\mathcal{T}(1) + \pi(1, 0, -1))$$

contains infinitely many points by Proposition 5.30. Since the quadruple point graph contains only finitely many infinite paths (see Figure 6.3) there is certainly a walk in the triple point graph starting at $[2, \mathbf{0}, 3, \pi(1, 0, -1), 1]$ that does not occur in the quadruple point graph. This shows that Condition (1) holds.

Checking Condition (2): Take $N = 4$, $\mathbf{v}_1 = \pi(1, 0, -1)$, $\mathbf{v}_2 = \pi(2, 1, -3)$ and $\mathbf{v}_3 = \pi(2, 0, -2)$. First, by iterating $\mathbf{E}_1$ four times for the argument $[\mathbf{0}, 2]$ we obtain

$$\begin{aligned}\mathbf{E}_1^4[\mathbf{0}, 2] \;=\; \{&[\pi(2, 1, -3), 1],\ [\pi(2, 1, -3), 2],\ [\pi(2, 0, -2), 1],\ [\pi(2, 0, -2), 2],\\ &[\pi(2, 0, -2), 3],\ [\pi(2, 2, -3), 1],\ [\pi(2, 1, -2), 1],\ [\pi(1, 0, -1), 3],\ [\pi(3, 1, -4), 1],\\ &[\pi(3, 1, -4), 2],\ [\pi(3, 0, -3), 3],\ [\pi(2, -1, -1), 3],\ [\pi(2, -1, -1), 1],\ [\pi(1, -2, 0), 3]\}.\end{aligned}$$

Looking at this list of values we notice that

$$\begin{aligned}&[\pi(1, 0, -1), 2] \notin \mathbf{E}_1^4[0, 2], \qquad [\pi(1, 0, -1), 3],\ [\pi(2, 0, -2), 1] \in \mathbf{E}_1^4[0, 2],\\ &[\pi(2, 1, -3), 3] \notin \mathbf{E}_1^4[0, 2], \qquad [\pi(2, 1, -3), 1],\ [\pi(3, 1, -4), 1] \in \mathbf{E}_1^4[0, 2],\\ &[\pi(3, 0, -3), 1] \notin \mathbf{E}_1^4[0, 2], \qquad [\pi(2, 0, -2), 2],\ [\pi(2, 0, -2), 3] \in \mathbf{E}_1^4[0, 2].\end{aligned}$$

Checking the conditions in the definition of Γ_{srs} in (3.1) for all occurring vectors we see that they all belong to Γ_{srs}. Thus Condition (2) is satisfied.

Now we may apply Theorem 6.18, in order to conclude that the subtile $\mathcal{T}(2)$ has nontrivial fundamental group.

Notice that we can check the condition on $\mathbf{E}_1^4$ by projecting each element of the self-replicating translation set Γ_{srs} to the anti-diagonal space with equation $x + y + z = 0$. Each piece $[\mathbf{x}, i]$ is represented by a rhombus; the rhombi occur in three different shapes depending on the letter i. We then have to place a given patch (consisting of three different rhombi) in three different places of the projection of Γ_{srs} such that the patch intersects the projection of $\mathbf{E}_1^4[0, 2]$ on exactly two pieces (in each of the three places the rhombus that does not intersect $\mathbf{E}_1^4[0, 2]$ has to be of a different shape so that each letter once corresponds to a rhombus lying outside $\mathbf{E}_1^4[0, 2]$). An illustration of this procedure is depicted in Figure 6.1.

EXAMPLE 6.20. In this example we outline hoe to prove that the subtile $\mathcal{T}(1)$ has nontrivial fundamental group. Indeed, the substitution σ_6 also satisfies the conditions of Theorem 6.18. This can be seen in the same way as in Example 6.19 when considering the

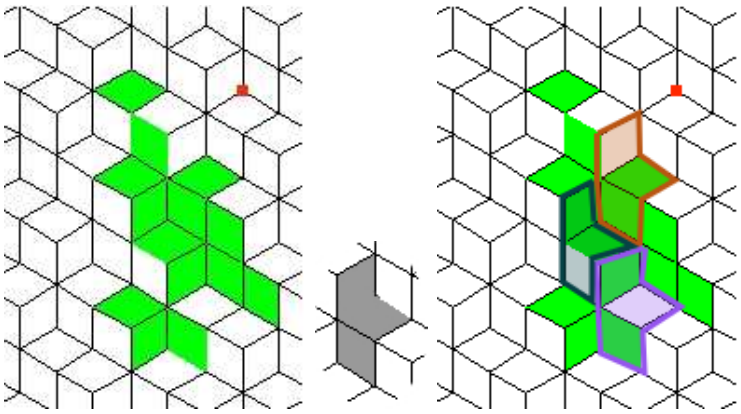

FIGURE 6.1. The substitution is $\sigma_5(1) = 123$, $\sigma_5(2) = 1$, $\sigma_5(3) = 31$. The left figure contains a geometric representation of $\mathbf{E}_1^4[0,2]$ in the self-replicating translation set Γ_{srs}. Each piece $[\mathbf{x}, i]$ is represented as a rhombus in the plane $x+y+z=0$; the shape of the rhombus depends of the letter used. In the right figure, we see that the shape $[(0,0,0),2],[(0,0,0),3],[\pi(1,0,-1),1]$ (depicted in the middle) can be translated such that two pieces of the shape belong to $\mathbf{E}_1^4[0,2]$ and the third belongs to $\Gamma_{srs} \setminus \mathbf{E}_1^4[0,2]$. This proves the second condition of Theorem 6.18.

elements $[\mathbf{0},1],[\pi(-1,0,2),2]$ and $[\pi(-1,1,1),2]$ of Γ_{srs}, the 7-th iteration $\mathbf{E}_1^7[0,1]$ and the translation vectors $\mathbf{v}_1 = \pi(-1,4,-4)$, $\mathbf{v}_2 = \pi(-4,4,2)$ and $\mathbf{v}_3 = \pi(1,3,-5)$. Since the node $[1,\pi(-1,0,2),2,\pi(-1,1,1),2]$ is the starting point of infinitely many infinite walks in the triple point graph and the quadruple point graph contains only finitely many infinite walks (see Figures 6.6 and 6.7), Theorem 6.18 applies and the central tile has a nontrivial fundamental group.

We can even do more and give the following result on uncountable fundamental groups.

THEOREM 6.21. *Let the same setting as in Theorem 6.18 be in force but assume that the following conditions hold.*

(1) *The intersection* $\mathcal{T}(i)\cap(\mathcal{T}(i_1)+\gamma_1)\cap(\mathcal{T}(i_2)+\gamma_2)$ *contains at least two elements* $\mathbf{x}_1,\mathbf{x}_2$. *The point* $\mathbf{x}_1$ *is contained in* $\mathrm{int}(\mathcal{T}(i)\cup(\mathcal{T}(i_1)+\gamma_1)\cup(\mathcal{T}(i_2)+\gamma_2))$.
(2) *Let* $[\gamma_0,i_0] := [0,i]$ *for convenience. Then there exists an integer* N *such that for all* $\ell\in\{0,1,2\}$ *one can find* $\mathbf{v}_\ell\in\mathbb{Z}^d$ *and* $[\mathbf{t}_\ell,j_\ell]\in\Gamma_{srs}$ *with* $[\mathbf{t}_\ell,j_\ell]\neq[0,i]$ *such that (indices are to be taken* mod 3*)*
   (i) $[i,\mathbf{t}_\ell,j_\ell]$ *is a node of the SR-boundary graph;*
   - *((ii))* $[\gamma_\ell+\mathbf{v}_\ell,i_\ell]\in\mathbf{E}_1^N[\mathbf{t}_\ell,j_\ell]$, $[\gamma_{\ell+1}+\mathbf{v}_\ell,i_{\ell+1}]\in\mathbf{E}_1^N[0,i]$, $[\gamma_{\ell+2}+\mathbf{v}_\ell,i_{\ell+2}]\in\mathbf{E}_1^N[0,i]$.

   (iii) *For each* $\ell\in\{0,1,2\}$, *there exists a node in the SR-boundary graph of the shape* $[i,\overline{\mathbf{t}_\ell},\overline{j_\ell}]$ *such that an infinite number of paths with an even number of edges of type 2 lead from* $[i,\overline{\mathbf{t}_\ell},\overline{j_\ell}]$ *to* $[i,\mathbf{t}_\ell,j_\ell]$.

Then the fundamental group $\pi_1(\mathcal{T}(i))$ *is uncountable and not free. Moreover,* $\mathcal{T}(i)$ *is not locally simply connected and admits no universal cover.*

PROOF. Since $[\mathbf{t}_\ell,j_\ell]\in\Gamma_{srs}$ and $[\mathbf{t}_\ell,j_\ell]\neq[0,i]$, the sets $\mathbf{E}_1^N[\mathbf{t}_\ell,j_\ell]$ and $\mathbf{E}_1^N[0,i]$ are disjoint (see Proposition 3.5). From $[\gamma_\ell+\mathbf{v}_\ell,i_\ell]\in\mathbf{E}_1^N[\mathbf{t}_\ell,j_\ell]$ we deduce that $[\gamma_\ell+\mathbf{v}_\ell,i_\ell]\notin\mathbf{E}_1^N[0,i]$ and the proof of Theorem 6.18 applies. This yields a complementary component U_0 of $\mathcal{T}(i)$ containing an inner point of $\mathbf{h}^N(\mathcal{T}(i_\ell)+\gamma_\ell+\mathbf{v}_\ell)$ for some $\ell\in\{0,1,2\}$. From $[\gamma_\ell+\mathbf{v}_\ell,i_\ell]\in\mathbf{E}_1^N[\mathbf{t}_\ell,j_\ell]$ and the GIFS equation $\mathcal{T}(j_\ell)+\mathbf{t}_\ell=\bigcup_{[\lambda,k]\in\mathbf{E}_1^N[\mathbf{t}_\ell,j_\ell]}\mathcal{T}(k)+\lambda$ it follows that $\mathbf{h}^N(\mathcal{T}(i_\ell)+\gamma_\ell+\mathbf{v}_\ell)\subset\mathcal{T}(j_\ell)+\mathbf{t}_\ell$ so that U_0 intersects the interior of $\mathcal{T}(j_\ell)+\mathbf{t}_\ell$. Let us denote by $\mathbf{z}$ a point contained

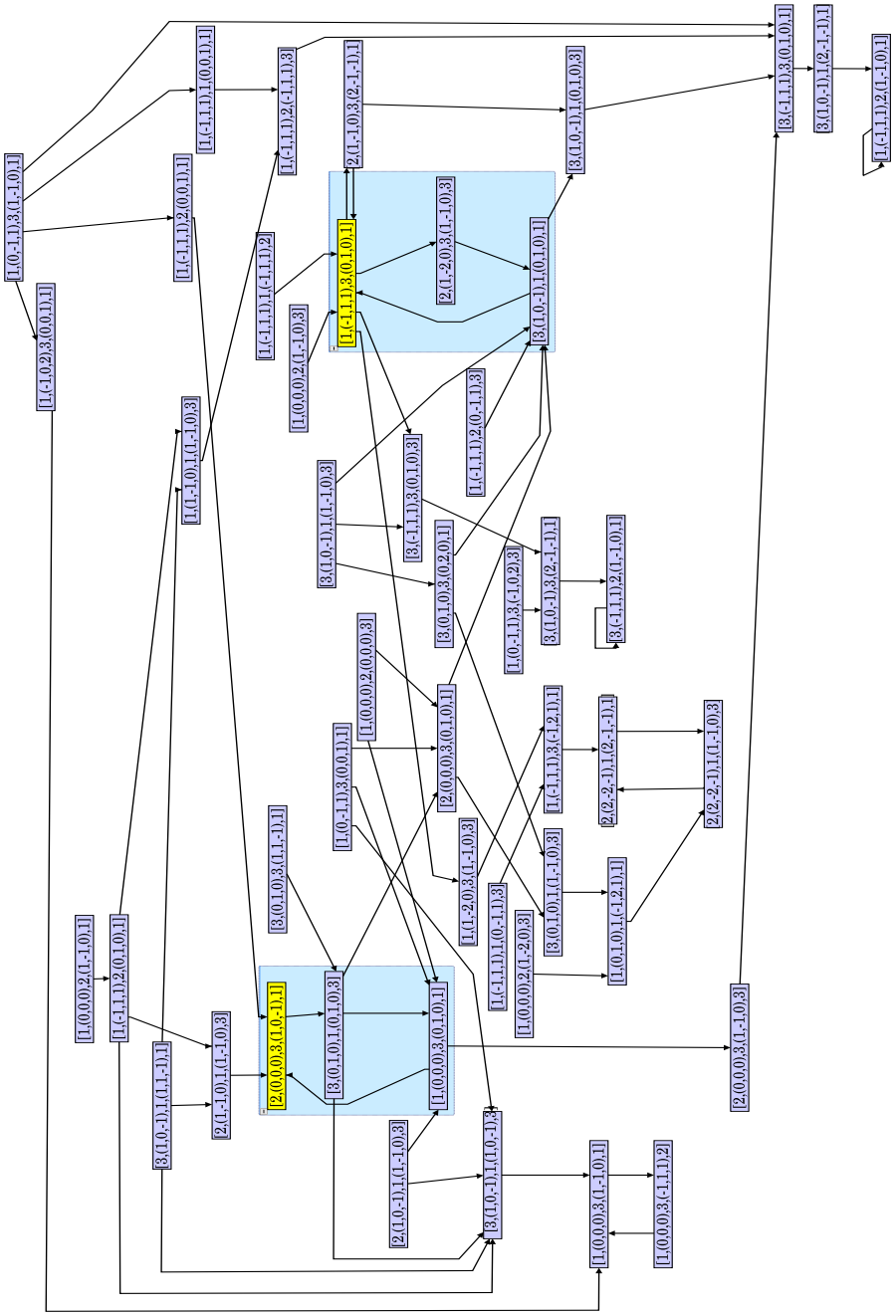

FIGURE 6.2. The triple point graph for the substitution $\sigma_5(1) = 123$, $\sigma_5(2) = 1$, $\sigma_5(3) = 31$. There are three internal loops in this graph, implying that some intersections between three tiles are infinite. This is especially true for $[2, \mathbf{0}, 3, \pi(1, 0, -1), 1]$ and $[1, \pi(-1, 1, 1), 3, \pi(0, 1, 0), 1]$. This is used to prove that the associated central tile has a non-trivial and even uncountable fundamental group (Theorems 6.18 and 6.21).

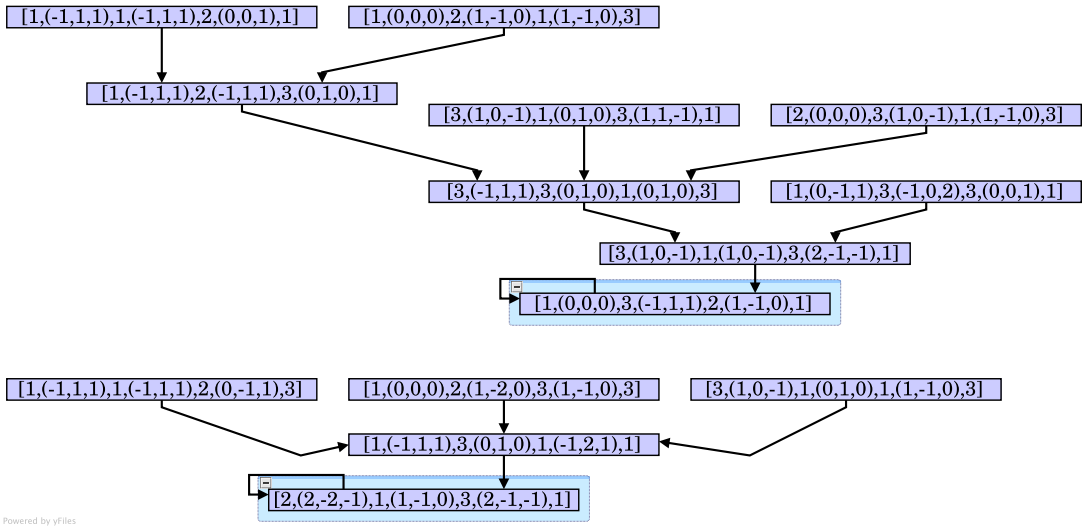

FIGURE 6.3. The quadruple point graph for the substitution $\sigma_5(1) = 123$, $\sigma_5(2) = 1$, $\sigma_5(3) = 31$. The graph has two independent connected components. Loops appear only at the end of path, therefore each intersection between four tiles is a single point. This is needed in order to apply Theorems 6.18 and 6.21.

in this intersection, *i.e.*,

$$\mathbf{z} \in U_0 \cap \mathrm{Int}(\mathcal{T}(j_\ell) + \mathbf{t}_\ell), \qquad U_0 \text{ bounded complementary component of } \mathcal{T}(i). \tag{6.10}$$

Now, comparing the definition of the edges in the SR-boundary graph (Definition 5.4) with the dual substitution $\mathbf{E}_1$ (Definition 3.4), we get the following. If there is an edge of type 1 from $[i, \gamma, j]$ to $[i', \gamma', j']$ labelled by $\mathbf{e}$, we have $\mathbf{e} = \pi\mathbf{l}(p_1)$ with $\sigma(i') = p_1 i s_1$. From Definition 3.4 we deduce that $[\mathbf{h}^{-1}\mathbf{e}, i'] \in \mathbf{E}_1[0, i]$. We also have $\mathbf{h}\gamma' = \gamma + \pi(\mathbf{l}(p_2) - \mathbf{l}(p_1))$ with $\sigma(j') = p_2 j s_2$. This implies that $[\mathbf{h}^{-1}(\gamma + \pi\mathbf{l}(p_2), j'] \in \mathbf{E}_1[\gamma, j]$ and $\mathbf{h}^{-1}(\gamma + \pi\mathbf{l}(p_2)) = \gamma' + \mathbf{h}^{-1}\pi\mathbf{l}(p_1) = \gamma' + \mathbf{h}^{-1}\mathbf{e}$. Hence,

$$[\mathbf{h}^{-1}\mathbf{e}, i'] \in \mathbf{E_1}[0, i], \qquad [\gamma' + \mathbf{h}^{-1}\mathbf{e}, j'] \in \mathbf{E_1}[\gamma, j].$$

If the edge is of type 2, we have $\mathbf{e} = \pi\mathbf{l}(p_2) + \gamma$ with $\sigma(i') = p_2 j s_2$, $\sigma(j') = p_1 i s_1$ and $-\mathbf{h}\gamma' = \gamma + \pi\mathbf{l}(p_2) - \pi\mathbf{l}(p_1) = \mathbf{e} - \pi\mathbf{l}(p_1)$. From $\sigma(j') = p_1 i s_1$ we have $[\mathbf{h}^{-1}\pi\mathbf{l}(p_1), j'] \in \mathbf{E}_1[0, i]$. From $\sigma(i') = p_2 j s_2$ we have $[\mathbf{h}^{-1}(\pi\mathbf{l}(p_2) + \gamma), i'] \in \mathbf{E_1}[\gamma, j]$. We deduce that

$$[\gamma' + \mathbf{h}^{-1}\mathbf{e}, j'] \in \mathbf{E}_1[0, i], \qquad [\mathbf{h}^{-1}\mathbf{e}, j'] \in \mathbf{E}_1[\gamma, j].$$

From these equations and the definition of $\mathbf{E}_1$, we deduce that if a path of length n leads from $[i, \gamma, j]$ to $[i', \gamma', j']$ with labels $\mathbf{e}^{(1)}, \dots, \mathbf{e}^{(n)}$ with an even number of edges of type 2, we have

$$[\mathbf{h}^{-n}\mathbf{e}^{(1)} + \cdots + \mathbf{h}^{-1}\mathbf{e}^{(n)}, i'] \in \mathbf{E}_1^n[0, i], \qquad [\gamma' + \mathbf{h}^{-n}\mathbf{e}^{(1)} + \cdots + \mathbf{h}^{-1}\mathbf{e}^{(n)}, j'] \in \mathbf{E}_1[\gamma, j]$$

(if the number of edges of type 2 was odd, we simply had to reverse $[0, i]$ and $[\gamma, j]$ in the equation).

Let us apply this result to the paths from $[i, \overline{\mathbf{t}_\ell}, \overline{j_\ell}]$ to $[i, \mathbf{t}_\ell, j_\ell]$ that are supposed to exist by the hypotheses. We classify each path by its length $L_\ell^{(n)}$ and we denote by $\mathbf{w}_\ell^{(n)}$ the sum $\mathbf{h}^{-L_\ell^{(n)}}\mathbf{e^{(1)}} + \cdots + \mathbf{h}^{-1}\mathbf{e}^{(L_\ell^{(n)})}$. This implies that

$$[\mathbf{w}_\ell^{(n)}, i] \in \mathbf{E}_1^{L_\ell^{(n)}}[0, i] \quad \text{and} \quad [\mathbf{w}_\ell^{(n)} + \mathbf{t}_\ell, j_\ell] \in \mathbf{E}_1^{L_\ell^{(n)}}[\overline{\mathbf{t}_\ell}, \overline{j_\ell}].$$

Since $[i, \overline{\mathbf{t}_\ell}, \overline{j_\ell}]$ is a node of the SR-boundary graph, the pair $[\overline{\mathbf{t}_\ell}, \overline{j_\ell}]$ belongs to Γ_{srs} therefore $\mathbf{E}_1^{L_\ell^{(n)}}[\overline{\mathbf{t}_\ell}, \overline{j_\ell}]$ is disjoint from $\mathbf{E}_1^{L_\ell^{(n)}}[0, i]$. Hence,

$$[\mathbf{w}_\ell^{(n)}, i] \in \mathbf{E}_1^{L_\ell^{(n)}}[0, i] \quad \text{and} \quad [\mathbf{w}_\ell^{(n)} + \mathbf{t}_\ell, j_\ell] \notin \mathbf{E}_1^{L_\ell^{(n)}}[0, i].$$

We now consider the GIFS equation of $\mathcal{T}(i)$ at different ranks M, *i.e.*,

$$\mathbf{h}^{-M}\mathcal{T}(i) = \bigcup_{[\lambda,k]\in\mathbf{E_1}^M[0,i]} \mathcal{T}(k) + \lambda.$$

From the tiling assumption we deduce that

$$\mathbf{h}^{L_\ell^{(n)}}(\mathcal{T}(i) + \mathbf{w}_\ell^{(n)}) \subset \mathcal{T}(i) \quad \text{and} \quad \operatorname{Int}\left(\mathbf{h}^{L_\ell^{(n)}}(\mathcal{T}(j_\ell) + \mathbf{w}_\ell^{(n)} + \mathbf{t}_\ell)\right) \cap \mathcal{T}(i) = \emptyset.$$

From (6.10) we have that $\mathbf{h}^{L_\ell^{(n)}}(\mathbf{z} + \mathbf{w}_\ell^{(n)}) \in \mathbf{h}^{L_\ell^{(n)}}(U_0 + \mathbf{w}_\ell^{(n)})$ and that $\mathbf{h}^{L_\ell^{(n)}}(\mathbf{z} + \mathbf{w}_\ell^{(n)}) \in \operatorname{Int}\left(\mathbf{h}^{L_\ell^{(n)}}(\mathcal{T}(j_\ell) + \mathbf{t}_\ell)\right)$, implying $\mathbf{h}^{L_\ell^{(n)}}(\mathbf{z} + \mathbf{w}_\ell^{(n)}) \notin \mathcal{T}(i)$. This yields that $\mathbf{h}^{L_\ell^{(n)}}(U_0 + \mathbf{w}_\ell^{(n)})$ intersects a complementary component of $\mathcal{T}(i)$, say U_n.

Since $\mathbf{h}^{L_\ell^{(n)}}(\mathcal{T}(i) + \mathbf{w}_\ell^{(n)}) \subset \mathcal{T}(i)$, each complementary component of $\mathcal{T}(i)$ is a subset of exactly one complementary component of $\mathbf{h}^{L_\ell^{(n)}}(\mathcal{T}(i) + \mathbf{w}_\ell^{(n)})$, among which we find $\mathbf{h}^{L_\ell^{(n)}}(U_0 + \mathbf{w}_\ell^{(n)})$. We deduce that

$$U_n \subset \mathbf{h}^{L_\ell^{(n)}}(U_0 + \mathbf{w}_\ell^{(n)}).$$

We have exhibited a sequence of complementary components to $\mathcal{T}(i)$ whose diameter tends to zero. Thus, there is an infinite subsequence of (U_k) consisting of pairwise disjoint complementary components of $\mathcal{T}(i)$. So $\mathbb{S}^2 \setminus \mathcal{T}(i)$ has infinitely many components. The result now follows from Lemma 6.17. □

Items (1), (2.i) and (2.ii) of Theorem 6.21 can be checked in the same way as for Theorem 6.18. Item (2.iii) can be checked by inspecting the loops of the SR-boundary graph.

REMARK 6.22. Note that we get analogues of Theorems 6.18 and 6.21 for $\mathcal{T}$ instead of $\mathcal{T}(i)$ by replacing $\mathbf{E}_1^N[0, i]$ by $\mathbf{E}_1^N\mathcal{U}$. The proof remains exactly the same.

EXAMPLE 6.23. In this example we deal with the substitution $\sigma_6(1) = 12$, $\sigma_6(2) = 31$, $\sigma_6(1) = 1$. We want to apply Theorem 6.21 for showing the uncountability of $\pi_1(\mathcal{T}(1))$.

To this matter take $i = 1$ and consider the elements $[0, 1]$, $[\pi(-1, 1, 1), 1]$ and $[\pi(0, 0, 1), 1]$ of Γ_{srs}. We will now check the items of Theorem 6.21.

Item (1): First observe that Proposition 5.30 implies that

$$\mathcal{T}(1) \cap \mathcal{T}(1) + \pi(-1, 1, 1) \cap \mathcal{T}(1) + \pi(0, 0, 1)$$

has infinitely many elements. Indeed, the node $[1, (-1, 1, 1), 1, (0, 0, 1), 1]$ of the triple point graph from which infinitely many infinite paths lead away (see Figure 6.6). At least one of these elements is contained in the interior of

$$\mathcal{T}(1) \cup \mathcal{T}(1) + \pi(-1, 1, 1) \cup \mathcal{T}(1) + \pi(0, 0, 1)$$

because the quadruple point graph accepts only a finite number of walks (see Figure 6.7).

Item 2.(i): Take

$$[\mathbf{t}, j] = [\mathbf{t}_0, j_0] = [\mathbf{t}_1, j_1] = [\mathbf{t}_2, j_2] = [\pi(0, 0, 1), 2].$$

We check that $[1, \pi(0, 0, 1), 2]$ appears in the SR-boundary graph.

Item 2.(ii): Take the translation vectors $\mathbf{v}_1 = [\pi(-2, 6, -5), 1]$, $\mathbf{v}_2 = [\pi(-2, 4, -1), 1]$ and $\mathbf{v}_3 = [\pi(0, 5, -6), 1]$. This item holds for these vectors with $N = 7$. An illustration is given in Figure 6.4.

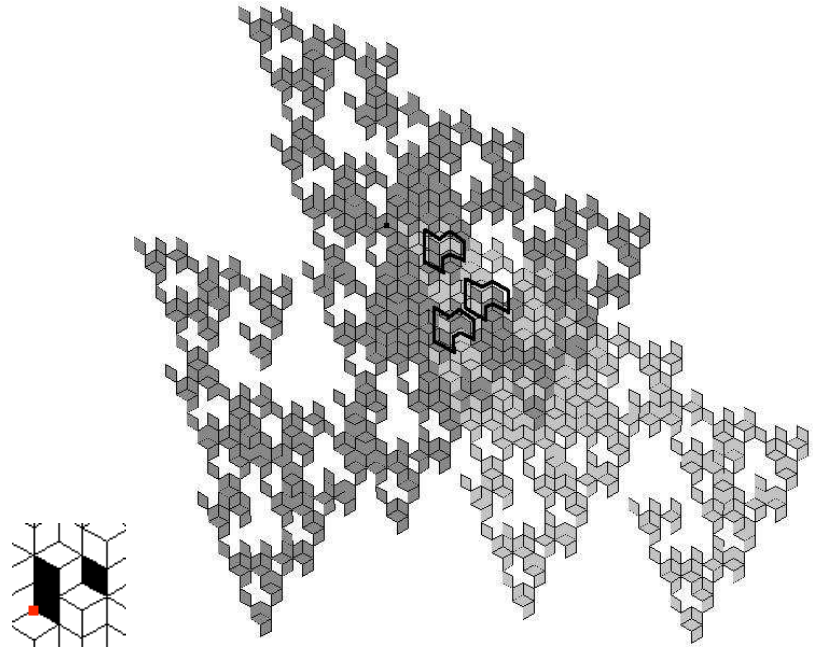

FIGURE 6.4. Consider the substitution $\sigma_6(1) = 12$, $\sigma_6(2) = 31$, $\sigma_6(1) = 1$. The figure contains a geometric representation of ${\mathbf{E_1}}^7[0,1]$ (dark grey) and ${\mathbf{E_1}}^7[\pi(0,0,1),2]$ (light grey) among the self-replicating translation set Γ_{srs}. The shape $[(0,0,0),1],[(-1,1,1),1],[\pi(0,0,1),1]$ (depicted in the left hand side) can be translated such that two pieces of the shape belong to ${\mathbf{E_1}}^7[0,1]$ and the third only belongs to ${\mathbf{E_1}}^7[\pi(0,0,1),2]$. The appropriate translation vectors are the ones given in Example 6.23. This proves Item (2.ii) of Theorem 6.21.

: the node $[1,\pi(0,0,1),2]$ appears in the SR-boundary graph and belongs to a loop, implying that an infinite number of paths with an even number of edges of type 2 start and end at this node (see Figure 6.5). Taking

$$[i,\overline{\mathbf{t}_0},\overline{j_0}] = [i,\overline{\mathbf{t}_1},\overline{j_1}] = [i,\overline{\mathbf{t}_2},\overline{j_2}] = [i,\mathbf{t},j] = [1,\pi(0,0,1),2]$$

this item is shown to hold.

Hence the conditions of Theorem 6.21 are satisfied and we deduce that the fundamental group of $\mathcal{T}(1)$ is uncountable and not free.

EXAMPLE 6.24. Theorem 6.21 also applies to $\sigma_5(1) = 123$, $\sigma_5(2) = 1$, $\sigma_5(3) = 31$. For instance, we can show that $\mathcal{T}(1)$ has uncountable fundamental group in the following way.

First take $i = 0$, $[\gamma_1, i_1] = [\pi(-1,1,1),3]$ and $[\gamma_2, i_2] = [\pi(0,1,0),1]$. For the elements $[\overline{\mathbf{t}_\ell},\overline{j_\ell}]$ and $[\mathbf{t}_\ell, j_\ell]$ $(0 \le \ell \le 2)$ always take $[(0,0,0),3]$. Moreover, choose $\mathbf{v}_1 = [\pi(1,2,-2),1]$, $\mathbf{v}_2 = [\pi(1,1,-1),3]$ and $\mathbf{v}_3 = [\pi(1,1,-1),1]$ for the translation vectors and take $N = 7$, *i.e.* look at the patches in $\mathbf{E}_1^7$. By considering the SR-boundary graph, the triple point graph and the quadruple point graph (see Figures 6.2, 6.3, and 6.8) one easily checks that Theorem 6.21 applies.

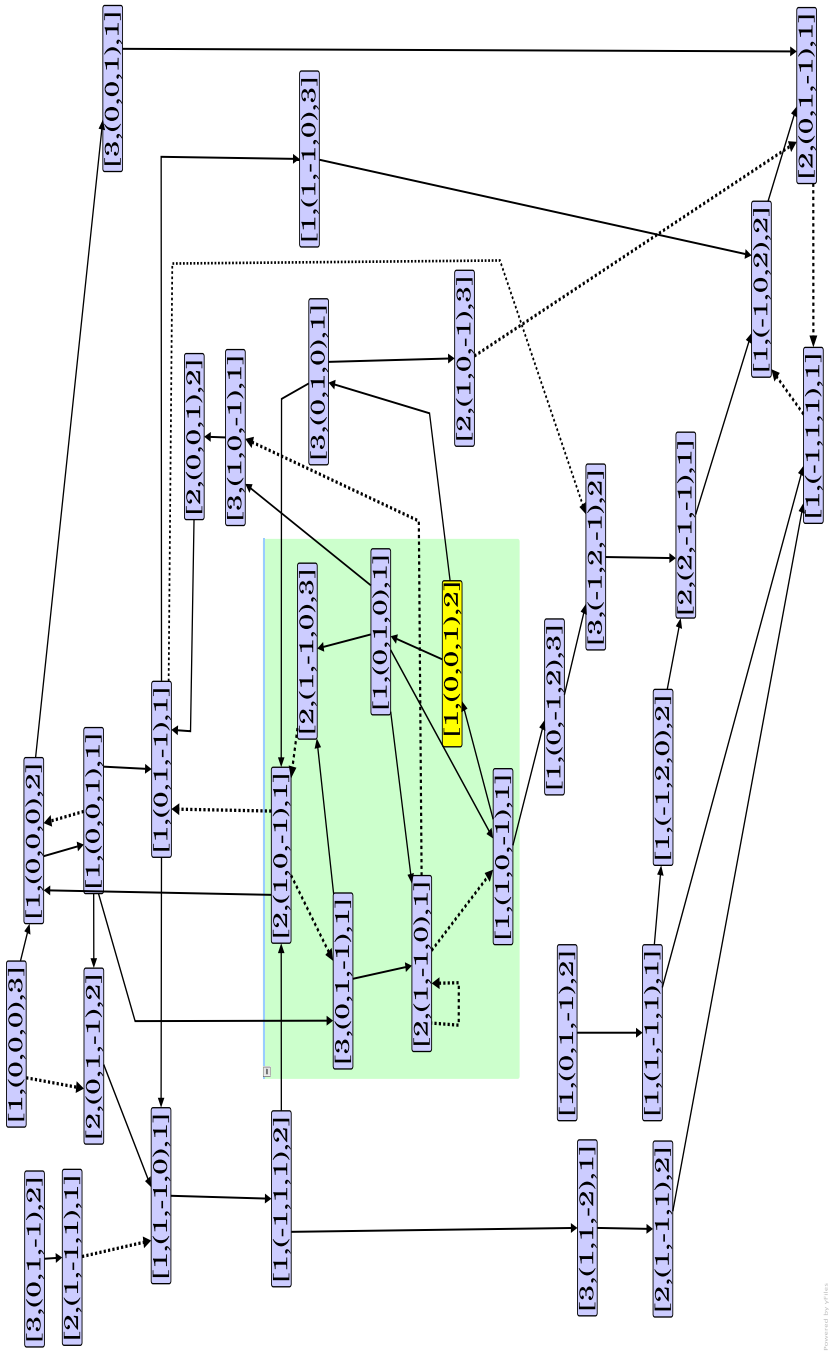

FIGURE 6.5. SR-boundary graph for the substitution $\sigma_6(1) = 12$, $\sigma_6(2) = 31$, $\sigma_6(3) = 1$. Dotted edges stand for edges of type 2. To apply Theorem 6.21, we notice that $[1, \pi(0,0,1), 2]$ belongs to a loop, so that an infinite number of paths with an even number of type 2 edges reach this node.

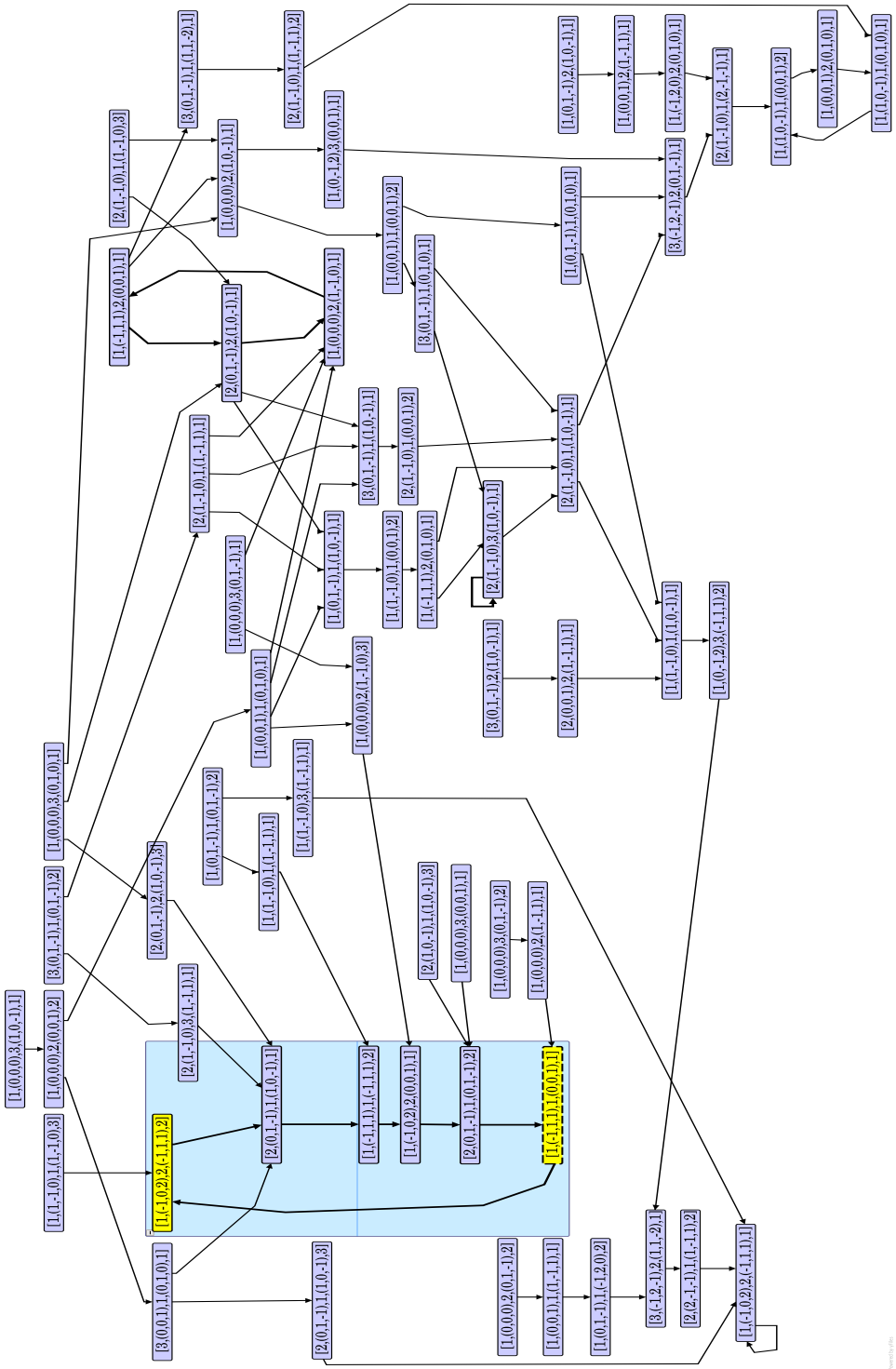

FIGURE 6.6. The triple point graph for the substitution $\sigma_6(1) = 12$, $\sigma_6(2) = 31$, $\sigma_6(3) = 1$. There are three internal loops in this graph (boxes with dotted nodes) and two terminal loops (also rounded by a box). To apply Theorems 6.18 and 6.21, we check that an infinite number of paths lead away from $[1, \pi(-1, 0, 2), 2, \pi(-1, 1, 1), 2]$ and $[1, \pi(-1, 1, 1), 1, \pi(0, 0, 1), 1]$.

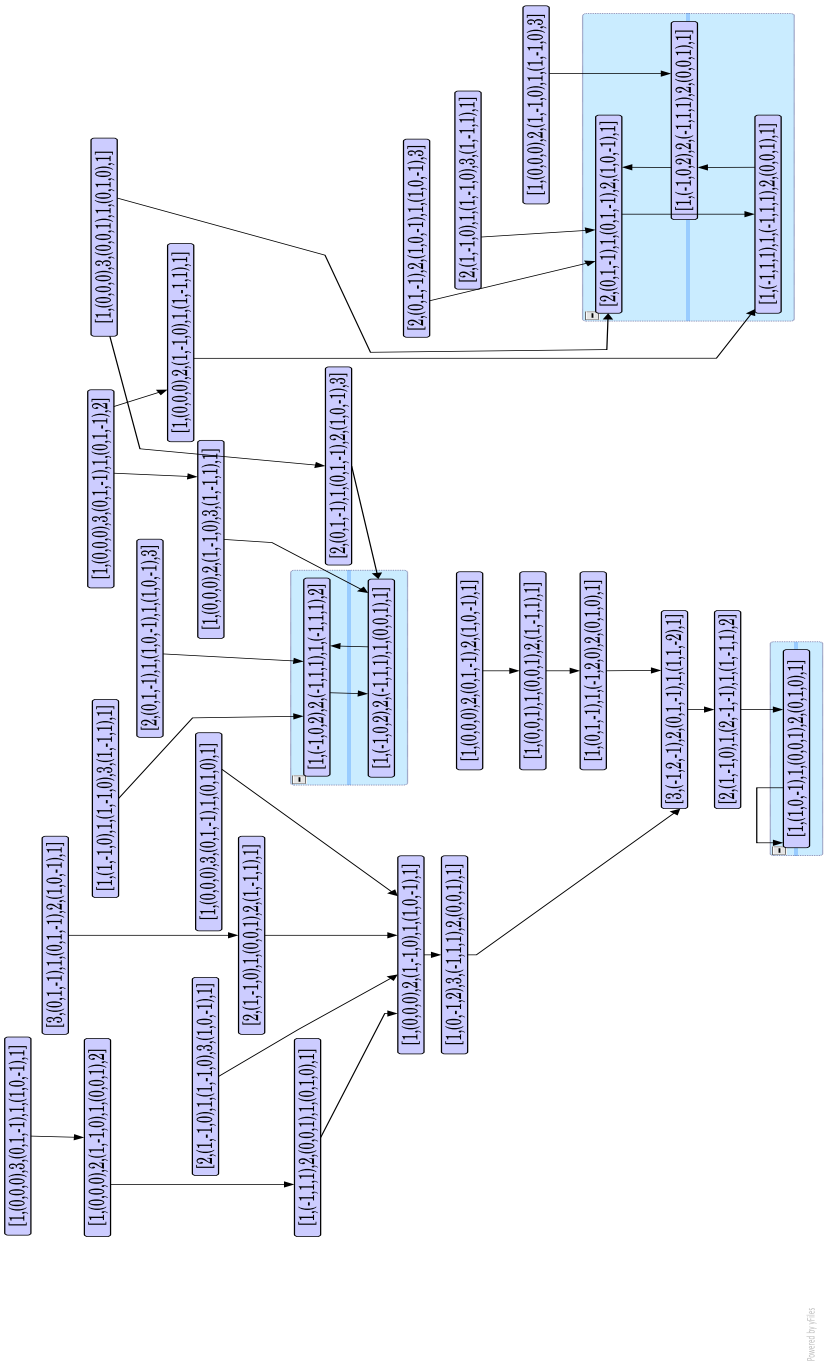

FIGURE 6.7. The quadruple point graph for the substitution $\sigma_6(1) = 12$, $\sigma_6(2) = 31$, $\sigma_6(3) = 1$. Loops appear only at the end of path, therefore each intersection between four tiles is a single point. To apply Theorems 6.18 and 6.21, we check that the number of recognized paths, corresponding to quadruple points, is finite.

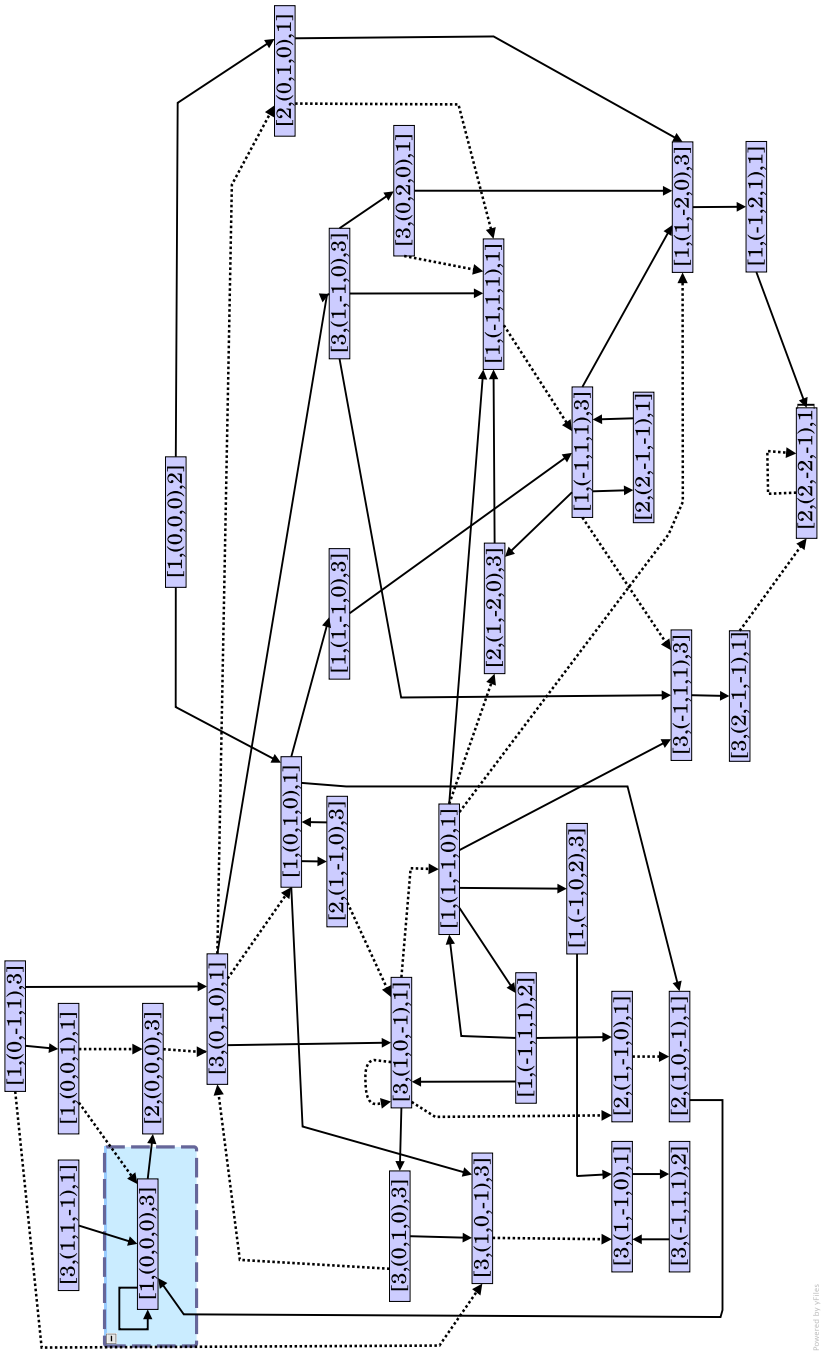

FIGURE 6.8. The SR-boundary graph for the substitution $\sigma_5(1) = 123$, $\sigma_5(2) = 1$, $\sigma_5(3) = 31$. To apply Theorem 6.21, we notice that $[1, (0, 0, 0), 3]$ belongs to a loop, hence an infinite number of finite paths join this node.

CHAPTER 7

Perspectives

In the present monograph we show many topological results for central tiles of primitive unit Pisot substitutions. The main objects used in our study are different kinds of graphs. We consider these graphs as powerful tools that can be used in order to derive various results on substitutions, their associated Dumont-Thomas numeration as well as their tiles and tilings. In this chapter we want to give some perspectives for future work in this direction.

7.1. Topology

A first direction of research consists in pursuing the research on the topological structure of the central tiles corresponding to primitive unit Pisot substitutions. In the examples we considered throughout this monograph, we exhibited compact subsets of the plans whose fundamental groups are uncountable and not free. Such sets are "pathological" from a topological point of view. Describing explicitly the structure of the fundamental group in such cases is a first task for future research. The fact that a central tile has uncountable fundamental group has the consequence that it is not locally simply connected. Fundamental groups of such spaces are studied in the literature. The easiest example of a space with this property is the so-called Hawaiian Earring (see for instance [**56**]). Its fundamental group has been studied in great detail in [**47**], where it has been described by means of words. Another example for a non-locally connected space whose fundamental group has been described is the Sierpiński gasket (see [**13**]). Structural results on fundamental groups of non-locally simply connected spaces can be found for instance in [**52, 59**]. The main challenge in calculating the fundamental group of a central tile in the plane comes from the fact that its topological dimension is 2. All the other examples for that calculations that have been performed so far have topological dimension 1. And this fact is heavily used in the calculations.

Other questions in this context are related to components of the interior of a central tile. There are several connected Rauzy fractals whose interior is disconnected. It would be interesting to get results on the structure of the components of their interior. Is the closure of a component of the interior a graph directed self-affine set (see [**87**], where this question has been studied for an example of a self-similar lattice tile)? Is it homeomorphic to a closed disk? Similar questions have been studied in the setting of self-affine tiles (see for instance [**93, 101, 102, 103**]). However, the fact that the central tile and its subtiles are *graph directed* self-affine sets makes things much more complicated. In view of Torhorst's theorem (see [**82**, §61, II, Theorem 4]) and the tiling property, the disklikeness of the components of the interior of the central tile is linked with the question whether this tile has cut points or not. Therefore, a criterion for cut points in terms of our graphs would be a desirable tool in this circle of problems.

Another direction is concerned with topological properties of higher dimensional central tiles. Most of our topological properties are obtained for substitutions whose corresponding central tiles are subsets of the plane. The reason for restricting to this case is that we based our proofs on separation properties of the Euclidean plane; such properties (like the Jordan curve theorem) are no longer satisfied in higher dimensions. However, the definition of boundary or contact graphs is independent from the dimension that is considered. The challenge here would be to obtain for instance connectivity or simple-connectivity criteria in dimension 3, that are based on the self-affinity of the central tile and that can be checked by using contact and boundary graphs. One theorem which could be useful in this context is the Moore-van

Kampen-Zippin Theorem (see for instance [**125**]). This theorem gives a characterization of $\mathbb{S}^2$ in terms of properties of cut sets. For the case of boundaries if three dimensional central tiles these properties can probably be checked with help of our graphs in order to exhibit a three dimensional central tile whose boundary is homeomorphic to a sphere.

7.2. Number theory

As mentioned in the introduction, one historical reason for introducing central tiles refers to the study of number systems [**123**]. Let us detail now the potential applications of our methods in this field.

When studying a numeration system, the first questions one may ask is to characterize the set of admissible expansions, then identifying which numbers have a finite, an eventually periodic or a purely periodic expansion. For number systems with integer basis or continued fractions, these questions are completely solved. For beta-numeration, however, the question of purely periodic expansions is not clearly understood. A classical method to study numbers with a purely periodic expansion is to build a suitable natural extension of the dynamics; in this natural extension periodic expansion correspond to finite orbits and thus can be identified. In this setting, the central tile plays a crucial role regarding to beta-numeration since Ito and Rao [**77**] proved that a suitable natural extension is obtained by adding an expanding component to the central tile of the corresponding beta-substitution. This geometrical characterization builds a bridge between number theory and topology. As an example, based on our geometrical characterization, the geometric property (F) implies that all rational number sufficiently near to zero have a purely periodic beta-expansion in the primitive unit Pisot case [**9, 77**]. In other words, the topology of the central tiles (in particular, the question whether $\mathbf{0}$ is an inner point or not) relates to unexpected properties of beta-numeration (note that the behavior of rational numbers with respect to purely periodic beta-expansion is far from random). A challenging question is now: does connectivity, or simple-connectivity of central tile have an influence on the structure of the subset of real numbers with a purely periodic expansion?

To go further, we know that when β is still Pisot but *not* a unit, a suitable natural extension is not built from the central tile itself but it requires additional p-adic components (see [**9, 39**]). In spite of that, the construction of the natural extension remains very similar to the unit case and boundary graphs can be defined as well in this situation. However, the previous relation between the geometric property (F) and purely periodic expansions of all rationals near to zero becomes false: The geometric property (F) still implies that $\mathbf{0}$ is an inner point of the central tile, but for instance for $\beta = 2 + \sqrt{7}$, there exists a sequence of rationals converging to zero and having non-purely periodic expansion. The proof of this fact is based on boundary graphs (see [**9**]). Then a challenging question is to find good topological conditions characterizing purely periodic expansions near zero in the non-unit case.

We then can turn to understanding better the expansion of some specific points. For instance, what is the expansion of the infimum of all rationals with a non-purely periodic expansion. Computations showed for $\beta^3 = \beta + 1$ that this number is close to $2/3$ but differs from it [**14**]. Is this number rational? Does it belong to $\mathbb{Q}(\beta)$? Is it transcendental? The technical purpose is to describe properly the intersection of a fractal curve with a line. Another example of interest is to compute the largest ball centered at zero which is contained in the central tile, in relation with diophantine approximation [**72, 73**]. Here the challenge is to describe and compute the exact intersection between a fractal curve and a circle.

In order to check the associativity of the so-called Fibonacci multiplication (see for instance [**33**]) one needs to consider the set $\mathcal{T} \cdot \mathcal{T} = \{\mathbf{xy}\,;\, \mathbf{x}, \mathbf{y} \in \mathcal{T}\}$ and its boundary (here $\mathcal{T} \subset \mathbb{C}$ denotes *e.g.* the tile associated to the Tribonacci substitution). Also in this context versions of our graphs might be useful to get further results.

Another topic is to generalize those approaches to other numeration systems. We present two types of dynamical systems that are close and deserve a specific study.

The first class of dynamical systems are shift radix systems (see [**10**]). We recall their definition. For $\mathbf{r} \in \mathbb{R}^d$ define the function

$$\begin{aligned}\tau_{\mathbf{r}} : &\mathbb{Z}^d \to \mathbb{Z}^d,\\ &\mathbf{z} = (z_0, \dots, z_{d-1}) \mapsto (z_1, \dots, z_{d-1}, -\lfloor \mathbf{rz} \rfloor),\end{aligned}$$

where $\mathbf{rz}$ is the scalar product of the vectors $\mathbf{r}$ and $\mathbf{z}$. The mapping $\tau_{\mathbf{r}}$ is called a *shift radix system (SRS)* if for each $\mathbf{z} \in \mathbb{Z}^d$ there exists a $k \in \mathbb{N}$ such that $\tau_{\mathbf{r}}^k(\mathbf{z}) = \mathbf{0}$. These dynamical systems form a generalization of beta-numeration (see [**10**]). Their arithmetic properties have been studied thoroughly (see for instance [**10, 11, 12**]). One can also attach central tiles to SRS, however, in general they are not graph directed self-affine. For this reason the topology as well as the tiling properties of them are much harder to study. A first step here would be to describe their boundary by means of (possibly infinite) graphs related to the SR-boundary graph of our paper. Moreover, tiling and connectivity properties of such tiles deserve to be investigated. As the parameter $\mathbf{r}$ varies in a compact subset of $\mathbb{R}^d$ (related to the Schur-Cohn region defined in terms of coefficients of contracting polynomials) this would lead to new types of Mandelbrot sets.

The second family of related number systems is Dumont-Thomas numeration [**58**]; it can be seen as an extension of beta-numeration to the substitutive case [**28, 38**]. We expect that this kind of numeration can be studied with help of our graphs. The SR-boundary as well as the contact graph should be related to addition of certain quantities to $\mathbf{h}$-ary representations. We think that these graphs can act as odometers for these number systems. For number systems related to full shifts a correspondence between boundary graphs and addition automata has been observed for instance in [**34, 115**]. Moreover in the framework of β-numeration the structure of pure periods occurring in β-expansions with respect to quadratic Pisot numbers as bases has been investigated (see [**107**]). Our graphs might be the appropriate tools to extend these considerations to Dumont-Thomas numeration.

7.3. Invariants in dynamics and geometry

A second and independent historical reason for the introduction of central tiles refers to the study of dynamical systems. This story started with Rauzy [**110**] who aimed at building an example of a domain exchange in $\mathbb{R}^2$ that generalized the theory on interval exchange transformations [**79, 126**]. This tile was proved to generate a Markov partition for the action of the incidence matrix of the substitution on a torus [**75, 105**]. Notice that the Markov partition is nothing else but the natural extension mentioned above to recover purely periodic beta-expansions. This story can be revisited in the framework of hyperbolic attractors as detailed in [**30**]: from the considerations in [**17, 31, 127**] it follows that every orientable hyperbolic one-dimensional attractor is either a substitution tiling space or a classical solenoid. It is thus proposed to study the topology of tiling spaces in order to understand the flow acting on an arc component of the attractor. The relation with central tiles is that the Markov partition, build from the central tile, is also a suitable geometric representation of the substitution tiling space. The substitutive dynamical system appears here to be an expanding foliation in the space tiling [**31**]. In [**30**], the authors prove that branch loci in tiling spaces are invariant for homeomorphic tiling spaces. A natural question is then how to characterize branch loci in the central tile as intersections of tiles and to derive from SR-boundary or contact graphs an explicit criterion for orientable hyperbolic one-dimensional attractors.

This question can be seen from a more general point of view. Indeed, branch loci or other topological invariants concern the substitutive tiling flow; whereas the Rauzy fractal represents the substitutive dynamical system, or, in other words, a section of the substitutive tiling flow. Then, if branch loci are invariants of the full tiling flow, they should appear in each section of the flow, hence, in several Rauzy fractals. A natural question then becomes to identify substitutions that produce (*i.e*, they are sections of) the same tiling flow. However, several pictures showed that the central tiles for substitutions that are conjugate to each other look *globally* the same

(see [**22**]). Therefore, a related challenge is to check which topological properties are invariant under the action of invertible substitutions. We assume that some (local) topological properties of central tiles are invariant under conjugacy, such as the existence of (local) cut points or connectivity. To go further in that direction, we need both to propose a topological criterion to characterize the existence of cut points (as already mentioned in Section 7.1) and to make explicit how boundary and contact graphs change when applying an invertible substitution to a given substitution.

A motivation is to generate new invariants for automorphisms of the free group. It is obvious that any substitution naturally extends to an endomorphism of the free group, and those that extend to an automorphism are called *invertible* substitutions. Although invertibility does not play a significant role in the case of substitutions, it does in the case of morphisms of the free group mainly because most geometric constructions lead to automorphisms. A specific case is given by homeomorphisms of orientable surfaces with nonempty boundary: the homeomorphism of the surface can be coded into an automorphism of the homotopy group of the surface, which is called *geometrical*. Notice that even if all automorphisms of the group free group of rank two F_2 are geometrical, most automorphisms of free groups are not: for instance, the Tribonacci automorphism $1 \mapsto 12$, $2 \mapsto 13$, $3 \mapsto 1$ is not geometrical in the free group of rank three and more generally, no irreducible automorphism on a free group of odd rank comes from a homeomorphism of an orientable surface [**22**].

When considering automorphisms, the free group F_N of rank N plays the role of the alphabet $\mathcal{A}$ in the terminology of substitutions. The equivalent of infinite sequences as considered in this paper is given by the Gromov boundary of the free group. It is a Cantor set which compactifies F_N. Any automorphism of F_N extends to the boundary of F_N [**53**]. The analogue to a minimal symbolic dynamical system is then given by algebraic laminations. An attractive algebraic lamination of an automorphism is a set of geodesic lines in the free group which is closed (for the topology induced by the boundary topology), invariant under the action of the group and flip-invariant (*i.e.*, orientation-invariant); therefore it is the analog to a substitutive dynamical system [**54**]. However, explicitly building such an attractive algebraic lamination is far from trivial; indeed, the constructions used for substitution cannot be used since iterations of automorphisms of free groups produce cancellations so that infinite fixed words cannot be generated easily.

An impressive achievement was obtained by Bestvina, Feighn and Handel [**41**]; the idea is to represent an automorphism of F_N by a homotopy equivalence of a marked group G with fundamental group F_N. In [**42**], the authors consider irreducible automorphisms with irreducible power (*iwip*): they are the algebraic equivalent of pseudo-Anosov homeomorphisms of surfaces. They describe an algorithmic process to build a representative for the automorphism, called an improved relative train-track map, which takes care of cancellations so that one can build a reduced two-sided recurrent infinite word on which the automorphism acts without cancellation and which is fixed by some power of the automorphism. From this, one deduces a symbolic dynamical system that is proved to be a representation of the attractive algebraic lamination [**22**].

Introducing the symbolic representation of an attractive lamination by means of a train track allows to geometrically represent the lamination by a central tile, as soon as the automorphism has a unit Pisot dilation coefficient [**22**]. However, the construction depends on the train-track used to represent the automorphism; additionally automorphisms are considered in this context up to conjugacy by inner automorphisms. This is natural since a basic difference between the free monoid and the free group is that the free monoid has a canonical basis, which is not the case for the free group. Hence, although the attractive lamination is intrinsic, there exist several symbolic codings for it. It seems that deciding to choose a specific coding, hence a specific symbolic dynamical system, corresponds in particular to choosing a discrete time to move on the leaf of the formal lamination. The challenge here is to understand which topological and metric properties of the central tile is invariant through conjugacy and the choice

of the train-track representative. This will lead to the definition of a topological or metric invariant for free group automorphisms. The ultimate goal would be to propose a metric on the full lamination of an automorphism of the free group. In this direction, preliminary results in [**18, 19**] are of great interest: they illustrate why and how the central tile of the Tribonacci substitution is covered by an explicit Peano curve.

7.4. Effective constructions and generalizations

To finish these perspectives, let us mention some concrete applications of substitutive dynamical systems. As already mentioned, central tiles are the fundament of an explicit Markov partition for the action of the incidence matrix of σ on the torus. Let us consider this question in the reverse way. We consider a toral automorphism with a unit Pisot Perron-Frobenius eigenvalue and we look for a Markov partition. From the theory, we could actually choose as many partitions as we can build substitutions with the given matrix. In other words, we can build a substitution with the given matrix, then permute letters in the image of any letter, and we shall generate another Markov partition. At this stage, the crucial point is to propose criterions to choose a good Markov partition. By analogy with transformations of the interval, good Markov partitions shall be the ones for which two points located at a small distance have a quite long future in common. From this point of view, Markov partitions based on a central tile with a non trivial fundamental group are not useful, since in this case many points of a piece of the partition are located at a small distance from another piece. Therefore, the remaining question is: given a unit matrix with a Pisot expanding eigenvalue, can we find a substitution corresponding to this matrix such that the pieces of the central tile are homeomorphic to a disk, or at least simply connected?

Similar considerations can be made in the field of discrete geometry. Let us consider a hyperplane $\mathcal{P}$ in $\mathbb{R}^n$. The discrete approximation of $\mathcal{P}$ is defined as the union of faces of unit cubes with integral coordinates that intersect $\mathcal{P}$ [**21**]. A specific case occurs when the hyperplane is orthogonal to the dominant eigenvector of a matrix with positive entries and with a Pisot unit of degree n as eigenvalue. In this case, any substitution with the matrix as incidence matrix is an irreducible unit Pisot substitution. Therefore, following the results stated in Chapter 3, the map $\mathbf{E}_1$ defined in Definition 3.4 stabilizes the discrete approximation of $\mathcal{P}$. From this we can derive a process to *generate* the discrete approximation of $\mathcal{P}$: as soon as the substitution satisfies the property (F), applying $\mathbf{E}_1^k$ to the unit cube produces increasing pieces of the approximation. However, in order to obtain suitable approximations, we need to check that the pieces are uniform [**68**]. This suggests that the choice of a good generator of a discrete surface (that is, a substitution with the suitable incidence matrix) should be guided by topological considerations on the central tile, such as simple connectivity and the fact that $\mathbf{0}$ is an inner point. To go further in that direction, a first strategy is to exhibit a relation between the topological properties of the finite approximations and their renormalized limit, that is the central tile. A second strategy is to generalize the topological characterizations described in this monograph in the context of the finite approximations. In other words, does there exist a graph that describes the connectivity of a finite approximation or its disklikeness?

A final motivation of this work is to control the production of *any* discrete plane. This refers to what is called *Rauzy program* in [**36**]: "find generalizations of the Sturmian/rotation interaction which would naturally generate approximation algorithms". Revisited with the Arnoux-IO formalism [**25**], this means to start from a n-dimensional vector $\mathbf{u}$ in $\mathbb{R}^n$ and to decompose this vector with a continued fraction algorithm, $\mathbf{u} = \mathbf{M}_1\mathbf{M}_2 \dots \mathbf{M}_k\mathbf{u}_k$, say. By construction, the matrices $\mathbf{M}_k$ are in finite number, and we can choose a substitution σ_k for each matrix. Then, from [**23**], we know that the iterations of dual substitutions $\mathbf{E}_1(\sigma_1)\mathbf{E}_1(\sigma_2)\dots\mathbf{E}_1(\sigma_k)(\mathcal{U})$ [7.1] generate increasing pieces of the discrete approximation for the hyperplane orthogonal to $\mathbf{u}$. Many questions remain on this topic: can we cover the whole discrete plane with these iterations

[7.1] $\mathcal{U}$ is defined in (3.4).

[**76**]? Can we renormalize the approximations and associate a central tile to the vector $\mathbf{u}$? Is such a central tile useful to produce simultaneous rational approximations of the coordinates of $\mathbf{u}$? Coming back to discrete geometry, two main questions appear. The first is how to use this process to decide whether a discrete piece is indeed a part of a discrete approximation of an hyperplane. This question was tackled in [**37, 65**] by using modified Jacobi-Perron algorithm. The second question is how to ensure that the pieces that are produce by iterations have a suitable shape? As explained in the substitutive case, we expect that approximation contain no holes and are quite uniform. To answer this question, we need to build boundary graphs for the successive discrete approximations, considering that the substitution may change at each step and then take benefit of the structure of such (infinite) graph.

CHAPTER 8

Appendix: several technical proofs and definitions

This appendix is devoted to detailed technical proofs of results we stated throughout this monograph.

8.1. A technical proof from Chapter 3

PROOF OF PROPOSITION 3.13. We introduce the lattice $\mathcal{L} = \sum_{k=2}^{d} \mathbb{Z}(\pi(\mathbf{e}_{B(k)}) - \pi(\mathbf{e}_{B(1)})$ and the quotient map $\phi : \mathbb{H}_c \to \mathbb{T} = \mathbb{H}_c/\mathcal{L}$. In order to apply the scheme of the proof of Proposition 3.10, we first need to check that the quotient map condition implies the following assertions.

(1) $\mathcal{L}$ is indeed a lattice, that is, the generating family of $\mathcal{L}$ has rank $d-1$ in $\mathbb{H}_c$.
(2) $\phi(\{\pi(\mathbf{e}_i); 1 \leq i \leq n\})$ is reduced to a single point denoted by $\mathbf{t}$.
(3) The addition of $\mathbf{t}$ is minimal on the torus $\mathbb{T}$. The Kroneker theorem implies that this is true as soon as $\mathbf{t}$ is rationally independent from the generators of $\mathcal{L}$.

Let π_{e+c} denote the projection of $\mathbb{R}^n$ on the beta-expanding and contracting spaces $\mathbb{H}_c \oplus \mathbb{H}_e$ along the beta-supplementary space $\mathbb{H}_s$. We know that the left expanding eigenvector $\mathbf{v}_\beta$ of $\mathbf{M}$ is orthogonal to both the beta-contracting and the beta-supplementary space. Then an explicit formula for π_{e+c} is the following:

$$\forall \mathbf{x} \in \mathbb{R}^n, \quad \pi_{e+c}(\mathbf{x}) = \pi(\mathbf{x}) + \langle \mathbf{x}, \mathbf{v}_\beta \rangle \mathbf{u}_\beta = \sum_{i=1}^{d} \langle \mathbf{x}, \mathbf{v}_{\beta^{(i)}} \rangle \mathbf{u}_{\beta^{(i)}}. \tag{8.1}$$

From the quotient map condition (see (3.10)) we know that

$$\langle \mathbf{e}_j, \mathbf{v}_\beta \rangle \in \sum_{k=1}^{d} \mathbb{Z} \langle \mathbf{e}_{B(k)}, \mathbf{v}_\beta \rangle \qquad (j \in \mathcal{A}).$$

By applying the Galois morphisms this implies that also

$$\langle \mathbf{e}_j, \mathbf{v}_{\beta_i} \rangle \in \sum_{k=1}^{d} \mathbb{Z} \langle \mathbf{e}_{B(k)}, \mathbf{v}_{\beta_i} \rangle \qquad (j \in \mathcal{A})$$

holds for each conjugate β_i of β. We now apply (8.1) and deduce from this that $\pi_{e+c}(\mathbf{e}_i) \in \sum_{k=1}^{d} \mathbb{Z} \pi_{e+c}(\mathbf{e}_{B(k)})$. Hence the family $\pi_{e+c}(\mathbf{e}_{B(1)})$, ..., $\pi_{e+c}(\mathbf{e}_{B(d)})$ is a generating family of the d-dimensional space $\mathbb{H}_c \oplus \mathbb{H}_e$ so that it is a basis of this space.

(8.1) also implies that the coordinates of each $\pi_{e+c}(\mathbf{e}_i)$ are invariant by the application of any Galois morphism of β, hence these points have rational coordinates. We denote by $\mathbf{z}_1$, ..., $\mathbf{z}_d$ the dual basis in $\mathbb{H}_c \oplus \mathbb{H}_e$ of the family $\pi_{e+c}(\mathbf{e}_{B(1)})$, ..., $\pi_{e+c}(\mathbf{e}_{B(d)})$. Linear algebra considerations imply that $\mathbf{z}_1$, ..., $\mathbf{z}_d$ exist and have rational coordinates.

To prove item (1), assume that a combination of $\pi(\mathbf{e}_{B(2)}) - \pi(\mathbf{e}_{B(1)})$, ..., $\pi(\mathbf{e}_{B(d)}) - \pi(\mathbf{e}_{B(1)})$ equals zero. Then we have $\sum_{k=1}^{d} \lambda_k \pi(\mathbf{e}_{B(k)}) = \mathbf{0}$ with $\sum_{k=1}^{d} \lambda_k = 0$. Extending to the space $\mathbb{H}_c \oplus \mathbb{H}_e$, we deduce that $\sum_{k=1}^{d} \lambda_k \pi_{e+c}(\mathbf{e}_{B(k)}) = \nu \mathbf{u}_\beta$. Let us compute the scalar product of $\mathbf{u}_\beta$ with the sum of the dual basis vectors $\mathbf{z} = \mathbf{z}_1 + \cdots + \mathbf{z}_d$. Then we have $\nu \langle \mathbf{u}_\beta, \mathbf{z} \rangle = \sum_{k=1}^{d} \lambda_k = 0$. If $\langle \mathbf{u}_\beta, \mathbf{z} \rangle = 0$, we apply Galois morphisms to this relation. Since $\mathbf{z}$ is rational, we obtain that each $\mathbf{u}_{\beta^{(i)}}$ is orthogonal to $\mathbf{z}$, hence $\mathbf{z}$ is orthogonal to the full space $\mathbb{H}_c \oplus \mathbb{H}_e$ which is impossible. Hence $\nu = 0$ and each $\lambda_k = 0$, implying (1).

Item (2) is a direct consequence of Galois morphisms applied on the quotient map condition combined with (8.1). We have for instance $\mathbf{t} = \phi(\pi(\mathbf{e}_{B(1)})$ (actually, it is also equal to any $\phi(\pi(\mathbf{e}_i))$. Item (3) is equivalent to proving a rational independency between $\pi(\mathbf{e}_{B(1)})$ and $\pi(\mathbf{e}_{B(2)}) - \pi(\mathbf{e}_{B(1)})$, ..., $\pi(\mathbf{e}_{B(d)}) - \pi(\mathbf{e}_{B(1)})$. Assume that $\sum_{k=2}^{d} \lambda_k \pi(\mathbf{e}_{B(k)}) = (\lambda_d + \sum_{k=1}^{d-1} \lambda_k)\pi(\mathbf{e}_{B(1)})$ with $\lambda_k \in \mathbb{Q}$. By using (2.5), we extend this relation to a rational dependency between $\pi_{e+c}(\mathbf{e}_{B(1)})$, ..., $\pi_{e+c}(\mathbf{e}_{B(d)})$. Since these vectors are linearly independent, we deduce that $\lambda_k = 0$ for every k and (3) is proved.

Let us now introduce $\psi(\mathbf{x})$ to denote the number of tiles that contain a given point $\mathbf{x}$. By minimality, $\psi(\mathbf{x})$ is constant almost everywhere so that the covering is a multiple tiling (see the proof of Host in the irreducible case which is detailed in [**66**, Exercise 7.5.14]). □

8.2. Technical proofs from Chapter 5

Proof of Proposition 5.2. The nodes of $\mathcal{G}^{(\mathbf{0})}$ are elements of Γ_{srs}. Since this set is a Delaunay set, the graph has to be finite by condition (1) of its definition.

Consider a node $[\gamma, i]$ of $\mathcal{G}^{(\mathbf{0})}$. There exists an infinite walk $([\gamma_k, i_k])_{k\geq 0}$ starting from $[\gamma_0, i_0] = [\gamma, i]$. Let (p_k, i_k, s_k) with $\sigma(i_{k+1}) = p_k i_k s_k$ $(k \geq 0)$ be the labelling of this walk. By considering the definition of the edges, we obtain an expansion of γ as

$$\gamma = -\pi\mathbf{l}(p_0) - \mathbf{h}\pi\mathbf{l}(p_1) - \cdots - \mathbf{h}^k\pi\mathbf{l}(p_k) + \mathbf{h}^{k+1}\gamma_{k+1} \qquad (k \geq 0).$$

Since all γ_k's are bounded and $\mathbf{h}$ is a contraction, for $k \to \infty$ the power series is convergent and $\gamma = -\sum_{k\geq 0} \mathbf{h}^k\pi\mathbf{l}(p_k)$. This means that $-\gamma$ can be expanded as the prefix-suffix expansion of a path of the prefix-suffix graph starting in the node i. By Corollary 2.7 this implies that $-\gamma \in \mathcal{T}(i)$ and, hence, $\mathbf{0} \in \mathcal{T}(i) + \gamma$.

Suppose conversely that $\mathbf{0} \in \mathcal{T}(i) + \gamma$ with $[\gamma, i] \in \Gamma_{srs}$. Then $-\gamma$ can be expanded as $-\gamma = \sum_{k\geq 0} \mathbf{h}^k\pi\mathbf{l}(p_k)$, with $(p_k, i_k, s_k)_{k\geq 0}$ a suitable walk in the prefix-suffix graph starting in i by Corollary 2.7. Let $\gamma_\ell = -(\sum_{k\geq 0} \mathbf{h}^k\pi\mathbf{l}(p_{k+\ell}))$. Each γ_ℓ obviously satisfies (5.1) and $\mathbf{h}\gamma_{\ell+1} = \gamma_\ell + \pi\mathbf{l}(p_\ell)$.

We now deduce by induction that $[\gamma_{\ell+1}, i_{\ell+1}] \in \Gamma_{srs}$. Indeed, $\gamma_{\ell+1} = \pi(\mathbf{x}_{\ell+1})$ with $\mathbf{x}_{\ell+1} = \mathbf{M}^{-1}(\mathbf{l}(p) + \mathbf{x}_\ell)$ and, hence, $\gamma_{\ell+1} \in \pi(\mathbb{Z}^n)$ by the unimodularity of $\mathbf{M}$. It remains to show that $0 \leq \langle \mathbf{x}_{\ell+1}, \mathbf{v}_\beta\rangle < \langle \mathbf{e}_{i_{\ell+1}}, \mathbf{v}_\beta\rangle$ (assuming that this relation is satisfied at rank ℓ). Indeed, we have (note that $\mathbf{e}_a = \mathbf{l}(a)$ for each $a \in \mathcal{A}$)

$$\begin{aligned}\langle \mathbf{x}_{\ell+1}, \mathbf{v}_\beta\rangle &= \langle \mathbf{M}^{-1}(\mathbf{l}(p_\ell) + \mathbf{x}_\ell), \mathbf{v}_\beta\rangle = \beta^{-1}\langle \mathbf{l}(p_\ell) + \mathbf{x}_\ell, \mathbf{v}_\beta\rangle < \beta^{-1}\langle \mathbf{l}(p_\ell) + \mathbf{e}_{i_\ell}, \mathbf{v}_\beta\rangle \\ &= \beta^{-1}\langle \mathbf{l}(p_\ell) + \mathbf{l}(i_\ell), \mathbf{v}_\beta\rangle \leq \beta^{-1}\langle \mathbf{l}(\sigma(i_{\ell+1})), \mathbf{v}_\beta\rangle \\ &= \beta^{-1}\langle \mathbf{M}\mathbf{l}(i_{\ell+1}), \mathbf{v}_\beta\rangle = \langle \mathbf{l}(i_{\ell+1}), \mathbf{v}_\beta\rangle = \langle \mathbf{e}_{i_{\ell+1}}, \mathbf{v}_\beta\rangle\end{aligned}$$

and

$$\langle \mathbf{x}_{\ell+1}, \mathbf{v}_\beta\rangle = \langle \mathbf{M}^{-1}(\mathbf{l}(p_\ell) + \mathbf{x}_\ell), \mathbf{v}_\beta\rangle = \beta^{-1}\langle \mathbf{l}(p_\ell) + \mathbf{x}_\ell, \mathbf{v}_\beta\rangle \geq \beta^{-1}\langle \mathbf{l}(p_\ell), \mathbf{v}_\beta\rangle \geq 0.$$

Hence $([\gamma_k, i_k])_{k\geq 0}$ is an infinite walk in the zero-expansion graph starting from $[\gamma, i]$. We deduce that $[\gamma, i]$ belongs to the zero-expansion graph. □

Proof of Proposition 5.5. We first prove that every set of points $[i, \gamma, j]$ that satisfies conditions (1) and (3) of Definition 5.4 is finite. If $[i, \gamma, j]$ satisfies these conditions, there exists a finite path $[i_0, \gamma_0, j_0] \to [i_1, \gamma_1, j_1] \to \ldots [i_k, \gamma_k, j_k] \to [i, \gamma, j]$, with $\gamma_0 \in \mathcal{S}$, *i.e.*, in a finite set. For each $\ell \in \{0, \ldots, k\}$, let $\mathbf{x}_\ell \in \mathbb{Z}^n$ be such that $\gamma_\ell = \pi(\mathbf{x}_\ell)$. Moreover, let $\mathbf{x}$ be such that $\gamma = \pi(\mathbf{x})$.

From the definition of the edges of the boundary graph, we deduce that $\mathbf{h}\gamma = \pi(\mathbf{M}\mathbf{x}) = \pm\gamma_k + \pi\mathbf{l}(p_2^{(k)}) - \pi\mathbf{l}(p_1^{(k)}) = \pi(\pm\mathbf{x}_k + \mathbf{l}(p_2^{(k)}) - \mathbf{l}(p_1^{(k)}))$. By iterating this procedure and setting $\mathbf{l}(p^{(\ell)}) = \mathbf{l}(p_2^{(\ell)}) - \mathbf{l}(p_1^{(\ell)})$, we obtain a representation of γ as

$$\gamma = \pi(\mathbf{x}) = \pi(\pm\mathbf{M}^{-1}\mathbf{l}(p^{(k)}) \pm \cdots \pm \mathbf{M}^{-k}\mathbf{l}(p^{(1)}) \pm \mathbf{M}^{-k-1}\mathbf{l}(p^{(0)}) \pm \mathbf{M}^{-k-1}\mathbf{x}_0)$$

(note that the signs $\pm$ are independent from each other).

From (2.5) we deduce that

$$\begin{aligned}\langle \mathbf{x}, \mathbf{v}_\beta\rangle &= \pm\langle \mathbf{M}^{-1}\mathbf{l}(p^{(k)}), \mathbf{v}_\beta\rangle \pm \dots \langle \mathbf{M}^{-k}\mathbf{l}(p^{(1)}), \mathbf{v}_\beta\rangle \pm \langle \mathbf{M}^{-k-1}\mathbf{l}(p^{(0)}), \mathbf{v}_\beta\rangle \pm \langle \mathbf{M}^{-k-1}\mathbf{x}_0, \mathbf{v}_\beta\rangle \\ &= \pm\beta^{-1}\langle \mathbf{l}(p^{(k)}), \mathbf{v}_\beta\rangle \pm \dots \pm \beta^{-k}\langle \mathbf{l}(p^{(1)}), \mathbf{v}_\beta\rangle \pm \beta^{-k-1}\langle \mathbf{l}(p^{(0)}), \mathbf{v}_\beta\rangle \pm \beta^{-k-1}\langle \mathbf{x}_0, \mathbf{v}_\beta\rangle.\end{aligned}$$

Since $\mathbf{x}_0$ is taken from a finite set, we deduce that $\langle \mathbf{x}, \mathbf{v}_\beta\rangle$ is bounded. In view of Condition (5.2) and by the definition of the norm (2.1), $\langle \mathbf{x}, \mathbf{v}_{\beta^{(i)}}\rangle$ is also bounded for each contracting eigenvalue β_i.

Thus $\langle \mathbf{x}, \mathbf{v}_\beta\rangle$ belongs to a bounded subset of $\mathbb{Z}[\beta]$ all whose Galois conjugates are bounded. This subset has to be finite which implies that there are only finitely many possibilities for $\langle \mathbf{x}, \mathbf{v}_\beta\rangle$. Since in view of (2.5) $\gamma = \pi(\mathbf{x})$ is uniquely determined by $\langle \mathbf{x}, \mathbf{v}_\beta\rangle$ there are only finitely many possibilities for γ and we are done.

Now each set of nodes that satisfies conditions (1) and (3) is finite with a uniform bound. So the union of two sets that satisfy the conditions also satisfies the conditions, hence it is finite. We conclude that the largest graph exists. □

Proof of Theorem 5.6. Suppose that $[i, \gamma, j]$ is a node of the boundary graph. By definition, $[i, \gamma, j]$ is the starting point of an infinite path in the graph $\mathcal{G}^{(B)}(\mathcal{S})$ Let $[i, \gamma, j] = [i_0, \gamma_0, j_0] \to \dots \to [i_k, \gamma_k, j_k] \to \dots$ be this path and let $[i, \gamma, j] = [m_0, \alpha_0, n_0] \to \dots \to [m_k, \alpha_k, n_k] \to \dots$ be its type one analogue. From this we build two sequences in the prefix-suffix graph $(p_k, a_k, s_k)_{k\geq 0}$ and $(q_k, b_k, r_k)_{k\geq 0}$ such that

$$\mathbf{h}\alpha_k = \alpha_{k-1} + \pi\mathbf{l}(q_{k-1}) - \pi\mathbf{l}(p_{k-1}).$$

This yields

$$\mathbf{h}^k\alpha_k = \gamma_0 + \sum_{i=0}^{k-1}\mathbf{h}^i\pi\mathbf{l}(q_i) - \sum_{i=0}^{k-1}\mathbf{h}^i\pi\mathbf{l}(p_i).$$

Since α_k belongs to a finite set and $\mathbf{h}$ is strictly contracting on $\mathbb{H}_c$, we deduce

$$\gamma_0 = -\sum_{i\geq 0}\mathbf{h}^i\pi\mathbf{l}(q_i) + \sum_{i\geq 0}\mathbf{h}^i\pi\mathbf{l}(p_i).$$

But $\sum_{i\geq 0}\mathbf{h}^i\pi\mathbf{l}(q_i)$ is build from a path of the prefix-suffix graph that starts in j_0, hence $\sum_{i\geq 0}\mathbf{h}^i\pi\mathbf{l}(q_i) \in \mathcal{T}(j_0)$. Similarly, $\sum_{i\geq 0}\mathbf{h}^i\pi\mathbf{l}(p_i) \in \mathcal{T}(i_0)$. Hence $\mathcal{T}(i_0) \cap (\mathcal{T}(j_0) + \gamma_0)$ is nonempty.

Conversely, if the intersection is nonempty, we build an explicit infinite path of the boundary graph starting in $[i, \gamma, j]$ in view of Corollary 2.7. More precisely, there exist two walks $(p_k, i_k, s_k)_{k\geq 0}$ and $(p'_k, i'_k, s'_k)_{k\geq 0}$ in the prefix-suffix graph starting in i and j such that $\gamma = \sum_{k\geq 0}\mathbf{h}^k\pi\mathbf{l}(p_k) - \sum_{k\geq 0}\mathbf{h}^k\pi\mathbf{l}(p'_k)$. We build inductively as follows an infinite path of the boundary graph starting in $[i, \gamma, j]$.

Let $\gamma_1 = \sum_{k\geq 0}\mathbf{h}^k\pi\mathbf{l}(p_{k+1}) - \sum_{k\geq 0}\mathbf{h}^k\pi\mathbf{l}(p'_{k+1})$. The points γ_1 and $-\gamma_1$ obviously satisfy (5.2). It remains to choose the one that belongs to the set $\mathfrak{D}$. We know that $\gamma = \pi(\mathbf{x})$, $\mathbf{x} \in \mathbb{Z}^n$. From the definition of γ_1 we deduce that $\gamma_1 = \pi(\mathbf{x}_1)$ with $\mathbf{M}\mathbf{x}_1 = \mathbf{x} + \mathbf{l}(p_0) - \mathbf{l}(p'_0)$. If $\langle \mathbf{x}_1, \mathbf{v}_\beta\rangle > 0$ then $[i_1, \gamma_1, j_1]$ belongs to $\mathfrak{D}$ and there is an edge of type 1 from $[i, \gamma, j]$ to $[i_1, \gamma_1, j_1]$. If $\langle \mathbf{x}_1, \mathbf{v}_\beta\rangle < 0$, then $[j_1, \gamma_1, i_1]$ belongs to $\mathfrak{D}$ and there is an edge of type 2 from $[i, \gamma, j]$ to $[i_1, -\gamma_1, j_1]$. If $\langle \mathbf{x}_1, \mathbf{v}_\beta\rangle = 0$ and $i_1 \leq j_1$, there is an edge of type 1 from $[i, \gamma, j]$ to $[i_1, \gamma_1, j_1]$. If $\langle \mathbf{x}_1, \mathbf{v}_\beta\rangle = 0$ and $i_1 > j_1$, there is an edge of type 2 from $[i, \gamma, j]$ to $[j_1, -\gamma_1, i_1]$.

The process can continue and we obtain an infinite walk in the graph starting in $[i, \gamma, j]$. Hence $[i, \gamma, j]$ is a node of the boundary graph. □

PROOF OF THEOREM 5.7. To prove the first assertion we need to check that for every node $[i,\gamma,j]$ of SR-boundary graph, $[\gamma,j]$ belongs to the self-replicating set. This is done by induction on the length of the path leading to a node from a starting node contained in $\mathcal{S}_{srs}$. Assume that $[\gamma,j]\in\Gamma_{srs}$ and that there exists an edge from $[i,\gamma,j]$ to $[i_1,\gamma_1,j_1]$. If the edge is of type 1 we have $\gamma_1=\mathbf{h}^{-1}(\gamma+\pi\mathbf{l}(p_2)-\pi\mathbf{l}(p_1))$ with $\sigma(j_1)=p_2js_2$. Since $[i_1,\gamma_1,j_1]$ is a node of the graph, it belongs to $\mathfrak{D}$, hence, $\langle\gamma_1,\mathbf{v}_\beta\rangle\geq 0$. Since $[\gamma,j]\in\Gamma_{srs}$, we also have $\gamma=\pi(\mathbf{x})$ with $0\leq\langle\mathbf{x},\mathbf{v}_\beta\rangle<\langle\mathbf{v}_\beta,\mathbf{e}_j\rangle$. We deduce that $\gamma_1=\pi(\mathbf{x}_1)$ with $\mathbf{x}_1=\mathbf{M}^{-1}(\mathbf{x}+\mathbf{l}(p_2)-\mathbf{l}(p_1))$. Then

$$\begin{aligned}\langle\mathbf{x}_1,\mathbf{v}_\beta\rangle &= \langle\mathbf{M}^{-1}(\mathbf{x}+\mathbf{l}(p_2)-\mathbf{l}(p_1)),\mathbf{v}_\beta\rangle=\beta^{-1}\langle\mathbf{x}+\mathbf{l}(p_2)-\mathbf{l}(p_1),\mathbf{v}_\beta\rangle\\ &< \beta^{-1}\langle\mathbf{e}_j+\mathbf{l}(p_2),\mathbf{v}_\beta\rangle\leq\beta^{-1}\langle\mathbf{l}(\sigma(j_1)),\mathbf{v}_\beta\rangle=\langle\mathbf{e}_{j_1},\mathbf{v}_\beta\rangle.\end{aligned}$$

Hence $[\gamma_1,j_1]\in\Gamma_{srs}$.

Assume now that the edge from $[i,\gamma,j]$ to $[i_1,\gamma_1,j_1]$ is of type 2. Then $\gamma_1=\pi(\mathbf{x}_1)$ with $\mathbf{x}_1=\mathbf{M}^{-1}(-\mathbf{x}+\mathbf{l}(p_1)-\mathbf{l}(p_2))$ and $\sigma(j_1)=p_1is_1$. We already know that $\langle\mathbf{x}_1,\mathbf{v}_\beta\rangle\geq 0$, and $\langle\mathbf{x},\mathbf{v}_\beta\rangle\geq 0$. Then

$$\langle\mathbf{x}_1,\mathbf{v}_\beta\rangle\leq\beta^{-1}\langle\mathbf{l}(p_1),\mathbf{v}_\beta\rangle=\beta^{-1}\langle\mathbf{l}(p_1),\mathbf{v}_\beta\rangle<\beta^{-1}\langle\mathbf{l}(p_1is_1),\mathbf{v}_\beta\rangle=\beta^{-1}\langle\mathbf{l}(\sigma(j_1)),\mathbf{v}_\beta\rangle=\langle\mathbf{e}_{j_1},\mathbf{v}_\beta\rangle.$$

Hence $[\mathbf{x}_1,j_1]\in\Gamma_{srs}$ which concludes the proof.

The second assertion is proved as follows. Let $\overline{B}[i,\gamma,j]=\mathcal{T}(i)\cap(\mathcal{T}(j)+\gamma)$ for the moment. By (2.6), we know that

$$\begin{aligned}\overline{B}[i,\gamma,j] &= \mathcal{T}(i)\cap(\mathcal{T}(j)+\pi(\gamma))\\ &= \left(\bigcup_{\sigma(i_1)=p_1is_1}\mathbf{h}\mathcal{T}(i_1)+\pi\mathbf{l}(p_1)\right)\cap\left(\gamma+\bigcup_{\sigma(j_1)=p_2js_2}\mathbf{h}\mathcal{T}(j_1)+\pi\mathbf{l}(p_2)\right).\end{aligned}$$

It remains to express each term $\mathbf{h}\mathcal{T}(i_1)+\pi\mathbf{l}(p_1))\cap(\gamma+\mathbf{h}\mathcal{T}(j_1)+\pi\mathbf{l}(p_2))$ in terms of $\overline{B}[\cdot]$. The two following equalities hold:

$$\begin{aligned}\mathbf{h}\mathcal{T}(i_1)+\pi\mathbf{l}(p_1))\cap(\gamma+\mathbf{h}\mathcal{T}(j_1)+\pi\mathbf{l}(p_2)) &= \pi\mathbf{l}(p_1)+\mathbf{h}\overline{B}[i_1,\mathbf{h}^{-1}(\gamma+\pi\mathbf{l}(p_2)-\pi\mathbf{l}(p_1)),j_1]\\ &= \pi\mathbf{l}(p_2)+\gamma+\mathbf{h}\overline{B}[j_1,\mathbf{h}^{-1}(-\gamma-\pi\mathbf{l}(p_2)+\pi\mathbf{l}(p_1)),i_1].\end{aligned}$$

By the definition of the boundary graph, if $[i_1,\mathbf{h}^{-1}(\mathbf{x}+\pi\mathbf{l}(p_2)-\pi\mathbf{l}(p_1)),j_1]\in\mathfrak{D}$, there is an edge of type 1 from $[i,\gamma,j]$ to $[i_1,\mathbf{h}^{-1}(\gamma+\pi\mathbf{l}(p_2)-\pi\mathbf{l}(p_1)),j_1]$ in the graph. But the node belongs to $\mathfrak{D}$ if and only if $\langle\pi\mathbf{l}(p_1),\mathbf{v}_\beta\rangle\leq\langle\mathbf{x}+\pi\mathbf{l}(p_2),\mathbf{v}_\beta\rangle$, hence the label of the graph is $\mathbf{e}=\pi\mathbf{l}(p_1)$.

The second possibility is $[j_1,\mathbf{h}^{-1}(-\gamma-\pi\mathbf{l}(p_2)+\pi\mathbf{l}(p_1)),j_1]\in\mathfrak{D}$ and there is an edge of type 2 from $[i,\gamma,j]$ to $[j_1,\mathbf{h}^{-1}(-\gamma-\pi\mathbf{l}(p_2)+\pi\mathbf{l}(p_1)),i_1]$ in the graph. The label is then $\mathbf{e}=\pi\mathbf{l}(p_2)+\gamma$. In each case, we then have

$$\overline{B}([i,\gamma,j])=\bigcup_{[i,\gamma,j]\xrightarrow{\mathbf{e}}[i_1,\gamma_1,j_1]\in\mathcal{G}^{(B)}_{SRT}}\mathbf{h}(\overline{B}([i_1,\gamma_1,j_1]))+\mathbf{e}.$$

Since the solutions of a GIFS are uniquely defined we deduce that the intersections $\mathcal{T}(i)\cap(\mathcal{T}(j)+\gamma)$ are solutions of the GIFS.

The third assertion allows follows from the tiling property: we have

$$\partial\mathcal{T}(i):=\bigcup_{[\gamma,j]\neq[\mathbf{0},i]\in\Gamma_{srs}}\mathcal{T}(i)\cap(\mathcal{T}(j)+\gamma).$$

Assume that $\gamma\neq\mathbf{0}$ and $\mathcal{T}(i)\cap(\mathcal{T}(j)+\gamma)\neq 0$. Then γ satisfies (5.2). From $\gamma\neq\mathbf{0}$ and $[\gamma,j]\in\Gamma_{srs}$ we deduce $\gamma=\pi(\mathbf{x})$ with $\langle\mathbf{x},\mathbf{v}_\beta\rangle>0$. Hence $[i,\gamma,j]\in\mathcal{S}_{srs}$. Since $\mathcal{T}(i)\cap(\mathcal{T}(j)+\gamma)$ is nonempty, $[i,\gamma,j]$ is a node of the boundary graph. Assume now that $\gamma=\mathbf{0}$. If $i<j$, by the definition of the boundary graph, $\mathcal{T}(i)\cap\mathcal{T}(j)\neq 0$ if and only if $[i,\mathbf{0},j]$ is a node of the graph. If $i>j$, the set $\mathcal{T}(i)\cap\mathcal{T}(j)$ is nonempty if and only if $[j,\mathbf{0},i]$ is a node of the graph. □

PROOF OF PROPOSITION 5.17. This proof is extracted from [**124**]. We only give a sketch for the sake of completeness. Let $[i,\gamma,j]$ be a node of a contact graph. Then γ can be written as $\gamma = \mathbf{h}^k\pi[\mathbf{l}(q_k)-\mathbf{l}(p_k)]+\cdots+\mathbf{h}^0\pi[\mathbf{l}(q_0)-\mathbf{l}(p_0)]+\gamma_0$ with γ_0 in a finite set. Hence γ is bounded.

Let $[i,\gamma,j]\in\mathfrak{D}$ with $\gamma=\pi(\mathbf{x})$ and $0\leq\langle\mathbf{x},\mathbf{v}_\beta\rangle<\langle\mathbf{e}_j,\mathbf{v}_\beta\rangle$. Suppose that $[i,\gamma,j]\to[i_1,\gamma_1,j_1]$ satisfies condition (2) of Definition 5.19 with $\gamma_1=\pi(\mathbf{x}_1)$. Then by the definition of edges, one can show that $0\leq\langle\mathbf{x}_1,\mathbf{v}_\beta\rangle<\langle\mathbf{e}_{j_1},\mathbf{v}_\beta\rangle$ (see the proof of Theorem 5.7 or [**124**] for details).

For every node $[i,\gamma,j]$ of the contact graph, with $\gamma=\pi(\mathbf{x})$, the projection $\pi_e(\mathbf{x})$ on the expanding line is bounded since $\mathbf{h}\ [\gamma_j]\in\Gamma_{srs}$. Since we have also proved that $\gamma=\pi(\mathbf{x})$ is bounded, there are only a finite number of possibilities (by the same arguments as in the proof of Proposition 5.5). □

PROOF OF PROPOSITION 5.18. This result is proved in [**124**]. The main idea is the following: If there is a path of length n between a node $[i,\gamma,j]$ and $[i_0,\gamma_0,j_0]$, then the polygons $\mathcal{T}_n(i_0)$ and $\mathcal{T}_n(j_0)+\gamma_0$ share a common edge related to $[i,\gamma,j]$. □

PROOF OF LEMMA 5.23. To preserve the set $\{\mathbf{e}_i,\mathbf{e}_j+\gamma_1,\mathbf{e}_k+\gamma_2\}$ associated with $[i,\gamma_1,j,\gamma_2,k]$ we can act either by translation or by reversing the order. Then $\{\mathbf{e}_i,\mathbf{e}_j+\gamma_1,\mathbf{e}_k+\gamma_2\}$ is equal to $\{\mathbf{e}_i,\mathbf{e}_k+\gamma_2,\mathbf{e}_j+\gamma_1\}$, $\gamma_1+\{\mathbf{e}_j,\mathbf{e}_i-\gamma_1,\mathbf{e}_k+\gamma_2-\gamma_1\}$,$\gamma_1+\{\mathbf{e}_j,\mathbf{e}_k+\gamma_2-\gamma_1,\mathbf{e}_i-\gamma_1\}$, $\gamma_2+\{\mathbf{e}_k,\mathbf{e}_i-\gamma_2,\mathbf{e}_j+\gamma_1-\gamma_2\}$, $\gamma_2+\{\mathbf{e}_k,\mathbf{e}_j+\gamma_1-\gamma_2,\mathbf{e}_i-\gamma_2,\}$. We deduce that the equivalence class of $[i,\gamma_1,j,\gamma_2,k]$ contains the six following elements (depending on the value of the node, some of them can be equal):

$$\begin{array}{rcl}[i,\gamma_1,j,\gamma_2,k] & \simeq_t & [i,\gamma_2,k,\gamma_1,j]\simeq_t[j,-\gamma_1,i,\gamma_2-\gamma_1,k]\\ & \simeq_t & j,\gamma_2-\gamma_1,k,-\gamma_1,i]\simeq_t[k,-\gamma_2,i,\gamma_1-\gamma_2,j]\simeq_t[k,\gamma_1-\gamma_2,j,-\gamma_2,i].\end{array}$$

In order to choose a unique candidate, we set $\gamma_0=\mathbf{0}$ and we denote $a_0=i$, $a_1=j$, $a_2=k$. For each γ_i there exists $\mathbf{x}_i\in\mathbb{Z}^n$ such that $\gamma_i=\pi(\mathbf{x}_i)$. By (2.5), $\langle\mathbf{x}_i,\mathbf{v}_\beta\rangle$ depends only on γ_i. We choose a permutation μ on $\{0,1,2\}$ such that the quantities $\langle\mathbf{x}_i,\mathbf{v}_\beta\rangle$ are ordered and, when there is an ambiguity, the associated letters a_i are also ordered:

$$\left\{\begin{array}{l}\langle\mathbf{x}_{\mu(0)},\mathbf{v}_\beta\rangle\leq\langle\mathbf{x}_{\mu(1)},\mathbf{v}_\beta\rangle\leq\langle\mathbf{x}_{\mu(2)},\mathbf{v}_\beta\rangle\\ \langle\mathbf{x}_{\mu(\alpha)},\mathbf{v}_\beta\rangle=\langle\mathbf{x}_{\mu(\beta)},\mathbf{v}_\beta\rangle\implies a_{\mu(\alpha)}<a_{\mu(\beta)}.\end{array}\right.$$

A unique permutation satisfies these conditions. The unique equivalent node to $[i,\gamma_1,j,\gamma_2,k]$ in $\overline{\mathfrak{T}}$ is then obtained by translating the smallest quantity $\langle\mathbf{x}_{\mu(0)},\mathbf{v}_\beta\rangle$ to zero, that is, $[a_{\mu(0)},\gamma_{\mu(1)}-\gamma_{\mu(0)},a_{\mu(1)},\gamma_{\mu(2)}-\gamma_{\mu(0)},a_{\mu(2)}]$. □

PROOF OF THEOREM 5.25. The proof of finiteness is the same as in Proposition 5.5. Consider a node $[i,\gamma_1,j,\gamma_2,k]$ that satisfies (1) and (3). Then γ_1 and γ_2 can be expanded as

$$\gamma_{1,2}=\pi(\mathbf{x}_{1,2})=\pi(\pm\mathbf{M}^{-1}\mathbf{l}(p_{1,2}^{(k)})\pm\cdots\pm\mathbf{M}^{-k}\mathbf{l}(p_{1,2}^{(1)})\pm\mathbf{M}^{-k-1}\mathbf{l}(p_{1,2}^{(0)})\pm\mathbf{M}^{-k-1}\mathbf{x}_{1,2}^{(0)}).$$

By the argument used in Proposition 5.5, γ_1 and γ_2 are in contained in a finite set, so that the triple point graph is finite.

We mimic the proof of Theorem 5.6 to demonstrate the assertion about intersections of tiles. Consider a path $[i^{(n)},\gamma_1^{(n)},j^{(n)},\gamma_2^{(n)},k^{(n)}]$ in the graph. By the definition of edges, there exist three walks in the prefix-suffix graph respectively starting in i_0, j_0 and k_0 such that

$$\begin{array}{rcl}\gamma_1^{(0)} & = & -\displaystyle\sum_{n\geq0}\mathbf{h}^n\pi\mathbf{l}(p_1^{(n)})+\sum_{n\geq0}\mathbf{h}^n\pi\mathbf{l}(p_0^{(n)}),\\ \gamma_2^{(0)} & = & -\displaystyle\sum_{n\geq0}\mathbf{h}^n\pi\mathbf{l}(p_2^{(n)})+\sum_{n\geq0}\mathbf{h}^n\pi\mathbf{l}(p_0^{(n)}).\end{array}$$

We deduce that $\mathcal{T}(j_0)+\gamma_1^{(0)}$ and $\mathcal{T}(k_0)+\gamma_2^{(0)}$ both contain the point $\sum_{n\geq0}\mathbf{h}^n\pi\mathbf{l}(p_0^{(n)})$ that belongs to $\mathcal{T}(i_0)$. This yields a nonempty intersection $\mathcal{T}(i)\cap(\mathcal{T}(j)+\gamma_1^{(0)})\cap(\mathcal{T}(k)+\gamma_2^{(0)})$.

Conversely, assume that $\mathcal{T}(i)\cap(\mathcal{T}(j)+\gamma_1)\cap(\mathcal{T}(k)+\gamma_2)$ is nonempty, with $[i,\gamma_1,j,\gamma_2,k]\in\mathfrak{T}$ and $[\gamma_1,j]\in\Gamma_{srs}$, $[\gamma_2,k]\in\Gamma_{srs}$. Set $[i^{(0)},\gamma_1^{(0)},j^{(0)},\gamma_2^{(0)},k^{(0)}]=\phi_{\overline{\mathfrak{T}}}[i,\gamma_1,j,\gamma_2,k]$. By the definition of $\phi_{\overline{\mathfrak{T}}}$, we also have $[\gamma_1^{(0)},j^{(0)}]\in\Gamma_{srs}$ and $[\gamma_2^{(0)},k^{(0)}]\in\Gamma_{srs}$.

Since the intersection is nonempty we exhibit three walks in the prefix-suffix graph (starting in i_0, j_0, k_0) with $\gamma_1^{(0)} = -\sum_{n\geq 0} \mathbf{h}^n \pi \mathbf{l}(p_1^{(n)}) + \sum_{n\geq 0} \mathbf{h}^n \pi \mathbf{l}(p_0^{(n)})$ and $\gamma_2^{(0)} = -\sum_{n\geq 0} \mathbf{h}^n \pi \mathbf{l}(p_2^{(n)}) + \sum_{n\geq 0} \mathbf{h}^n \pi \mathbf{l}(p_0^{(n)})$. We define $\gamma_{1,2}^{(k)} = -\sum_{n\geq 0} \mathbf{h}^n \pi \mathbf{l}(p_2^{(n+k)}) + \sum_{n\geq 0} \mathbf{h}^n \pi \mathbf{l}(p_0^{(n+k)})$.

Then the nodes $\phi_{\overline{\mathfrak{T}}}[i^{(n)}, \gamma_1^{(n)}, j^{(n)}, \gamma_2^{(n)}, k^{(n)}]$ belong to $\overline{\mathfrak{T}}$; they satisfy condition (1) and they give rise to an infinite path in the graph, hence they belong to the triple point graph.

As in the proof of Theorem 5.7, we deduce a GIFS equation between the triple intersections:

$$T[i, \gamma_1, j, \gamma_2, k] = \bigcup_{[i,\gamma_1,j,\gamma_2,k] \xrightarrow{\mathbf{e}} [i',\gamma_1',j',\gamma_2',k'] \in \mathcal{G}_{SRT}^{(T)}} \mathbf{h} T[i', \gamma_1', j', \gamma_2', k'] + \mathbf{e}.$$

This implies that any point in $T[i, \gamma_1, j, \gamma_2, k]$ can be expanded by using the labels of a path of the triple point graph starting from $[i, \gamma_1, j, \gamma_2, k]$. □

Proof of Proposition 5.30. The proof is given in the case of the SR-boundary graph. The cases of triple or quadruple point graphs are similar.

Assume that a point x corresponds to infinitely many different walks starting from a node $N_0 = [i^{(0)}, \gamma^{(0)}, j^{(0)}]$ of the SR-boundary graph. We denote these walks by $w_k = N_0 \xrightarrow{\mathbf{e}_k^{(1)}} N_k^{(1)} \xrightarrow{\mathbf{e}_k^{(2)}} N_k^{(2)} \xrightarrow{\mathbf{e}_k^{(3)}} \cdots$ with $N_k^{(l)} = [i_k^{(l)}, \gamma_k^{(l)}, j_k^{(l)}]$. By the local finiteness of the self-replicating multiple tiling (see Remark 3.8), there exists a positive integer P such that each point of $\mathbb{H}_c$ is covered at most P times by the tiles of this multiple tiling. Since the walks w_k are all distinct, there exists a positive integer n and $P+1$ walks, say $w_1, \ldots, w_{P+1}$, such that the prefixes of length n of $w_1, \ldots, w_{P+1}$ are pairwise distinct. From Theorem 5.7 we have that

$$\mathcal{T}(i^{(0)}) \cap (\mathcal{T}(j^{(0)}) + \gamma^{(0)}) = \bigcup (\mathbf{h}^n \mathcal{T}(i^{(n)}) \cap (\mathcal{T}(j^{(n)}) + \gamma^{(n)})) + \mathbf{e}^{(1)} + \mathbf{h}\mathbf{e}^{(2)} + \cdots + \mathbf{h}^{n-1}\mathbf{e}^{(n)},$$

where the union is extended over all walks

$$N^{(0)} \xrightarrow{\mathbf{e}^{(1)}} N^{(1)} \xrightarrow{\mathbf{e}^{(2)}} N^{(2)} \xrightarrow{\mathbf{e}^{(3)}} \cdots \xrightarrow{\mathbf{e}^{(n)}} N^{(n)}$$

of length n in the SR-boundary graph. In particular, the tiles $\mathbf{e}_k^{(1)} + \mathbf{h}\mathbf{e}_k^{(2)} + \cdots + \mathbf{h}^{n-1}\mathbf{e}_k^{(n)} + \mathbf{h}_k^n \mathcal{T}(i_k^{(n)})$ are pairwise distinct tiles of the self-replicating multiple tiling. However, by Corollary 5.9, the point x belongs to each of these $P+1$ tiles, which is impossible by the choice of P, a contradiction.

Consider now a path $w : N^{(0)} \xrightarrow{\mathbf{e}^{(1)}} N^{(1)} \xrightarrow{\mathbf{e}^{(2)}} N^{(2)} \xrightarrow{\mathbf{e}^{(3)}} \cdots$ in the SR-boundary graph that is not ultimately periodic. Since the SR-boundary graph is finite, two nodes in this path are equal, *i.e.*, there exist positive integers n and p such that $N^{(n)} = N^{(n+p)}$. Thus w contains a piece

$$v : N^{(n)} \xrightarrow{\mathbf{e}^{(n+1)}} \cdots \xrightarrow{\mathbf{e}^{(n+p)}} N^{(n+p)}.$$

Thus there is a prefix w_1 of length n and an infinite suffix w_2 such that $w = w_1 v w_2$. Denote the r-fold repetition of the walk v by v^r. Since w is not ultimately periodic, the walks

$$w_k = w_1 v^k w_2 \qquad (k \geq 1)$$

are infinitely many different walks starting at $N^{(0)}$.

Consequently, if only a finite number of paths lead away from a given node $\mathcal{N}$ of the SR-boundary graph, these paths all have to be ultimately periodic. This implies that the corresponding points can be calculated exactly from the formula $\mathbf{x} = \sum_{n\geq 0} \mathbf{h}^n \mathbf{e}^{(n)}$, since the ultimate periodicity of the sequence $(\mathbf{e}^{(n)})_{n\geq 1}$ makes this formula to a "rational function" in $\mathbf{h}$. □

8.3. Details for the quadruple point graph

To deal with quadruple intersections, we reduce the set of all possible intersections defined in (5.11).

$$\overline{\mathfrak{Q}} = \left\{ \begin{array}{l} [i,\gamma_1,j,\gamma_2,k,\gamma_3,l] \in \mathfrak{Q} \\ \gamma_1 = \pi(\mathbf{x}_1),\ \gamma_2 = \pi(\mathbf{x}_2),\ \gamma_3 = \pi(\mathbf{x}_3)\ ; \\ \mathbf{x}_1,\mathbf{x}_2,\mathbf{x}_3 \in \mathbb{Z}^n \end{array} \left| \begin{array}{l} 0 \le \langle \mathbf{x}_1,\mathbf{v}_\beta\rangle \le \langle \mathbf{x}_2,\mathbf{v}_\beta\rangle \le \langle \mathbf{x}_3,\mathbf{v}_\beta\rangle \\ \text{if } \gamma_1 = 0 \text{ then } i<j \\ \text{if } \gamma_2 = \gamma_1 \text{ then } j<k \\ \text{if } \gamma_3 = \gamma_2 \text{ then } k<l \end{array} \right. \right\}.$$

As for the triple point graph, the set $\overline{\mathfrak{Q}}$ provides a unique representant of intersections between four tiles.

LEMMA 8.1. *Let us define the following equivalence relation on $\mathfrak{Q}$. 4-tuples are equivalent, i.e.,*

$$[i,\gamma_1,j,\gamma_2,k,\gamma_3,l]) \simeq_q [i',\gamma_1',j',\gamma_2',k',\gamma_3',l']$$

if and only if the sets $\{\mathbf{e}_i, \mathbf{e}_j+\gamma_1, \mathbf{e}_k+\gamma_2, \mathbf{e}_l+\gamma_3\}$ and $\{\mathbf{e}_{i'}, \mathbf{e}_{j'}+\gamma_1', \mathbf{e}_{k'}+\gamma_2', \mathbf{e}_{l'}+\gamma_3'\}$ are equal up to a translation. The set $\overline{\mathfrak{Q}}$ is a quotient set for the equivalence relation $\simeq_q$: for every $[i,\gamma_1,j,\gamma_2,k,\gamma_3,l]$, there exists a unique element in $\overline{\mathfrak{Q}}$, denoted by $\phi_{\overline{\mathfrak{Q}}}([i,\gamma_1,j,\gamma_2,k,\gamma_3,l]) \in \overline{\mathfrak{Q}}$ such that $[i,\gamma_1,j,\gamma_2,k,\gamma_3,l] \simeq_q \phi_{\overline{\mathfrak{Q}}}([i,\gamma_1,j,\gamma_2,k,\gamma_3,l])$.

PROOF. As in the case of intersection between three tiles, we reorder the labels of tiles and use translation process. We deduce that there are a-priori 24 sets being equivalent to $[i,\gamma_1,j,\gamma_2,k,\gamma_3,l]$ (some of them can be equal):

$$\begin{array}{rll} [i,\gamma_1,j,\gamma_2,k,\gamma_3,l] \simeq_q & [i,\gamma_2,k,\gamma_1,j,\gamma_3,l] & \text{and all permutations between } j,k,l \\ \simeq_q & [j,-\gamma_1,i,\gamma_2-\gamma_1,k,\gamma_3-\gamma_1,l] & \text{and all permutations between } i,k,l \\ \simeq_q & [k,-\gamma_2,i,\gamma_1-\gamma_2,j,\gamma_3-\gamma_2,l] & \text{and all permutations between } i,j,l \\ \simeq_q & [l,-\gamma_3,i,\gamma_1-\gamma_3,j,\gamma_2-\gamma_3,k] & \text{and all permutations between } i,j,k. \end{array}$$

We fix $\gamma_0 = \mathbf{0}$ and we consider integer pre-images for γ's: $\gamma_i = \pi(\mathbf{x}_i)$, $\mathbf{x}_i \in \mathbb{Z}^n$. Then we consider a permutation of $\{0,1,2,3\}$ such that the quantities $\langle \mathbf{x}_i,\mathbf{v}_\beta\rangle$ are ordered and, when there is an ambiguity, the associated letters a_i are also ordered. There exists a unique permutation μ like that. We translate all γ_i by $-\gamma_{\mu(0)}$ to get the representant of $[i,\gamma_1,j,\gamma_2,k,\gamma_3,l]$ in $\overline{\mathfrak{Q}}$. □

As for the triple intersection, we deduce that if $Q[i,\gamma_1,j,\gamma_2,k,\gamma_3,l]$ denotes the intersection between the four associated tiles, *i.e.*,

$$Q[i,\gamma_1,j,\gamma_2,k,\gamma_3,l] = \mathcal{T}(i) \cap (\mathcal{T}(j)+\gamma_1) \cap (\mathcal{T}(k)+\gamma_2) \cap (\mathcal{T}(l)+\gamma_3)),$$

then $Q[i,\gamma_1,j,\gamma_2,k,\gamma_3,l]$ and $Q\phi_{\overline{\mathfrak{Q}}}[i,\gamma_1,j,\gamma_2,k,\gamma_3,l]$ are equal up to a translation vector.

The quadruple point graph is then defined as follows.

DEFINITION 8.2 (Quadruple point graph). The *quadruple point graph* of σ is denoted by $\mathcal{G}^{(Q)}$. It the largest[8.1] graph such that

(1) If $[i,\gamma_1,j,\gamma_2,k,\gamma_3,l]$ is a node of $\mathcal{G}^{(Q)}$, then $[i,\gamma_1,j,\gamma_2,k,\gamma_3,l] \in \overline{\mathfrak{Q}}$ and

$$\max\{||\gamma_1||,||\gamma_2||,||\gamma_3||\} \le \frac{2\max\{||\pi\mathbf{l}(p)||;(p,a,s)\in\mathcal{P}\}}{1-\max\{|\beta^{(j)}|;j=2\dots d\}}. \tag{8.2}$$

(2) There is an edge from a node $[i,\gamma_1,j,\gamma_2,k,\gamma_3,l]$ to the node $[i',\gamma_1',j',\gamma_2',k',\gamma_3',k']$ if and only if there exists $[\overline{i},\overline{\gamma_1},\overline{j},\overline{\gamma_2},\overline{k},\overline{\gamma_3},\overline{l}] \in \mathfrak{Q}$ and (p_0,a_0,s_0), (p_1,a_1,s_1), (p_2,a_2,s_2),

[8.1] The meaning of "largest" is explained in Definition 5.1.

(p_3, a_3, s_3) such that

$$\begin{cases} [i', \gamma_1', j', \gamma_2', k'] = \Phi_{\overline{\mathfrak{Q}}}[\bar{i}, \overline{\gamma_1}, \bar{j}, \overline{\gamma_1}, \bar{k}, \overline{\gamma_3}, \bar{l}] \\ a_0 = i \text{ and } p_0 a_0 s_0 = \sigma(\bar{i}) \\ a_1 = j \text{ and } p_1 a_1 s_1 = \sigma(\bar{j}) \\ a_2 = k \text{ and } p_2 a_2 s_2 = \sigma(\bar{k}) \\ a_3 = l \text{ and } p_3 a_3 s_3 = \sigma(\bar{l}) \\ \mathbf{h}\overline{\gamma_1} = \gamma_1 + \pi\mathbf{l}(p_1) - \pi\mathbf{l}(p_0) \\ \mathbf{h}\overline{\gamma_2} = \gamma_2 + \pi\mathbf{l}(p_2) - \pi\mathbf{l}(p_0) \\ \mathbf{h}\overline{\gamma_3} = \gamma_3 + \pi\mathbf{l}(p_3) - \pi\mathbf{l}(p_0). \end{cases}$$

The edge is labelled by $\mathbf{e} \in \{\pi\mathbf{l}(p_0), \pi\mathbf{l}(p_1) + \gamma_1, \pi\mathbf{l}(p_2) + \gamma_2, , \pi\mathbf{l}(p_3) + \gamma_3\}$ such that $\langle \mathbf{e}, \mathbf{v}_\beta \rangle = \min\{\langle \mathbf{l}(p_0), \mathbf{v}_\beta \rangle, \langle \mathbf{l}(p_1) + \mathbf{x}_1, \mathbf{v}_\beta \rangle, \langle \mathbf{l}(p_2) + \mathbf{x}_2, \mathbf{v}_\beta \rangle, \langle \mathbf{l}(p_3) + \mathbf{x}_3, \mathbf{v}_\beta \rangle\}$. Here $\pi(\mathbf{x}_\ell) = \gamma_\ell$, $\mathbf{x}_\ell \in \mathbb{Z}^n$ $(\ell \in \{1, 2, 3\})$.

(3) Every node belongs to an infinite path starting from a node $[i, \gamma_1, j, \gamma_2, k, \gamma_3, l]$ such that $[\gamma_1, j] \in \Gamma_{srs}$, $[\gamma_2, k] \in \Gamma_{srs}$ and $[\gamma_3, l] \in \Gamma_{srs}$.

With a treatment similar to the triple point graph, we prove that this graph is finite and identifies quadruple points in the self-replicating tiling.

Proof of Theorem 5.31. The proof is exactly the same as in Theorem 5.25. Finiteness property is deduced from Condition (8.2). Then, if $[i, \gamma_1, j, \gamma_2, k, \gamma_3, l] \in \overline{\mathfrak{Q}}$ is a node of the quadruple point graph, we can express as a power series a point that lies at the intersection of the four tiles. □

Remark 8.3. It is now clear how to define n-tuple graphs for $n \geq 5$ also.

Bibliography

[1] B. Adamczewski and Y. Bugeaud. On the complexity of algebraic numbers. I. Expansions in integer bases. *Ann. of Math. (2)*, 165(2):547–565, 2007.

[2] B. Adamczewski, Y. Bugeaud, and L. Davison. Continued fractions and transcendental numbers. *Ann. Inst. Fourier (Grenoble)*, 56(7):2093–2113, 2006. Numération, pavages, substitutions.

[3] R. L. Adler. Symbolic dynamics and Markov partitions. *Bull. Amer. Math. Soc. (N.S.)*, 35(1):1–56, 1998.

[4] R. L. Adler and B. Weiss. *Similarity of automorphisms of the torus*. Memoirs of the American Mathematical Society, No. 98. American Mathematical Society, Providence, R.I., 1970.

[5] S. Akiyama. Pisot numbers and greedy algorithm. In *Number theory (Eger, 1996)*, pages 9–21. de Gruyter, Berlin, 1998.

[6] S. Akiyama. Cubic Pisot units with finite beta expansions. In *Algebraic number theory and Diophantine analysis (Graz, 1998)*, pages 11–26. de Gruyter, Berlin, 2000.

[7] S. Akiyama. On the boundary of self affine tilings generated by Pisot numbers. *J. Math. Soc. Japan*, 54:283–308, 2002.

[8] S. Akiyama. Pisot number system and its dual tiling. In *Physics and Theoretical Computer Science (Cargese, 2006)*, pages 133–154. IOS Press, 2007.

[9] S. Akiyama, G. Barat, V. Berthé, and A. Siegel. Boundary of central tiles associated with pisot beta-numeration and purely periodic expansions. *Monashefte für Mathematik*, 2008, to appear.

[10] S. Akiyama, T. Borbély, H. Brunotte, A. Pethő, and J. M. Thuswaldner. Generalized radix representations and dynamical systems. I. *Acta Math. Hungar.*, 108(3):207–238, 2005.

[11] S. Akiyama, H. Brunotte, A. Pethő, and J. M. Thuswaldner. Generalized radix representations and dynamical systems. II. *Acta Arith.*, 121(1):21–61, 2006.

[12] S. Akiyama, H. Brunotte, A. Pethő, and J. M. Thuswaldner. Generalized radix representations and dynamical systems. III. *Osaka J. Math.*, to appear, 2008.

[13] S. Akiyama, G. Dorfer, J. Thuswaldner, and R. Winkler. On the fundamental group of the Sierpiński-gasket. *preprint*, 2008.

[14] S. Akiyama and K. Scheicher. Intersecting two-dimensional fractals with lines. *Acta Sci. Math. (Szeged)*, 71(3-4):555–580, 2005.

[15] C. Allauzen. Une caractérisation simple des nombres de Sturm. *J. Théor. Nombres Bordeaux*, 10(2):237–241, 1998.

[16] J.-P. Allouche and J. O. Shallit. *Automatic sequences: Theory and Applications*. Cambridge University Press, 2002.

[17] J. Anderson and I. Putnam. Topological invariants for substitution tilings and their associated C^*-algebras. *Ergodic Theory Dynam. Systems*, 18:509–537, 1998.

[18] P. Arnoux. Un exemple de semi-conjugaison entre un échange d'intervalles et une translation sur le tore. *Bull. Soc. Math. France*, 116(4):489–500 (1989), 1988.

[19] P. Arnoux, J. Bernat, and X. Bressaud. Geometrical models for substitutions. *in preparation*, 2008.

[20] P. Arnoux, V. Berthé, H. Ei, and S. Ito. Tilings, quasicrystals, discrete planes, generalized substitutions, and multidimensional continued fractions. In *Discrete models: combinatorics, computation, and geometry (Paris, 2001)*, Discrete Math. Theor. Comput. Sci. Proc., AA, pages 059–078 (electronic). Maison Inform. Math. Discrèt. (MIMD), Paris, 2001.

[21] P. Arnoux, V. Berthé, T. Fernique, and D. Jamet. Functional stepped surfaces, flips, and generalized substitutions. *Theoret. Comput. Sci.*, 380(3):251–265, 2007.

[22] P. Arnoux, V. Berthé, A. Hilion, and A. Siegel. Fractal representation of the attractive lamination of an automorphism of the free group. *Ann. Inst. Fourier (Grenoble)*, 56(7):2161–2212, 2006. Numération, pavages, substitutions.

[23] P. Arnoux, V. Berthé, and S. Ito. Discrete planes, $\mathbb{Z}^2$-actions, Jacobi-Perron algorithm and substitutions. *Ann. Inst. Fourier (Grenoble)*, 52(2):305–349, 2002.

[24] P. Arnoux, M. Furukado, E. Harriss, and S. Ito. Algebraic numbers and automorphisms of free groups. submitted, 2007.

[25] P. Arnoux and S. Ito. Pisot substitutions and Rauzy fractals. *Bull. Belg. Math. Soc. Simon Stevin*, 8(2):181–207, 2001.

[26] V. Baker, M. Barge, and J. Kwapisz. Geometric realization and coincidence for reducible non-unimodular pisot tiling spaces with an application to beta-shifts. *Ann. Inst. Fourier*, 56(7):2213–2248, 2006.
[27] C. Bandt and G. Gelbrich. Classification of self-affine lattice tilings. *J. London Math. Soc. (2)*, 50(3):581–593, 1994.
[28] G. Barat, V. Berthé, P. Liardet, and J. Thuswaldner. Dynamical directions in numeration. *Ann. Inst. Fourier (Grenoble)*, 56(7):1987–2092, 2006. Numération, pavages, substitutions.
[29] M. Barge and B. Diamond. Coincidence for substitutions of Pisot type. *Bull. Soc. Math. France*, 130:619–626, 2002.
[30] M. Barge, B. Diamond, and R. Swanson. The branch locus for one-dimensional pisot tiling spaces. *preprint*, 2008.
[31] M. Barge and J. Kwapisz. Geometric theory of unimodular Pisot substitutions. *Amer. J. Math.*, 128(5):1219–1282, 2006.
[32] M.-P. Béal and D. Perrin. Symbolic dynamics and finite automata. In G. Rozenberg and A. Salomaa, editors, *Handbook of Formal Languages*, volume 2, pages 463–503. Springer, 1997.
[33] J. Bernat. Computation of L_+ for several cases of cubic pisot numbers. *Discrete Mathematics and Theoretical Computer Science*, 2008. to appear.
[34] J. Bernat. Arithmetic automaton for perron numbers. *Discrete Mathematics and Theoretical Computer Science*, to appear.
[35] J. Berstel and D. Perrin. The origins of combinatorics on words. *European J. Combin.*, 28(3):996–1022, 2007.
[36] V. Berthé, S. Ferenczi, and L. Q. Zamboni. Interactions between dynamics, arithmetics and combinatorics: the good, the bad, and the ugly. In *Algebraic and topological dynamics*, volume 385 of *Contemp. Math.*, pages 333–364. Amer. Math. Soc., Providence, RI, 2005.
[37] V. Berthé and T. Fernique. Brun expansions of stepped surfaces. preprint, 2008.
[38] V. Berthé and A. Siegel. Tilings associated with beta-numeration and substitutions. *INTEGERS (Electronic Journal of Combinatorial Number Theory)*, 5(3):A2, 2005.
[39] V. Berthé and A. Siegel. Purely periodic β-expansions in the Pisot non-unit case. *J. Number Theory*, 127(2):153–172, 2007.
[40] A. Bertrand-Mathis. Développement en base θ; répartition modulo un de la suite $(x\theta^n)_{n\geq 0}$; langages codés et θ-shift. *Bull. Soc. Math. France*, 114(3):271–323, 1986.
[41] M. Bestvina, M. Feighn, and M. Handel. Laminations, trees, and irreducible automorphisms of free groups. *Geom. Funct. Anal.*, 7:215–244, 1997.
[42] M. Bestvina and M. Handel. Train tracks and automorphisms of free groups. *Ann. of Math. (2)*, 135:1–51, 1992.
[43] F. Blanchard. β-expansions and symbolic dynamics. *Theoret. Comput. Sci.*, 65:131–141, 1989.
[44] E. Bombieri and J. E. Taylor. Which distributions of matter diffract? An initial investigation. *J. Physique*, 47(7, Suppl. Colloq. C3):C3–19–C3–28, 1986. International workshop on aperiodic crystals (Les Houches, 1986).
[45] R. Bowen. *Equilibrium states and the ergodic theory of Anosov diffeomorphisms*. Springer-Verlag, Berlin, 1975. Lecture Notes in Mathematics, Vol. 470.
[46] R. Bowen. Markov partitions are not smooth. *Proc. Amer. Math. Soc.*, 71(1):130–132, 1978.
[47] J. W. Cannon and G. R. Conner. The combinatorial structure of the Hawaiian earring group. *Topology Appl.*, 106(3):225–271, 2000.
[48] V. Canterini. Connectedness of geometric representation of substitutions of Pisot type. *Bull. Belg. Math. Soc. Simon Stevin*, 10(1):77–89, 2003.
[49] V. Canterini and A. Siegel. Geometric representation of substitutions of Pisot type. *Trans. Amer. Math. Soc.*, 353(12):5121–5144, 2001.
[50] E. Cawley. Smooth Markov partitions and toral automorphisms. *Ergodic Theory Dynam. Systems*, 11(4):633–651, 1991.
[51] A. Cobham. Uniform tag sequences. *Math. Systems Theory*, 6:164–192, 1972.
[52] G. R. Conner and J. W. Lamoreaux. On the existence of universal covering spaces for metric spaces and subsets of the euclidean plane. *preprint*, 2008.
[53] D. Cooper. Automorphisms of free groups have finitely generated fixed point sets. *J. Algebra*, 111:453–456, 1987.
[54] T. Coulbois, A. Hilion, and M. Lustig. $\mathbb{R}$-trees and laminations for free groups I: Algebraic laminations. preprint, 2007.
[55] D. Crisp, W. Moran, A. Pollington, and P. Shiue. Substitution invariant cutting sequences. *J. Théor. Nombres Bordeaux*, 5(1):123–137, 1993.
[56] B. de Smit. The fundamental group of the Hawaiian earring is not free. *Internat. J. Algebra Comput.*, 2(1):33–37, 1992.
[57] O. Delgrange and E. Rivals. Star: an algorithm to search for tandem approximate repeats. *Bioinformatics*, 20(16):2812–20, 2004.
[58] J.-M. Dumont and A. Thomas. Digital sum moments and substitutions. *Acta Arith.*, 64:205–225, 1993.

[59] K. Eda and K. Kawamura. The fundamental groups of one-dimensional spaces. *Topology Appl.*, 87(3):163–172, 1998.

[60] H. Ei and S. Ito. Tilings from some non-irreducible Pisot substitutions. *Discrete Math. Theor. Comput. Sci.*, 7:81–122, 2005.

[61] H. Ei, S. Ito, and H. Rao. Atomic surfaces, tilings and coincidences II. reducible case. *Ann. Inst. Fourier*, 56:2285–2313, 2006.

[62] M. Einsiedler and K. Schmidt. Markov partitions and homoclinic points of algebraic $\mathbf{Z}^d$-actions. *Tr. Mat. Inst. Steklova*, 216(Din. Sist. i Smezhnye Vopr.):265–284, 1997.

[63] K. Falconer. *Fractal geometry*. John Wiley & Sons Ltd., Chichester, 1990. Mathematical foundations and applications.

[64] D.-J. Feng, M. Furukado, S. Ito, and J. Wu. Pisot substitutions and the Hausdorff dimension of boundaries of atomic surfaces. *Tsukuba J. Math.*, 30(1):195–223, 2006.

[65] T. Fernique. Generation and recognition of digital planes using multi-dimensional continued fractions. In *DGCI'08: International Conference on Discrete Geometry for Computer Imagery*, 2008.

[66] N. P. Fogg. *Substitutions in dynamics, arithmetics and combinatorics*, volume 1794 of *Lecture Notes in Mathematics*. Springer-Verlag, Berlin, 2002. Edited by V. Berthé, S. Ferenczi, C. Mauduit and A. Siegel.

[67] C. Frougny and B. Solomyak. Finite beta-expansions. *Ergodic Theory Dynam. Systems*, 12:45–82, 1992.

[68] C. Fuchs and R. Tijdeman. Substitutions, abstract number systems and the space filling property. *Ann. Inst. Fourier (Grenoble)*, 56(7):2345–2389, 2006. Numération, pavages, substitutions.

[69] B. Gaujal, A. Hordijk, and D. V. der Laan. On the optimal open-loop control policy for deterministic and exponential polling systems. *Probability in Engineering and Informational Sciences*, 21:157–187, 2007.

[70] J.-P. Gazeau and J.-L. Verger-Gaugry. Geometric study of the beta-integers for a Perron number and mathematical quasicrystals. *J. Théor. Nombres Bordeaux*, 16(1):125–149, 2004.

[71] M. Hata. On the structure of self-similar sets. *Japan J. Appl. Math.*, 2(2):381–414, 1985.

[72] P. Hubert and A. Messaoudi. Best simultaneous Diophantine approximations of Pisot numbers and Rauzy fractals. *Acta Arith.*, 124(1):1–15, 2006.

[73] S. Ito, J. Fujii, H. Higashino, and S. Yasutomi. On simultaneous approximation to (α, α^2) with $\alpha^3+k\alpha-1 = 0$. *J. Number Theory*, 99(2):255–283, 2003.

[74] S. Ito and M. Kimura. On Rauzy fractal. *Japan J. Indust. Appl. Math.*, 8(3):461–486, 1991.

[75] S. Ito and M. Ohtsuki. Modified Jacobi-Perron algorithm and generating Markov partitions for special hyperbolic toral automorphisms. *Tokyo J. Math.*, 16(2):441–472, 1993.

[76] S. Ito and M. Ohtsuki. Parallelogram tilings and Jacobi-Perron algorithm. *Tokyo J. Math.*, 17(1):33–58, 1994.

[77] S. Ito and H. Rao. Purely periodic β-expansion with Pisot base. *Proc. Amer. Math. Soc.*, 133:953–964, 2005.

[78] S. Ito and H. Rao. Atomic surfaces, tilings and coincidences I. Irreducible case. *Israel J. Math.*, 153:129–155, 2006.

[79] M. Keane. Interval exchange transformations. *Math. Z.*, 141:25–31, 1975.

[80] J. Kellendonk and I. Putnam. Tilings, C^*-algebras, and K-theory. In M. B. et al., editor, *Directions in mathematical quasicrystals*, volume 13 of *AMS CRM Monogr. Ser.*, pages 177–206, Providence, RI, 2000.

[81] R. Kenyon and A. Vershik. Arithmetic construction of sofic partitions of hyperbolic toral automorphisms. *Ergodic Theory Dynam. Systems*, 18(2):357–372, 1998.

[82] K. Kuratowski. *Topology. Vol. II*. New edition, revised and augmented. Translated from the French by A. Kirkor. Academic Press, New York, 1968.

[83] J. C. Lagarias and Y. Wang. Substitution Delone sets. *Discrete Comput. Geom.*, 29:175–209, 2003.

[84] J.-Y. Lee, R. V. Moody, and B. Solomyak. Pure point dynamical and diffraction spectra. *Ann. Henri Poincaré*, 3(5):1003–1018, 2002.

[85] D. Lind and B. Marcus. *An introduction to symbolic dynamics and coding*. Cambridge University Press, Cambridge, 1995.

[86] A. Livshits. On the spectra of adic transformations of markov compacta. *Russian Math. Surveys*, 42, 1987.

[87] B. Loridant and J. M. Thuswaldner. Interior components of a tile associated to a quadratic canonical number system. *Topology Appl.*, 155:667–695, 2008.

[88] M. Lothaire. *Applied combinatorics on words*, volume 105 of *Encyclopedia of Mathematics and its Applications*. Cambridge University Press, 2005.

[89] J. M. Luck, C. Godrèche, A. Janner, and T. Janssen. The nature of the atomic surfaces of quasiperiodic self-similar structures. *J. Phys. A*, 26(8):1951–1999, 1993.

[90] J. Luo. A note on a self-similar tiling generated by the minimal Pisot number. *Fractals*, 10(3):335–339, 2002.

[91] J. Luo, S. Akiyama, and J. M. Thuswaldner. On the boundary connectedness of connected tiles. *Math. Proc. Cambridge Philos. Soc.*, 137(2):397–410, 2004.

[92] J. Luo, H. Rao, and B. Tan. Topological structure of self-similar sets. *Fractals*, 10:223–227, 2002.

[93] J. Luo and J. M. Thuswaldner. On the fundamental group of self-affine plane tiles. *Ann. Inst. Fourier (Grenoble)*, 56(7):2493–2524, 2006. Numération, pavages, substitutions.

[94] J. Luo and Z.-L. Zhou. Disk-like tiles derived from complex bases. *Acta Math. Sin. (Engl. Ser.)*, 20(4):731–738, 2004.
[95] R. D. Mauldin and S. C. Williams. Hausdorff dimension in graph directed constructions. *Trans. Amer. Math. Soc.*, 309(2):811–829, 1988.
[96] A. Messaoudi. Propriétés arithmétiques et dynamiques du fractal de Rauzy. *J. Théor. Nombres Bordeaux*, 10(1):135–162, 1998.
[97] A. Messaoudi. Frontière du fractal de Rauzy et système de numération complexe. *Acta Arith.*, 95(3):195–224, 2000.
[98] A. Messaoudi. Propriétés arithmétiques et topologiques d'une classe d'ensembles fractales. *Acta Arith.*, 121(4):341–366, 2006.
[99] R. V. Moody. Model sets: a survey. In F. Axel and e. J.-P. Gazeau, editors, *From Quasicrystals to More Complex Systems*, pages 145–166. Les Editions de Physique, Springer-Verlag, Berlin, 2000.
[100] H. M. Morse. Recurrent geodesics on a surface of negative curvature. *Trans. Amer. Math. Soc.*, 22(1):84–100, 1921.
[101] S.-M. Ngai and N. Nguyen. The Heighway dragon revisited. *Discrete Comput. Geom.*, 29(4):603–623, 2003.
[102] S.-M. Ngai and T.-M. Tang. A technique in the topology of connected self-similar tiles. *Fractals*, 12(4):389–403, 2004.
[103] S.-M. Ngai and T.-M. Tang. Topology of connected self-similar tiles in the plane with disconnected interiors. *Topology Appl.*, 150(1-3):139–155, 2005.
[104] W. Parry. On the β-expansion of real numbers. *Acta Math. Acad. Sci. Hungar.*, 11:401–416, 1960.
[105] B. Praggastis. Numeration systems and Markov partitions from self-similar tilings. *Trans. Amer. Math. Soc.*, 351(8):3315–3349, 1999.
[106] N. Priebe-Franck. A primer on substitution tilings of euclidean space. To appear in *Expositiones Mathematicae*, 2008.
[107] Y.-H. Qu, H. Rao, and Y.-M. Yang. Periods of β-expansions and linear recurrent sequences. *Acta Arith.*, 120(1):27–37, 2005.
[108] M. Queffélec. *Substitution dynamical systems—spectral analysis*. Lecture Notes in Mathematics, 1294. Springer-Verlag, Berlin, 1987.
[109] C. Radin. Space tilings and substitutions. *Geom. Dedicata*, 55(3):257–264, 1995.
[110] G. Rauzy. Nombres algébriques et substitutions. *Bull. Soc. Math. France*, 110(2):147–178, 1982.
[111] J.-P. Reveillès. *Géométrie discrète, calcul en nombres entiers et algorithmique*. Thèse de Doctorat, Université Louis Pasteur, Strasbourg, 1991.
[112] E. A. Robinson, Jr. Symbolic dynamics and tilings of $\mathbb{R}^d$. In *Symbolic dynamics and its applications*, volume 60 of *Proc. Sympos. Appl. Math., Amer. Math. Soc. Providence, RI*, pages 81–119, 2004.
[113] D. Roy. Approximation to real numbers by cubic algebraic integers. II. *Ann. of Math. (2)*, 158(3):1081–1087, 2003.
[114] Y. Sano, P. Arnoux, and S. Ito. Higher dimensional extensions of substitutions and their dual maps. *J. Anal. Math.*, 83:183–206, 2001.
[115] K. Scheicher and J. M. Thuswaldner. Canonical number systems, counting automata and fractals. *Math. Proc. Cambridge Philos. Soc.*, 133(1):163–182, 2002.
[116] K. Schmidt. On periodic expansions of Pisot numbers and Salem numbers. *Bull. London Math. Soc.*, 12(4):269–278, 1980.
[117] M. Senechal. What is. . .a quasicrystal? *Notices Amer. Math. Soc.*, 53(8):886–887, 2006.
[118] A. Siegel. Représentation des systèmes dynamiques substitutifs non unimodulaires. *Ergodic Theory Dynam. Systems*, 23(4):1247–1273, 2003.
[119] A. Siegel. Pure discrete spectrum dynamical system and periodic tiling associated with a substitution. *Ann. Inst. Fourier (Grenoble)*, 54(2):341–381, 2004.
[120] V. F. Sirvent and Y. Wang. Self-affine tiling via substitution dynamical systems and Rauzy fractals. *Pacific J. Math.*, 206(2):465–485, 2002.
[121] S. Smale. Differentiable dynamical systems. *Bull. Amer. Math. Soc.*, 73:747–817, 1967.
[122] B. Solomyak. Tilings and dynamics. In *EMS Summer School on Combinatorics, Automata and Number Theory*, Liege, 2006.
[123] W. P. Thurston. *Groups, tilings and finite state automata*. Lectures notes distributed in conjunction with the Colloquium Series, in *AMS Colloquium lectures*, 1989.
[124] J. M. Thuswaldner. Unimodular Pisot substitutions and their associated tiles. *J. Théor. Nombres Bordeaux*, 18(2):487–536, 2006.
[125] E. R. van Kampen. On some characterizations of 2-dimensional manifolds. *Duke Math. J.*, 1(1):74–93, 1935.
[126] W. A. Veech. Interval exchange transformations. *J. Anal. Math.*, 33:222–272, 1978.
[127] R. F. Williams. Classification of one dimensional attractors. In *Global Analysis (Proc. Sympos. Pure Math., Vol. XIV, Berkeley, Calif., 1968)*, pages 341–361. Amer. Math. Soc., Providence, R.I., 1970.